The Role of Sulforaphane in Microtubule Dynamics and Organisation in Health and Cancer

Miss Julia E. A. Mundy MSc
100017170

Thesis submitted for Degree of Master of Science (Research)

University of East Anglia
School of Biological Sciences

September 2018

Abstract

The cellular cytoskeleton, composed of filamentous actin, intermediate filaments and microtubules, is integral in organisation of cell contents, connection of cells to the external environment and cell migration. Cytoskeletal changes and increased migration have been linked to the pathogenesis of multiple diseases, including cancer. The isothiocyanate sulforaphane has been shown in epidemiological studies to exhibit a range of chemopreventive and chemotherapeutic effects, and has attracted attention as a potential therapeutic agent. It has been previously demonstrated that sulforaphane exerts its chemotherapeutic effects via interaction with a number of cellular pathways and processes, including responses to oxidative stress, activation of apoptosis and chromatin remodelling, however, very little of this research focuses on potential effects on microtubules. Recently it has been proposed that sulforaphane is able to bind to, and potentially modify, tubulin leading to disrupted polymerisation of microtubules, which could result in aberrant division, transient cell cycle arrest, mitotic catastrophe and changes in cell migration. The proposed project aimed to investigate the effects of sulforaphane on cell migration and microtubules and upstream signalling proteins in both cancerous and non-cancerous epithelial cell lines. Significant reduction of scratch wound closure was observed at sulforaphane concentrations as low as 10μM, with reduction of both cell velocity and distance travelled. An upregulation of the GTPase activating protein Rap1GAP, a tumour suppressor gene, was observed at the mRNA and protein level following treatment of Panc-1 cells with sulforaphane, which could explain why migration is reduced in these cells, and could translate into an anti-metastatic mechanism in cancer therapies.

Table of Contents

List of Figure Plates

List of Abbreviations

2D	2-Dimensional
3D	3-Dimensional
+TIP	Plus End Tracking Protein
γ-TuRC	γ-Tubulin Ring Complex
γ-TuSC	γ-Tubulin Small Complex
ABP	Actin Binding Protein
ADP	Adenosine Diphosphate
AJ	Adherens Junction
ARE	Antioxidant Response Element
ATAT1	α-Tubulin N-Acetyltransferase 1
ATP	Adenosine Triphosphate
bHLH	Basic Helix Loop Helix
BITC	Benzyl-Isothiocyanate
CD24	Cluster of differentiation 24
CH	Calponin Homology (Domain)
CML	Chronic Myeloid Leukaemia
CSC	Cancer Stem Cell
DAPI	4',6-diamidino-2-phenylindole
DMEM	Dulbecco's Modified Eagle Medium
DMSO	Dimethyl sulfoxide
EB	End Binding Protein
EDTA	Ethylenediaminetetraacetic acid
EMT	Epithelial-to-Mesenchymal Transition
EZH2	Enhancer of Zeste Homolog 2
F-Actin	Filamentious Actin
FA	Focal Adhesion
FAK	Focal Adhesion Kinase
FBS	Foetal Bovine Serum
G-Actin	Globular Actin
GAP	GTPase Activating Protein
GDP	Guanine Diphosphate
GEF	Guanine Nucleotide Exchange Factor

GPCR	G Protein-Coupled Receptor
GS	Goat Serum
GTP	Guanine Diphosphate
HDAC6	Histone Deacetylase 6
Id	Inhibitor of Differentiation
IF	Intermediate Filament
ITC	Isothiocyanate
MAP	Microtubule Associated Protein
MAT	Mesenchymal-to-Amoeboid Transition
MET	Mesenchymal-to-Epithelial Transition
MMP	Matrix Metalloproteinase
MT	Microtubule
MTA	Microtubule Targeting Agent
MTOC	Microtubule Organising Centre
nMTOC	Non-Centrosomal Microtubule Organising Centre
NQO1	NAD(P)H:quinone oxidoreductase
PBS	Phosphate Buffered Saline
PBST	Phosphate Buffered Saline plus 0.1% Tween 20
PRC2	Polycomb Repressive Complex 2
PTM	Post-Translational Modification
RIAM	Rap1-GTP-Interacting Adaptor Molecule
ROS	Reactive Oxygen Species
RTK	Receptor Tyrosine Kinase
SFN	Sulforaphane
TJ	Tight Junction
TSG	Tumour Suppressor Gene
TTL	Tubulin Tyrosine Ligase
ZO	Zonulae Occludens

Acknowledgements

I would first like to thank Dr Mette Mogensen for her supervision, understanding and advice during my time in the lab, and for reading and making comments throughout the writing process. Thanks also to the other members of my supervisory team, Dr Jelena Gavrilovic and Dr Elizabeth Lund for their advice, and Dr Paul Thomas for his help with imaging and analysis. For funding of the project, I must extend my thanks to BigC.

For their help with routine lab questions and tasks, thank you to Ben Rix and Tope Amodu. For use of images of EB1 and acetylated tubulin in breast cancer cells thanks to Olivia Hodges who worked with me for her undergraduate research project. Thank you to Yaser Alqurashi for tips on SFN dosing and use of microarray data, and additional thanks to Simon Moxon for help with processing and understanding of this data.

I would also like to thank my family and friends for their support during this time.

Chapter One

Introduction

1.1. Background

The eukaryotic cellular cytoskeleton is composed of three interconnected polymeric elements: actin, intermediate filaments (IFs) and microtubules (MTs), and a host of accessory proteins which facilitate their integration into a number of cellular processes. Much like the bony skeleton, the cellular cytoskeleton lends mechanical support and integrity to cells, however, in lieu of rigid mineralised bones, the cellular cytoskeleton comprises a system of multimeric protein filaments. The dynamics and organisation of these filaments are influenced by diverse hierarchical networks of regulatory proteins and signalling pathways (Frixione, 2000; Fletcher and Mullins, 2010). Functionally, the cytoskeleton serves a trio of broad purposes, namely the organisation of cellular contents, connection to the external environment, and force generation during cell movement and shape changes (Fletcher and Mullins, 2010; de Forges et al., 2012). As such, the ability of cells to withstand mechanical deformation, move and proliferate is largely dependent on the cytoskeleton, making it absolutely essential for normal tissue development, homeostasis and function.

Many fundamental cellular processes, such as migration and division, are perturbed or intensified during disease development and progression, with cancer being a prominent example. Cancers are a collection of diseases primarily characterised by aberrant cell division and invasion, and numerous links have previously been drawn between tumour development and proteins involved in cytoskeletal assembly and regulation (Hall, 2009; Yilmaz and Christofori, 2009). Thus, the cellular cytoskeleton, and by association its regulators, serve as viable targets for chemotherapeutics. The effectiveness of this strategy has already been demonstrated through the approval and successful clinical use of the MT-targeting spindle poisons paclitaxel and vinblastine, which provide better clinical outcomes when utilised as combination chemotherapeutics (Loehrer et al., 1992; Dumontet and Jordan, 2010). Unfortunately, as these drugs also disrupt MTs in healthy cells, they are associated with high levels of toxicity, particularly neurotoxicity involving both

central and peripheral nerves, which greatly restricts their efficacy (Steward et al., 1984; Dumontet and Jordan, 2010; Magge and DeAngelis, 2015). Furthermore, as is the case for many other clinical compounds, current MT targeting agents (MTAs), such as vinblastine, are not invulnerable to chemotherapeutic resistance (Ueda et al., 1987; Kavallaris, 2010). Therefore, further work into identification and characterisation of novel cytoskeletal targeting compounds that capitalise on the effectiveness of inhibiting both proliferation and invasion of cells while also being free from these pitfalls is paramount, with the overarching aim of introducing new clinical compounds in the future.

The isothiocyanate (ITC) sulforaphane (SFN), derived from hydrolysis of a glucosinolate secondary metabolite known as glucoraphanin present in broccoli and other brassicas, has been highlighted as a potential novel chemotherapeutic. Previous work has shown that SFN has multiple effects on a diverse array of cellular pathways and processes (Juge et al., 2007), including interactions with the cellular cytoskeleton, particularly MTs (Jackson and Singletary, 2004; Jackson et al., 2007; Azarenko et al., 2008). Epidemiological studies have linked consumption of brassicas, and therefore an elevated SFN intake, to the reduction of cancer risk at multiple sites, including the gastrointestinal tract (Hansson et al., 1993; Lin et al., 1998; Seow et al., 2002), lung (Spitz et al., 2000; Wang et al., 2004a), and breast (Ambrosone et al., 2004). Additionally, diets rich in brassicas have been associated with reduced malignant prostate cancer progression (Richman et al., 2012). Pairing these epidemiological observations with reports of growth inhibitory (Kanematsu et al., 2011), cytotoxic (Gamet-Payrastre et al., 1998; Gamet-Payrastre et al., 2000; Rudolf et al., 2009; Rudolf and Červinka, 2011) and anti-metastatic (Thejass and Kuttan, 2006; Shankar et al., 2008; Singh et al., 2009; Shan et al., 2013) activities, it appears that SFN could potentially prevent cancer development as well as targeting established cancers. This dual effect allows sulforaphane a greater potential than most chemotherapeutic agents, which are mainly utilised as destructive forces

against established cancers. Therefore, sulforaphane could potentially be utilised not only in clinical cases of established malignancies, but also as a prophylactic measure to reduce cancer incidence. However, the full potential of this compound will only be realised following comprehensive characterisation of its effects, of which there are many, on both healthy and cancerous cells. To that end, the project discussed herein aims to contribute to this field of research by investigating the effects of both low physiological and high therapeutic dose ranges of sulforaphane on the MT cytoskeleton within epithelial cells, from which roughly 90% of cancers are thought to originate (McCaffrey and Macara, 2011). This opening introduction chapter will present current knowledge in the field and discuss the key underpinning rationale to this work, so that subsequent data may be set into sufficient context.

1.2. The Eukaryotic Cytoskeleton

In order to successfully survive and reproduce cells must be able to control their shape throughout growth and partition genetic material during cell division. In order to achieve this both eukaryotes and, in a more simplified manner, prokaryotes, utilise networks of dynamic filamentous polymers which are collectively known as the cytoskeleton. Members of both tubulin (FtsZ and TubZ) and actin (MreB and ParM) families have been identified in all types of cells except the crenarchaea (Löwe and Amos, 2009), which instead use a system homologous to eukaryotic vesicular sorting and cytokinesis, even when their genomes encode FtsZ (Busiek and Margolin, 2011). As referenced earlier in the text, the eukaryotic cytoskeleton is a tripartite system, consisting of three families of polymeric filaments, each of which possess distinct structural and functional properties. The following section of text will outline the basic features of each polymer, and the relation of these to their function. MTs, the main focus of this investigation, will subsequently be discussed in more detail later in the text.

The highly conserved actin protein is the most abundant in eukaryotic cells and partakes in a greater number of protein-protein interactions than any other currently identified protein (Reisler and Egelman, 2007; Dominguez and Holmes, 2011). The actin cytoskeleton is primarily involved in the initial stages of cell protrusions, driven by the assembly of globular (G-actin) monomers into filamentous (F-actin) structures (Svitkina, 2018). The 375-amino acid actin polypeptide is folded into two major domains (α & β), although a traditional four-domain nomenclature has been used, with subdomains 2 and 4 inserted into structurally related domains 1 and 3 (Kabsch et al., 1990). Two clefts are present in the actin monomer, one into which the nucleotide and its associated divalent cation, magnesium (Mg^{2+}), are bound, and the other, lined with hydrophobic residues, that acts as the binding site for the majority of actin binding proteins (ABPs) and a mediator for longitudinal contacts in F-actin (Oda et al., 2009; Fujii et al., 2010). The proximity of these two binding clefts facilitates nucleotide-dependent changes in ABP binding affinities and inter-subunit contacts (Dominguez and Holmes, 2011).

Nucleotide hydrolysis from the relatively stable ATP to unstable ADP form of actin is a principle factor regulating G-actin to F-actin transition, with G-actin being a poor ATPase, while F-actin is the opposite. Assembled *in vitro*, G-actin will join a filament in the ATP state at the fast-growing barbed (+) end, with hydrolysis taking place in the filament while monomers dissociate in the ADP-bound monomers from the pointed (-) end (Wegner and Isenberg, 1983). This is known as actin treadmilling, however, the phenomenon is not observed in cells, where there is a cohort of ABPs which can nucleate, cap, cross link and cleave actin filaments as well as sequestering monomers (Pollard and Borisy, 2003). These accessory proteins allow the construction of complex and diverse actin arrays within the cell which constitute the primary force generating machinery for both pushing and pulling motions (Svitkina, 2018). Actin drives cell protrusions by polymerising closely under the plasma membrane, with large branched arrangements resulting in sheet like lamellipodia,

which drive cell migration, and bundled unbranched filaments producing spike like filopodia which are important in environmental sensing (Jacquemet et al., 2015). Control and organisation of these networks is multidimensional, affected by cell surface receptors, GTPases and nucleating/capping accessory proteins, and there is no straightforward relationship between certain receptors or GTPases and specific actin organisations (Insall and Machesky, 2009).

Branched actin filaments are created through interaction with the seven subunit Arp2/3 complex, within which are the actin-like proteins Arp2 and Arp3 plus five unique, yet highly conserved, proteins (Machesky and Gould, 1999). These arrays drive the protrusion of lamellipodia, large skirt-like protrusions formed at the leading edge of a cell during migration, a process that will be discussed in more depth later on. Actin arrays are also involved in certain membrane trafficking processes and cell-cell junction formation, which is important in epithelial cells (Svitkina, 2018). A distinct set of proteins, the formins, regulate the nucleation of unbranched actin structures such as those found in filopodia (Insall and Machesky, 2009), finger-like projections which extend out from the cell edge and are involved in environmental sensing and junctional contact formation (Jacquemet et al., 2015). Acting as ring-shaped dimers, formins sit on growing end of the actin filament to mediate addition of actin monomers in a linear manner (Insall and Machesky, 2009). As a result of the action of formins, rather than being composed of a branched network, filopodia consist of tightly packed, unidirectional actin filaments, with all barbed ends oriented towards the plasma membrane (Jacquemet et al., 2015). Further details of the assembly and dynamics of these actin-rich protrusions will be discussed in a later section focusing on cell migration.

In contrast to actin filaments, that are formed from only one well conserved protein building block, IFs are a diverse group of polymers composed from a large number of different protein families. Indeed, there are over 70 known IF proteins identified in humans (Snider and Omary, 2014), making them the largest family of

cytoskeletal proteins in mammals (Eira et al., 2016). Expression of these proteins varies between tissue types (Dey et al., 2014), for example keratin filaments are expressed in the epidermis to provide structural support and tissue integrity (Steinart, 1993). It was originally thought that assembled IFs were relatively static structures, principally important for maintaining tissue integrity, and that they did not participate in the process of cell movement, however, later evidence has indicated that IFs are dynamic polymers, much like actin filaments and MTs, which partake in a number of cell movements (Helfand et al., 2004).

The largest cytoskeletal elements, MTs, are non-covalent, hollow structures that are not only key in mechanical integrity, cell polarity and migration, but also play a fundamental role in segregation of chromosomes during cell division (Downing and Nogales, 1998; Conde and Cáceres, 2009), spatial distribution of organelles (Wade and Hyman, 1997; de Forges et al., 2012) and intracellular trafficking (Dumontet and Jordan, 2010). Similar to the other cytoskeletal filaments, MTs generate motility via orchestrated assembly and disassembly of filaments. Similar to treadmilling of actin, nucleotide triphosphate hydrolysis is key to polymer assembly and disassembly, however, in the case of MTs GTP, not ATP hydrolysis is key. MT dynamics are modulated by multiple categories of regulatory proteins, including factors promoting nucleation and polymerisation, anchoring proteins and depolymerising factors (Fletcher and Mullins, 2010).

The structure, dynamics and function of MTs will be discussed in detail in the next section of text, as these filaments constitute the principle focus of this investigation, however, it should be mentioned here that the three cytoskeletal subsystems do not exist in isolation within the cell; in certain situations, different filament types may interact with one another, allowing the construction of highly organised arrays which influence cell shape and mechanics (Huber et al., 2014).

1.3. Microtubule Structure and Dynamic Instability

MTs are hollow cylindrical polymers generated by longitudinal and lateral interactions between homologous α- and β-tubulin proteins, each approximately 450 amino acids in size (Downing and Nogales, 1998). Eight α- and seven β-tubulin isoforms are present in humans, and these exhibit cell- and tissue-type specific variation in their expression (Roll-Mecak, 2015). The main bodies of tubulin proteins are ordered and well folded, sharing 80-95% sequence identity, while the C-terminal tails are negatively-charged and disordered, with only around 50% sequence identity (Garnham and Roll-Mecak, 2012; Roll-Mecak, 2015). In constructing a MT, α- and β-tubulin heterodimers self-assemble head-to-tail into linear protofilaments, which subsequently associate laterally via further homotypic α- and β-tubulin contacts to form a sheet. This sheet is sealed into a tubule via further lateral interactions at a single seam, where homotypic α-β-tubulin interactions are present due to offset in protofilament alignment (Conde and Cáceres, 2009; Maurer et al., 2012; Roll-Mecak, 2015). The polarity originating from the tubulin heterodimers gives rise to a polarity over the MT as a whole, with α-tubulin exclusively present at a slow growing (minus) end and β-tubulin exposed at the opposite fast-growing (plus) end (Conde and Cáceres, 2009). MT assembly may occur spontaneously *in vitro* at high concentrations of purified tubulin (above 2.5mg/ml) and in the presence of 10mM Mg^{2+} (Fellous et al., 1977: Herzog and Weber, 1977), however, in most vertebrate cells, spontaneous polymerisation of tubulin is not favoured (Kollman et al., 2008). Consequently, the cellular MT network is nucleated and anchored by an organelle known as the centrosome, a structure consisting of two centrioles, each themselves composed of nine MT triplets surrounded by pericentriolar material. Most often located in the perinuclear region, the centrosome acts as the principle MT organising centre (MTOC) within the cell, from which MT arrays, held at the MTOC by their minus ends, extend towards the cell cortex in interphase cells (Bowne-Anderson et al.,

2015). A cloud of pericentriolar material surrounds the centrioles, and contains a number of proteins associated with MT nucleation and organisation. One of these proteins is γ-tubulin, another tubulin family member, that forms into two complexes along with other proteins, a heterotetrameric γ-tubulin small complex (γ-TuSC; Haren et al., 2008) and a larger γ-tubulin ring complex (γ-TuRC), which then act as a scaffold for the binding of α- and β-tubulin heterodimers during MT nucleation (de Forges et al., 2012). Within cells, due to nucleation by γ-tubulin complexes, MTs generally contain 13 individual protofilaments. However, there are exceptions to this, such as cochlear pillar cells, where MTs commonly contain 15 protofilaments (Tucker et al., 1992; Mogensen et al., 2002). MTs polymerised *in vitro*, due to the absence of nucleating complexes, may vary greatly in the number of protofilaments present (Pierson et al., 1978; Wade et al., 1990).

Following assembly, subsets of MTs may be rapidly growing or shrinking at any given time point. This occurs via the ability of MTs to swiftly and repeatedly switch between growing and shrinking states, sometimes segregated by a period of stasis known as pausing. Referred to as dynamic instability, this process facilitates rapid remodelling of MTs in response to environmental or mechanical cues (Burbank and Mitchison, 2006). This phenomenon arises from the intrinsic properties of the tubulin proteins themselves, rather than from the action of other proteins, although additional MT associated proteins may further modulate dynamic instability of MTs. In MTs, both α- and β-tubulin monomers act as GTPases, and each possess a binding site for a guanine nucleotide, however, the site in α-tubulin is rendered non-exchangeable (known as the N-site), as it is located at the dimer interface between the tubulin monomers (Nogales et al., 1998). The site in β-tubulin (E-site) is exposed and readily exchangeable. Hydrolysis of guanine triphosphate (GTP) at the E-site is important in dynamic instability, and for the assembly of MTs. Dimers are incorporated onto the growing MT end via initial transient association with the end of the MT followed by

formation of stronger longitudinal and lateral contacts. This incorporation increases the GTPase activity of tubulin and GTP at the E-site is hydrolysed to guanine diphosphate (GDP), rendering the E-site non-exchangeable (Downing and Nogales, 1998; Bowne-Anderson et al., 2015). In the GTP-bound state protofilaments possess a straight conformation, however, when GDP is present in the E-site, unless held by lateral contacts from neighbouring protofilaments, a curved conformation is adopted. A delay in GTP hydrolysis by tubulin maintains a GTP cap at the growing tip of the MT, further stabilising GDP bound protofilaments, however, if this GTP cap becomes hydrolysed prior to the addition of further dimers, the protofilaments bow outwards from the MT, destabilising the structure and leading to a rapid MT depolymerisation event known as catastrophe (Fig. 1, Conde and Caceres, 2009; Bowne-Anderson et al., 2015). In the cell, MTs explore the cytoplasm of the cell through polymerisation, and their function largely depends on making contact with other proteins on intracellular organelles or the plasma membrane, which allow them to generate pushing or pulling forces and perform other functions. If they do not form these contacts they will very often undergo catastrophe (Bowne-Anderson et al., 2015). Many such proteins, which, in capturing MTs and facilitating their mechanical and biological roles in the cell, modulate the dynamic instability of the MT network, are collectively known as MT associated proteins (MAPs). Other processes, such as MT nucleation and severing are also regulated by MAPs.

Amid the many families included in the MAP group are a diverse collection of proteins which are unified by their preferential binding to the plus end of MTs, leading to their collective nomenclature as plus-end tracking proteins (+TIPs; Schuyler and Pellman, 2001). In binding the plus-end these proteins influence the dynamic instability arising from tubulin GTP hydrolysis and facilitate interactions with various structures (Zhang et al., 2015). Among the +TIPs, the three-member end binding protein (EB) family is prominent (Honnappa et al., 2009). These conserved proteins, designated EB1, EB2 and EB3, are encoded by the genes *MAPRE1, MAPRE2* and

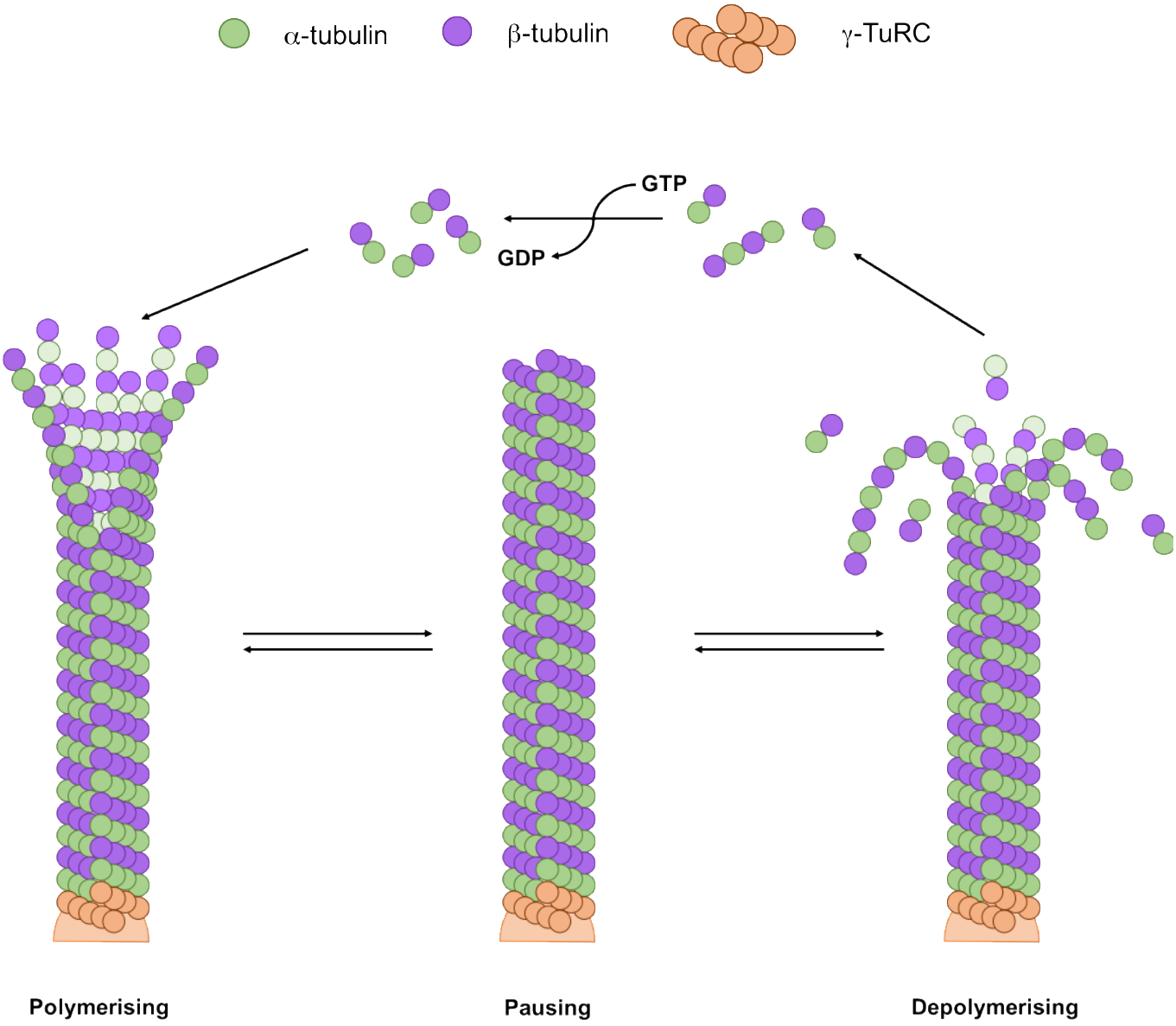

Figure 1 – Schematic to show MT polymerisation and dynamic instability. *In vivo* MTs are nucleated by g-TuRCs, and the MT minus ends are protected by capping proteins. During polymerisation a-b-tubulin heterodimers are added head-to-tail to form protofilaments, which also associate laterally and are connected at a single seam to form a hollow tubule. Hydrolysis of GTP bound to b-tubulin to GDP occurs following heterodimer addition, however, in growing MTs there is a cap of GTP-tubulin which acts to facilitate continued polymerisation. If this cap is lost, and tubulin at the end of the growing microtubule is hydrolysed to GDP the protofilaments adopt a curved conformation and peel outwards from the microtubule, an event known as catastrophe, leading to depolymerisation. In between these growing and shrinking states MTs may pause, during which time no subunits are added nor lost. (Adapted from Conde and Cáceres, 2009).

MAPRE3 respectively (Su and Qi. 2001). The EBs are characterised by their two functional domains, an N-terminal calponin homology (CH) domain and a C-terminal coiled coil, or dimerization, domain, which are separated by a 60-80 residue variable linker region (Buey et al., 2011). The CH domain, by binding over four tubulin proteins in the MT lattice, aside from those at the MT seam, can sense the nucleotide status of β-tubulin, and has a markedly greater affinity for GTP tubulin at the plus end of MTs. As a result, EB1 is observed only at the ends of growing MTs, as during depolymerisation the GTP cap is lost, and therefore EB1 no longer binds (Maurer et al., 2012). The coiled coil of the dimerization domain, along with a C-terminal EEY/F motif, facilitates both homo/hetero-dimerisation of EBs and binding to a number of other +TIP proteins and regulatory molecules (Fig.2), such as cytoplasmic linker protein-170 (CLIP-170), containing CAP-Gly domains or SxIP motifs, allowing them to act as a scaffold for functional protein assemblies at the plus end of MTs (Bieling et al., 2008; Dixit et al., 2009; Galjart, 2010).

On the assembled MT, the disordered C-terminal domains of tubulins are positioned on the exterior of the tubule and serve as binding sites for many molecular motors and other accessory proteins, including MAPs (Verhey and Gaertig, 2007; Roll-Mecak, 2015). These regions are also subject to the majority of sequence variation and post-translational tubulin modifications (PTMs), which along with the relative levels of different tubulin isotypes, can alter the dynamic properties of MTs, leading to more, or less, stable MTs. The full range of tubulin PTM functions has yet to be ascertained, however, a number of functions have been determined through experimental means (Hammond et al., 2008). Tubulin detyrosination, involves removal of the C-terminal tyrosine of α-tubulin within polymerised MTs by a carboxypeptidase. Detyrosination and its reverse reaction, tyrosination, addition of tyrosine back onto the C-terminal glutamate by tubulin tyrosine ligases (TTLs), may differentially recruit MT-binding proteins (Hammond et al., 2008). Kinesin-1, a motor

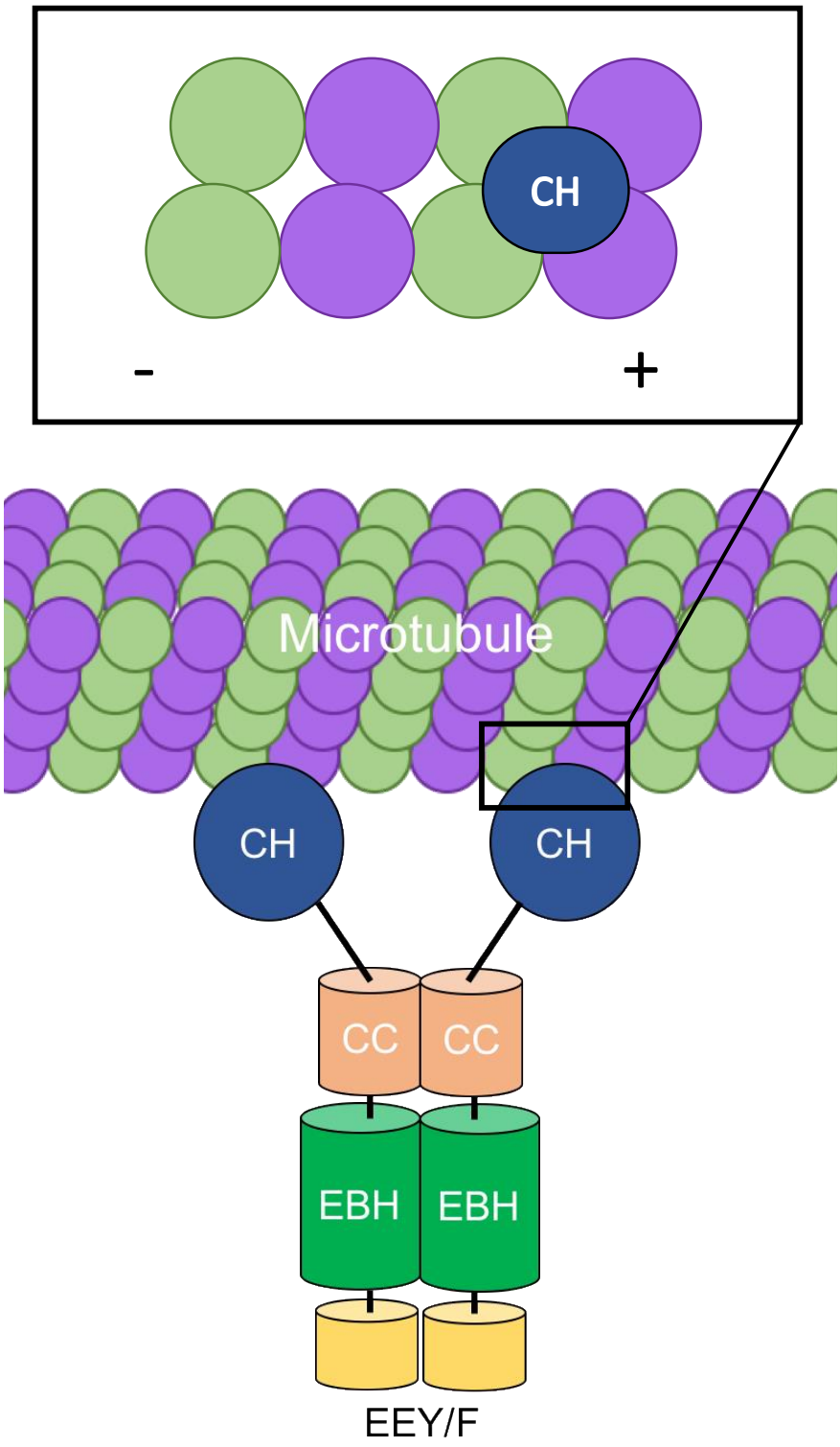

Figure 2 – Schematic representation of EB1 domain structure and CH domain binding across tubulin protofilaments. EBs function as homo- or hetero-dimers, and bind to microtubules via their N-terminal CH domain. The CH domain, by binding across four tubulin monomers the CH domain can detect the nucleotide status of β-tubulin, and has a markedly increased affinity for GTP tubulin over the GDP form. The C-terminal region of the protein, facilitates homo- and hetero-dimerisation through a coiled-coil domain and binding to other +TIPs via an EEY/F motif. Adapted from Buey et al., 2011.

protein charged with moving various cargoes, including the IF vimentin, along MTs, preferentially binds detyrosinated MTs (Liao and Gundersen, 1998; Reed et al., 2006). Conversely, CAP-Gly domain-containing +TIPs, such as CLIP-170 are recruited to tryosinated MTs. For example, presence of MTs lacking the C-terminal phenylalanine, mimicking detyrosinated tubulin, in *Saccharomyces cerevisiae* leads to mislocalisation of the CAP-Gly domain-containing CLIP-170 homologue, but not the EB1-type +TIP without a CAP-Gly domain (Badin-Larcon et al., 2004). A similar mislocalisation of CLIP-170, but not EB1, was seen in fibroblasts isolated from TTL null mice, which show a dramatic reduction in tyrosinated MTs and alterations in spindle orientation (Peris et al., 2006). This indicates that PTMs not only alter MT dynamics, but impact on the behaviour of MAPs. Increased levels of detyrosinated tubulin may provide some form of growth advantage, as TTLs are frequently down-regulated in animal and human cancers (Lafanechere et al., 1998; Soucek et al., 2006), and this may be correlated with poor prognoses (Mialhe et al., 2001; Kato et al., 2004).

Unlike detyrosination, which likely occurs on the outside of MTs, acetylation occurs on Lysine 40 of α-tubulin, which is located on the luminal face (Hammond et al., 2008). Originally it was thought that acetylation marked only long-lived stable MTs, however, it has since been shown that some cell types possess stabilised MTs that are not extensively acetylated (Piperno and Fuller, 1985; Schulze et al., 1987) some organisms, such as *Trypanosoma brucei*, exhibit global acetylation of MTs (Sasse and Gull, 1988). Nascent MTs, which have unusual abilities to simultaneously grow and resist depolymerisation are commonly acetylated (Perdiz et al., 2011).

1.4. Epithelial Cells

In order to protect the interior of the body whilst permitting controlled movement of vital components there must be an intuitive and dynamic barrier

separating the external and internal environments. In complex multicellular organisms, this barrier comes in the form of epithelia, which line or encapsulate most organs within the body, dividing it into distinct compartments with differing physiology or morphology (Chen and Zhang, 2013). Epithelial layers are generally one cell thick (simple epithelia) but some may contain multiple stratified layers (complex epithelia; Macara et al., 2014). This discussion will only focus on simple epithelia, such as those in the gut, kidneys and pancreatic ducts.

Simple epithelial layers possess three main characteristics, namely exhibition of distinct polarity over the apico-basal axis, formation of multiple intercellular adhesions and the orientation of mitotic spindles in register with the plane of the epithelial sheet (McCaffrey and Macara, 2011). Indeed, epithelia are thought to be the first tissue to arise during the evolution of multicellular animals, and they are the initial differentiated structure formed during embryonic development (McCaffrey and Macara, 2011), during which they may be folded into complex tissues (St Johnston and Sanson, 2011). In the adult, epithelia may respond to stretching or compressive forces via proliferation or extrusion of cells respectively, allowing expansion or shrinkage of the layer in response to environmental stimuli (Macara et al., 2014). *In vivo* most, yet not all, epithelial layers originate from, and are renewed by, discrete populations of stem cells present within the layer. These stem cells give rise to rapidly proliferating progenitors, which in turn often produce fully differentiated epithelial cells, however in some cases cells continue to divide to maintain homeostasis. This pool of stem cells often exists within a specific, protected, stem cell niche, and has the capacity to repopulate the epithelium with new, healthy cells in the event of damage from toxic agents in the environment, such as chemicals or radiation, which epithelial layers are more likely to be exposed to (Macara et al., 2014). Due to their prevalence in the body, and the aforementioned frequent exposure to harmful agents, epithelial cells have been suggested as the cell of origin of up to 90% of cancers (McCaffrey and Macara, 2011), including intestinal cancer (Barker et al., 2009), basal

cell carcinomas of the skin (Gerdes and Yuspa, 2005), prostate cancers (Wang et al., 2009) and certain breast cancer subtypes, such as those linked to *BRCA1* mutations (Lim et al., 2009; Molyneux et al., 2010).

Formation of junctions between cells in the layer, and between cells and the basement membrane, is important for the function and integrity of epithelial layers (Fig. 3; Yilmaz and Christofori, 2009). Near to the apical surface, net-like branched networks of transmembrane proteins form tight junctions (TJs), or zonulae occludens (ZO) which connect neighbouring cells. Each of the protein strands act to create a seal between the two neighbouring membranes, restricting paracellular and transcellular movement of ions and molecules, with increasing number of strands creating a tighter junction (Singh et al., 2018). Slightly basal to the TJs, still on the lateral membranes, are adherens junctions (AJs), or zonula adherens, which form belt structures around the cell periphery. In epithelial cells the transmembrane glycoprotein E-cadherin spans the gap between the cells and links intracellularly to the actin cytoskeleton through adaptor proteins and catenins (Singh et al., 2018). Tissue specific interactions are maintained by AJs, and their arrangement allows for control over cell shape and tension (Yilmaz and Christofori, 2009). The IFs of neighbouring cells are linked via desmosomes, which consist of inner plaques, connecting to IFs, and outer plaques which bind cadherins to allow contact with desmosomes on neighbouring cells. Desmosomes lend mechanical support to cells and are found more prominently in cells in areas of mechanical stress. Hemi-desmosomes are similar in their composition but connect to the underlying extracellular matrix (ECM) instead of desmosomes on adjacent cells (Singh et al., 2018). Intercellular communication is maintained by pore-like gap junctions between cells, composed of connexin proteins. These water-filled pores allow intercellular signals, small metabolites and ions to move between cells (Lee et al., 2006; Singh et al., 2018).

As mentioned earlier, epithelial layers display polarity, specifically a molecular asymmetry which means that the composition of the basal (bottom) membrane of a polarised epithelial cell is biochemically distinct from that of the apical (top) membrane. This polarity generates two distinct faces of the epithelial layer, with the basal surface generally connected to the underlying ECM, often referred to as the basal lamina or basement membrane, while the apical membrane tends to face outwards to the external environment, a division which is highly important in barrier function and nutrient transport (Chen and Zhang, 2013). Following certain cues, polarity originates from the activity of dedicated, evolutionarily conserved polarity proteins, reorganisation of the cytoskeleton and precise spatiotemporal changes in the distribution of certain lipids (St Johnston and Sanson, 2011; Tepass, 2012; Chen and Zhang, 2013; Raman et al., 2018; Singh et al., 2018). Polarity proteins form three complexes within the cell which initiate and maintain the discrete basal and apical regions of the cell. In the basal domain lies the Scrib complex, comprised of the tumour suppressors lethal giant larve (Lgl), discs large (Dlg) and scribble (Scrib), which acts to maintain the basolateral polarity of this domain. In the apical region of the cell, localising to tight junctions, are two complexes which contribute to maintenance of apical polarity. The PAR complex, consisting of atypical protein kinase C (aPKC), PAR3 and PAR6, acts to segregate the basal and apical domains, and possesses a mutual antagonistic relationship with the basal Scrib complex (Singh et al., 2018). Additionally, the PAR complex reinforces the action of the other apical complex, Crumbs, which aside from the namesake protein contains protein associated with Lin-1 (PALS1) and PALS1-associated tight junction (PATJ) complex and is involved in the establishment of the apical pole (Iden and Collard, 2008; Singh et al., 2018). Due to association of apical complexes with tight junctions, apical junctional complexes separate the apical and basolateral regions of the polarised cell by acting as a physical barrier between membrane domains (Fig. 4; Shin et al., 2005; Raman et al., 2018).

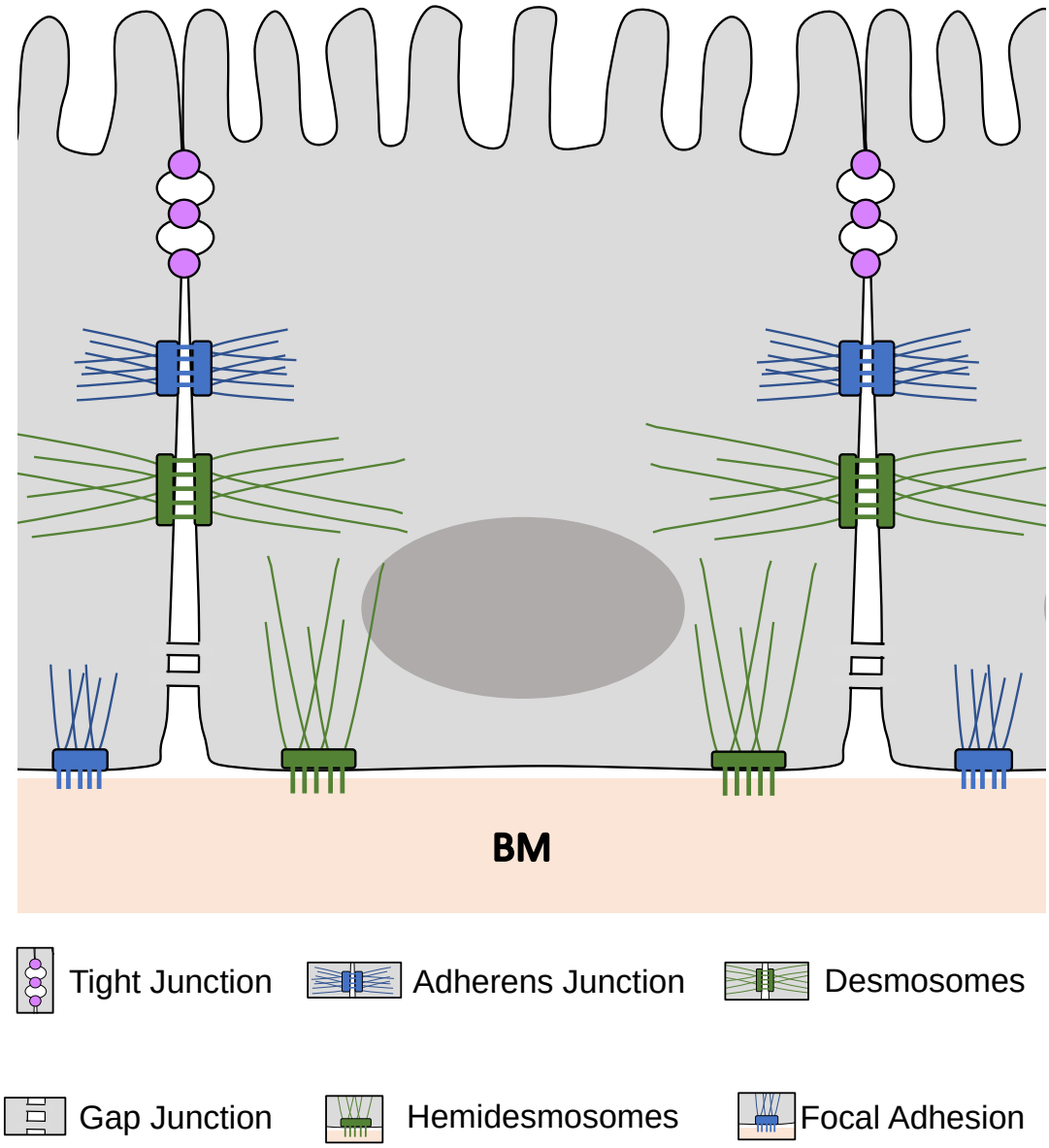

Figure 3 – Schematic representation of the junctions formed between epithelial cells and the basement membrane. Tight junctions are the most apical junctions, and form a seal between cells to restrict movements of ions and molecules between cells and across the epithelial layer. Below these are adherens junctions, which connect the actin cytoskeletons of cells to one another, allowing control over tension and cell shape. Desmosomes and hemidesmosomes allow connection of intermediate filaments to those in other cells and to the BM respectively. Adapted from Singh et al., 2018.

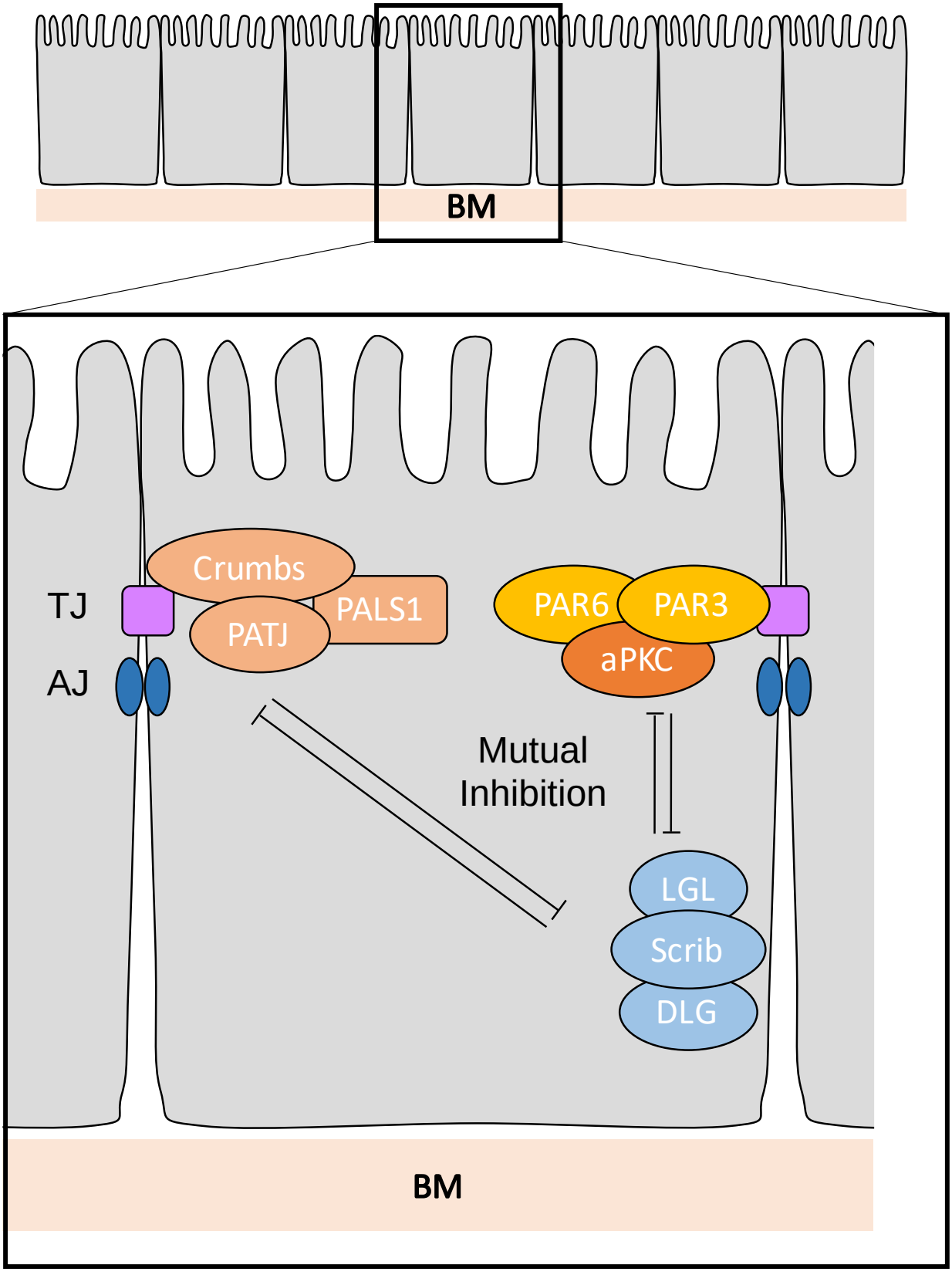

Figure 4 – Three key protein complexes establish and maintain epithelial cell polarity. The apical domain is partitioned by two complexes associating with TJs, namely the crumbs and PAR complexes, with the latter forming a barrier between the two domains and enhancing crumbs activity. The basolateral portion of the cell is governed by the Scrib complex, which is mutually antagonistic to both apical complexes. Adapted from Iden and Collard, 2008.

Of key relevance to the discussed project, the MT cytoskeleton undergoes remodelling during polarisation, from a radial array in undifferentiated cells to an apico-basal array, in which MTs, in some cases anchored at non-centrosomal MTOCs (nMTOCs), extend from the apical region to the basolateral portion of the cell. The following section will discuss the establishment and function of such arrays in epithelial cells in more detail.

1.5. Microtubule Organisation in Polarised Epithelial Cells

Relatively flat cells generally possess a radial MT array, with MTs anchored at the centrosome, located near the cell nucleus, growing out towards the cell periphery (Mogensen et al., 2000; Bellett et al., 2009). When cells differentiate into functional cell types in any particular organ or tissue, they generally lose this radial array and rearrange their MT cytoskeleton to favour their particular specialised function, including the formation of non-centrosomal arrays (Fig. 5; Mogensen, 2004). Epithelial cells are one predominant cell type within the body that possess non-centrosomal arrays of MTs.

Apico-basal polarisation of epithelial cells, stimulated by cell-cell contacts, is due to MT rearrangement, in which the radial array extending from the centrosome is repressed or lost completely and MTs are anchored at n-MTOCs located at apical adherens junctions, forming bundles for stability (Bellett et al., 2009). In some terminally differentiated cells, such as those in the intestine, the centrosome is disassembled, however, in others, including the kidney epithelium, it may remain near the apical cell surface, with only a few MTs anchored to it, while the majority of MT minus ends are associated with lateral n-MTOCs (Mogensen, 1999). The release and capture model has been proposed to explain these cytoskeletal rearrangements (Fig.6; Mogensen et al., 1997; Mogensen, 2000; Mogensen et al., 2002; Mogensen, 2004; Moss et al., 2007), formulated from observations made in cochlear epithelial cells and other cells which prominently display apico-basal arrays (Mogensen et al.,

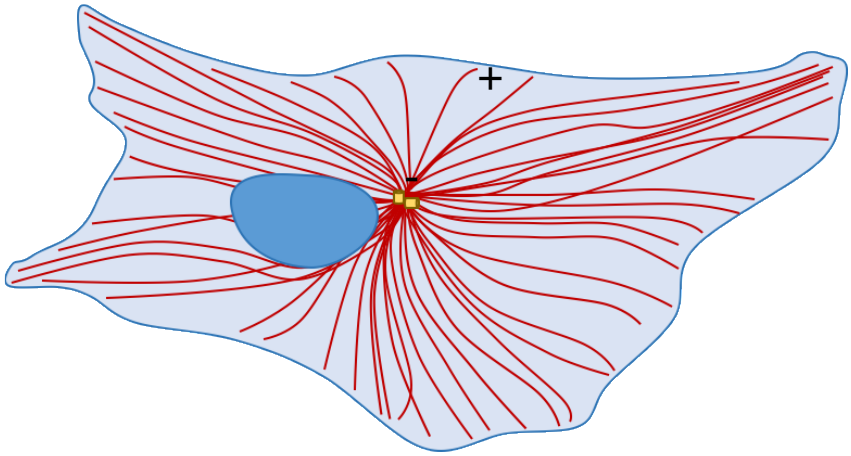

Undifferentiated Cell - Radial Array

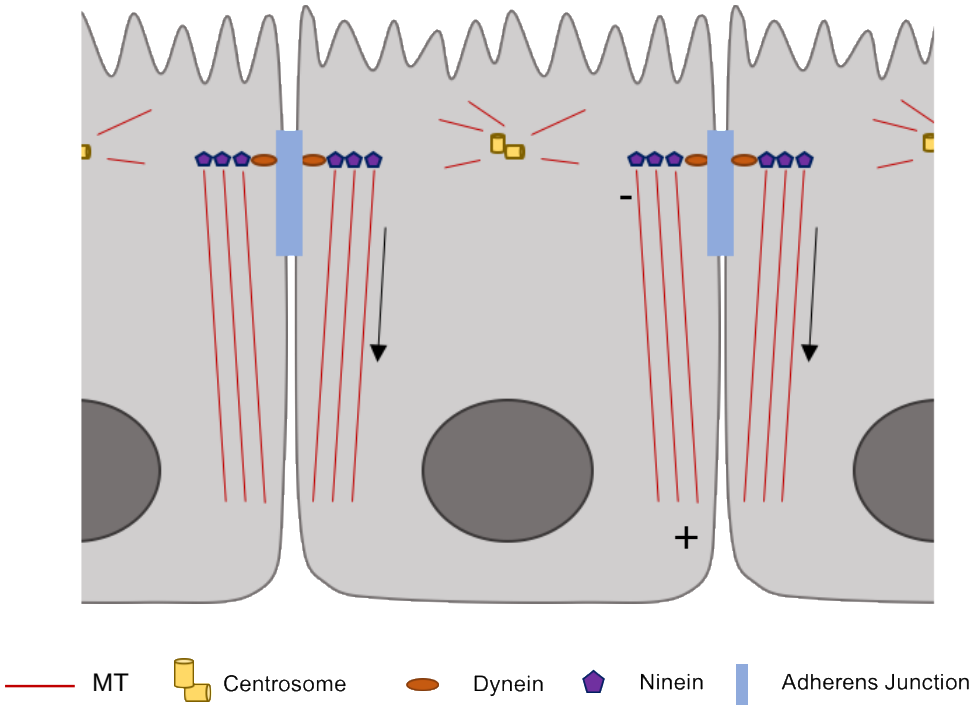

Differentiated Epithelial Cells - Apico-Basal Array

Figure 5 – Variation in microtubule arrays between undifferentiated cells and differentiated epithelial cells. Undifferentiated cells exhibit radial arrays, in which MTs extend from the centrosome, located near to the nucleus, towards the periphery of the cell. In differentiated epithelial sheets, in which cells have become polarised over the apico-basal axis, cells exhibit bundled MT arrays which span from the apical to the basal face of the cell, known as apico-basal arrays. These MTs are anchored at n-MTOCs on adherens juctions and bundled to add stability. Apico-basal arrays are integral to polarised cell function, for example in transport across epithelial sheets as in the gut. (Figure adapted from Bellett et al., 2009).

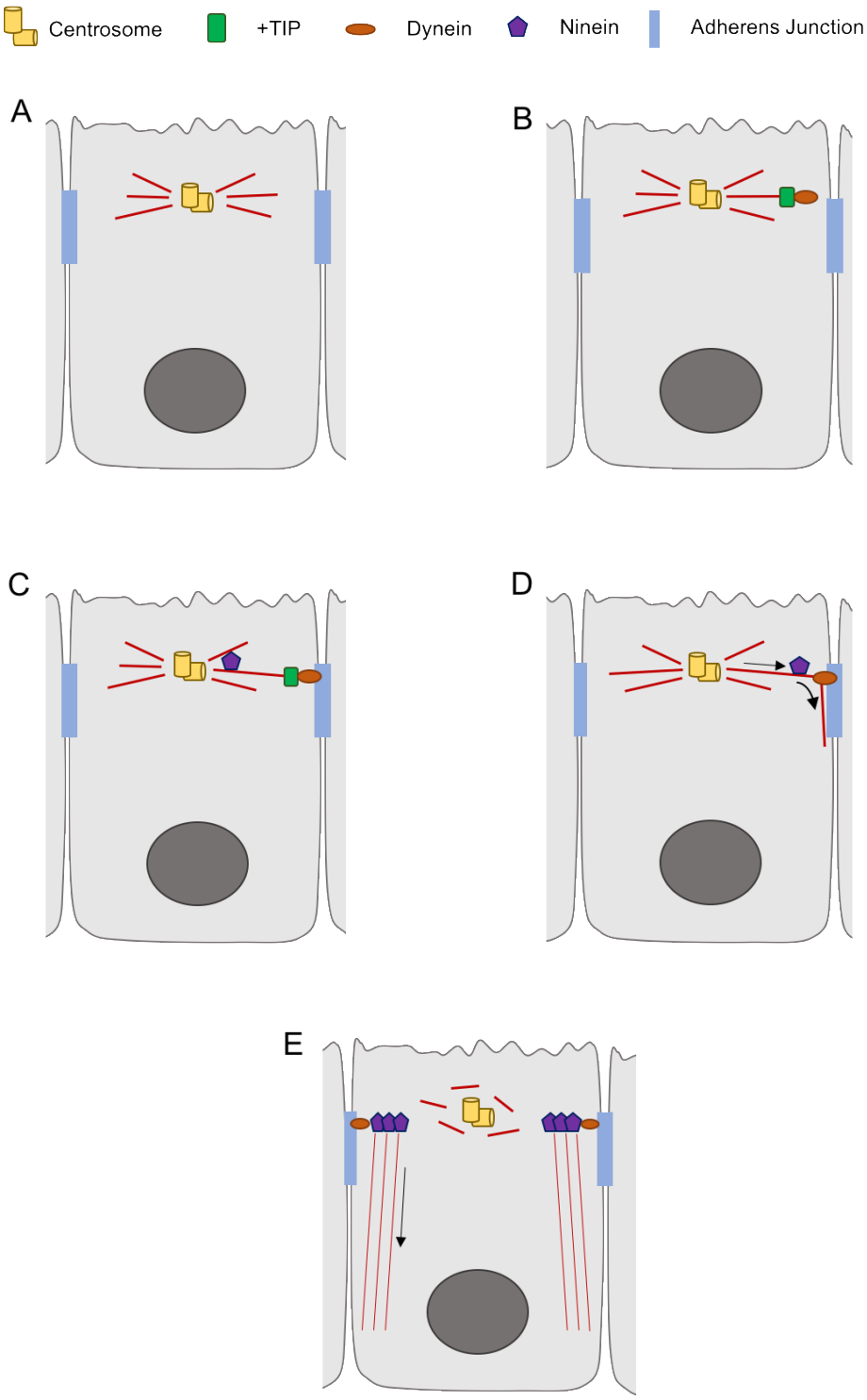

Figure 6 – The release and capture model of apico-basal array formation. In polarising cells the centrosome relocates to the apical surface and nucleates MTs in a radial manner (A). The plus-ends of these growing MTs are directed towards apically located adherens junctions and are captured by the motor protein dynein (B) which captures MTs at adherens junctions (C). Anchoring protein ninein is relocated from the centrosome to adherens junctions by travelling along adherens-captured MTs. Dynein translocates the growing MTs towards the basal surface (D) and exerts a force on the MT to break is attachment to the centrosome so the minus-end may be captured by the relocated ninein (E; Figure adapted from Bellett et al., 2009).

2000). Once nucleated at the centrosome, as part of a radial array, MT plus ends are targeted towards the cell cortex by +TIPs and anchored at junctional sites by the motor protein dynein. The minus end anchoring protein ninein is released from the centrosome and travels along MTs to adherens junctions where it co-localises with β-catenin (Moss et al., 2007, Goldspink et al., 2017). Dynein, in exerting force on the plus end, pulls captured MTs from their anchorage at the centrosome and begins to thread them towards the basal edge of the cell, allowing capture of the minus end by apical ninein, while the plus end extends basally. These apico-basal MTs are subsequently bundled to increase stability (Bellett et al., 2009).

1.6. Epithelial-to-Mesenchymal Transition, Migration and Cancer Progression

Cell migration is a fundamental, highly complex process involved in development, tissue repair and, when dysregulated, in cancer progression and other disease processes (Ridley et al., 2003). This complex process is orchestrated by both temporal and spatial regulation of multiple echelons of adhesion molecules, signalling proteins and cytoskeletal filaments. Crucial early stages of embryogenesis, such as gastrulation involve movement of cell layers, along with a number of later events throughout embryonic development where cells must migrate to the correct tissues and structures within the body (Aman and Piotrowski, 2010). In the adult cell migration holds important homeostatic roles including wound healing, where cells must close gaps in tissues, and immune responses, where leukocytes migrate to the site of infection or injury (Lauffenburger and Horwitz, 1996).

In the body, despite the presence of over 200 cell types, cells can be loosely grouped into either epithelial or mesenchymal phenotypes (Nakaya and Sheng, 2008; Lim and Thiery, 2012) Generally, there is very little cell migration where epithelial layers are concerned, and cells from epithelia-derived tumours must adopt

a motile fibroblastic, or mesenchymal, phenotype in order to invade out of the tumour into the surrounding ECM. This transient transdifferentiation process, arguably the tipping point for metastasis, is known as epithelial to mesenchymal transition (EMT; Carey et al., 2017). Its reverse process, mesenchymal to epithelial transition (MET) is undertaken by malignant cells once they have reached a distant site in the body in which to set up metastatic tumours and has been demonstrated as an essential process in the establishment of stable macrometastases (Ocana et al., 2012; Tsai et al., 2012). The precise mechanisms at play during the metastastatic cascade are still largely swathed by enigma (Chaffer and Weinberg, 2011), however it is widely regarded as the key differentiator between benign and malignant tumours, and could therefore be argued as the most important feature of cancers (Lazebnik 2010). Frequently, sheets, strings or clusters of cells begin to push into the ECM surrounding the tumour, with secretion of proteolytic enzymes at the invasive front carving a path into the tissue (Friedl et al., 2012). Additionally, certain single cells may break away from these collectively migrating groups and find their way into the blood or lymphatic vessels, providing access to distant bodily sites (Fig. 7; Chaffer and Weinberg, 2011). Once in these distant sites metastatic cells, termed micrometastases, may remain dormant and clinically silent for extended periods, following which, when conditions are right, tumour growth is resumed and a relapse occurs (Naumov et al., 2002). Single cells may employ either mesenchymal or amoeboid mechanisms of movement, and can switch between these if environmental or therapeutic stresses become inhibitory (Panková et al., 2010; Clark and Vignjevic, 2015). It is thought that only 0.01% of the millions of cells shed from a primary tumour are capable of completing the full metastatic cycle to yield macrometastases, indicating that it is a highly inefficient and stochastic process (Luzzi et al., 1998; Chambers et al., 2002).

There is a large influence of context on EMT, as it also plays important roles in fundamental developmental processes, during growth and differentiation of the embryo, and wound healing, where epithelial cells must acquire the ability to migrate

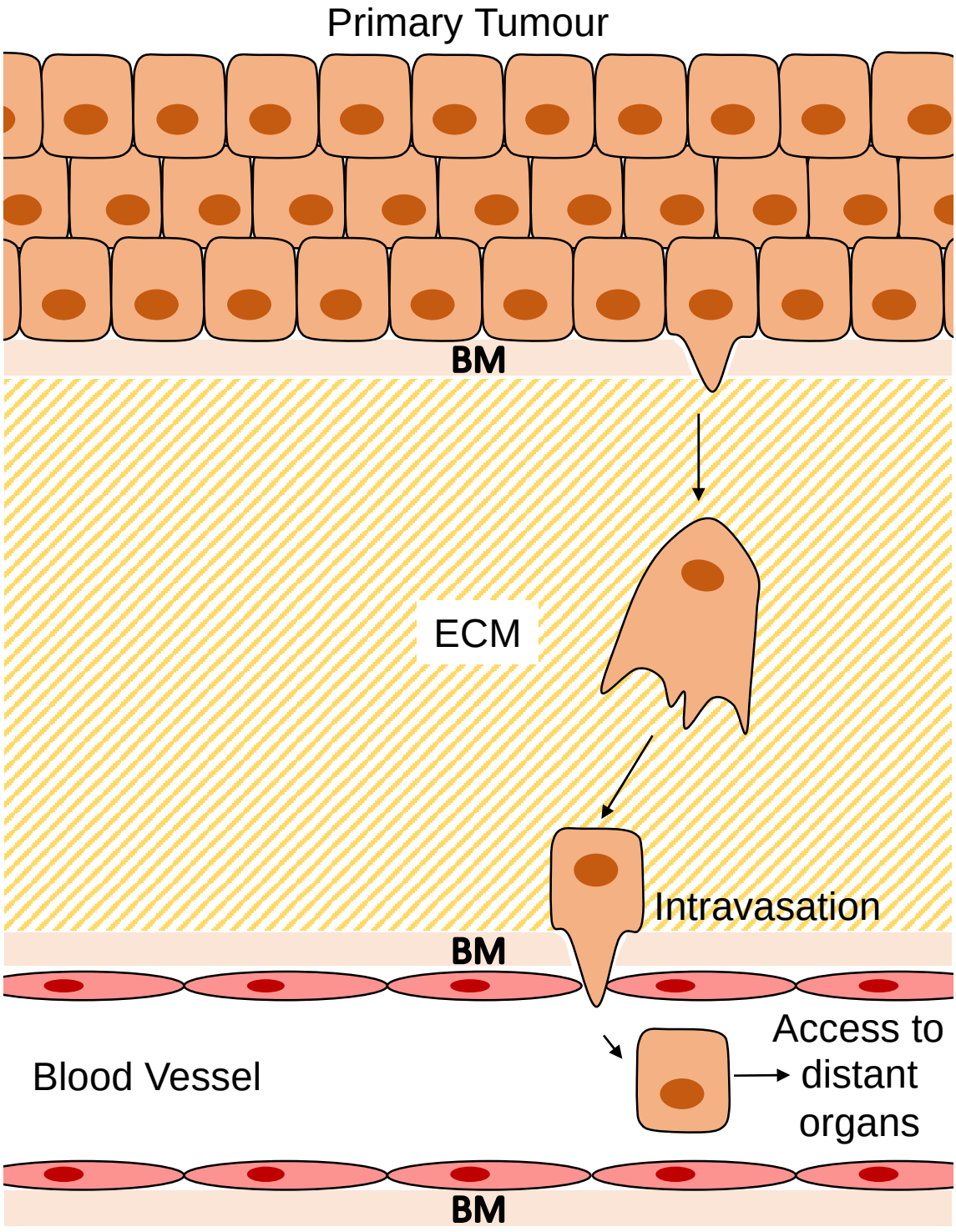

Figure 7 – The stages of cell invasion during metastasis. Cells from the primary tumour may undergo EMT and invade through the BM into the ECM surrounding the tumour. They move through the ECM and enter blood or lymphatic vessels via a process known as intravasation. Once in the circulatory system these metastatic cells potentially have access to distant sites in the body. Adapted from Bravo-Cordero et al., 2012.

and close the breach in the tissue. To reflect this, three classes of EMT have been defined, depending on the physiological context (Lamouille et al., 2014). EMT occurring in non-disease processes is tightly controlled and co-ordinated, however, in the case of EMT during tumour metastasis, the process becomes aggressive and unregulated (Singh et al., 2018). Despite this, in all contexts EMT involves the disassembly of cell-cell junctions, loss of apical-basal polarity, increased motility, and the ability to secrete proteolytic enzymes to degrade the ECM (Lamouille et al., 2014). EMT also involves multiple changes in gene expression and extensive reorganisation of the cytoskeleton, including actin, MTs and vimentin (Dinicola et al., 2016), which could potentially serve as targets for future therapeutics.

The switch in cell behaviour from an epithelial to mesenchymal phenotype is mediated by a number of key transcription factors, including Snail and Twist, which act to change expression programs in the epithelial cells to those resembling mesenchymal cells (Wang et al., 2016). These expression changes effect a number of genes, and act to alter cell adhesions and interactions with the ECM as well as promoting changes in cytoskeletal arrangement (Lamouille et al., 2014). Prominent among these expression changes, especially in terms of cancer progression, is the suppression of epithelial E-cadherin expression in favour of mesenchymal neural cadherin, which causes cells undergoing EMT to lose contact with their epithelial neighbours and form connections with mesenchymal cells through homotypic N-cadherin interactions (Yoshida et al., 2009; Lamouille et al., 2014). This dissolution of epithelial junctions consequently leads to a loss of apico-basal polarity, as key polarity proteins such as Scrib lose their ability to associate with the plasma membrane. Instead cells acquire a front-to-rear polarity which facilitates cell migration. Changes in IF composition also occur during EMT, with cytokeratins downregulated by Snail transcription factors while vimentin is upregulated. These changes are likely to increase cell motility via changes in the proteins being targeted to the plasma membrane, as keratin targets E-cadherin to the plasma membrane

while vimentin does not, and through interactions of vimentin with motor proteins (Lamouille et al., 2014).

The majority of knowledge pertaining to cell migration has come from studies of cells on 2D surfaces *in vitro*, perhaps giving a more simplistic view of migration than the true *in vitro* mechanisms, which involve cells having to negotiate a path through the ECM. However, a number of observations from 2D fibroblastic migration studies have been shown to also be relevant *in vivo*. In short, migration involves extension of a large actin-rich leading process, known as the lamellipodium, formation of new focal adhesions (FAs) at this frontal structure, contraction of the cell body and detachment of existing adhesions at the rear of the cell to avoid tearing (Fig. 8; Raftopoulou and Hall, 2004). Before moving a cell must become polarised, however, this is not the same form of molecular asymmetry as in polarised epithelial cells, although the Par6/Par3/aPKC complex is involved in both instances. As opposed to apico-basal polarity, migrating cells exhibit distinct front and rear polarity, with the former marked by the formation of the actin-rich protrusions lamellipodia and filopodia, which occurs under the direction of the small Rho GTPases Rac1 and Cdc42 (Ridley et al., 2003). Indeed, many aspects of migration are controlled and fine-tuned via the action of small GTPases (Fig. 8).

Small GTPases represent around 100 proteins in several subfamilies which possess intrinsic GTPase activity and play key roles in a number of cellular processes including cell migration and control of the cell cycle. Acting as molecular switches, GTPases are active when GTP-bound and inactive once this is hydrolysed to GDP. This hydrolysis may be carried out by relatively slow intrinsic activity of the GTPase, or by another set of proteins known as GTPase activating proteins (GAPs), which increase intrinsic GTPase activity by multiple orders of magnitude. Exchange of GDP for GTP is facilitated by guanine nucleotide exchange factors (GEFs), leading to restoration of the active state of GTPases (Caron, 2003). The most prominent group of these GTPases is the Ras family of proteins, which act to transduce signals

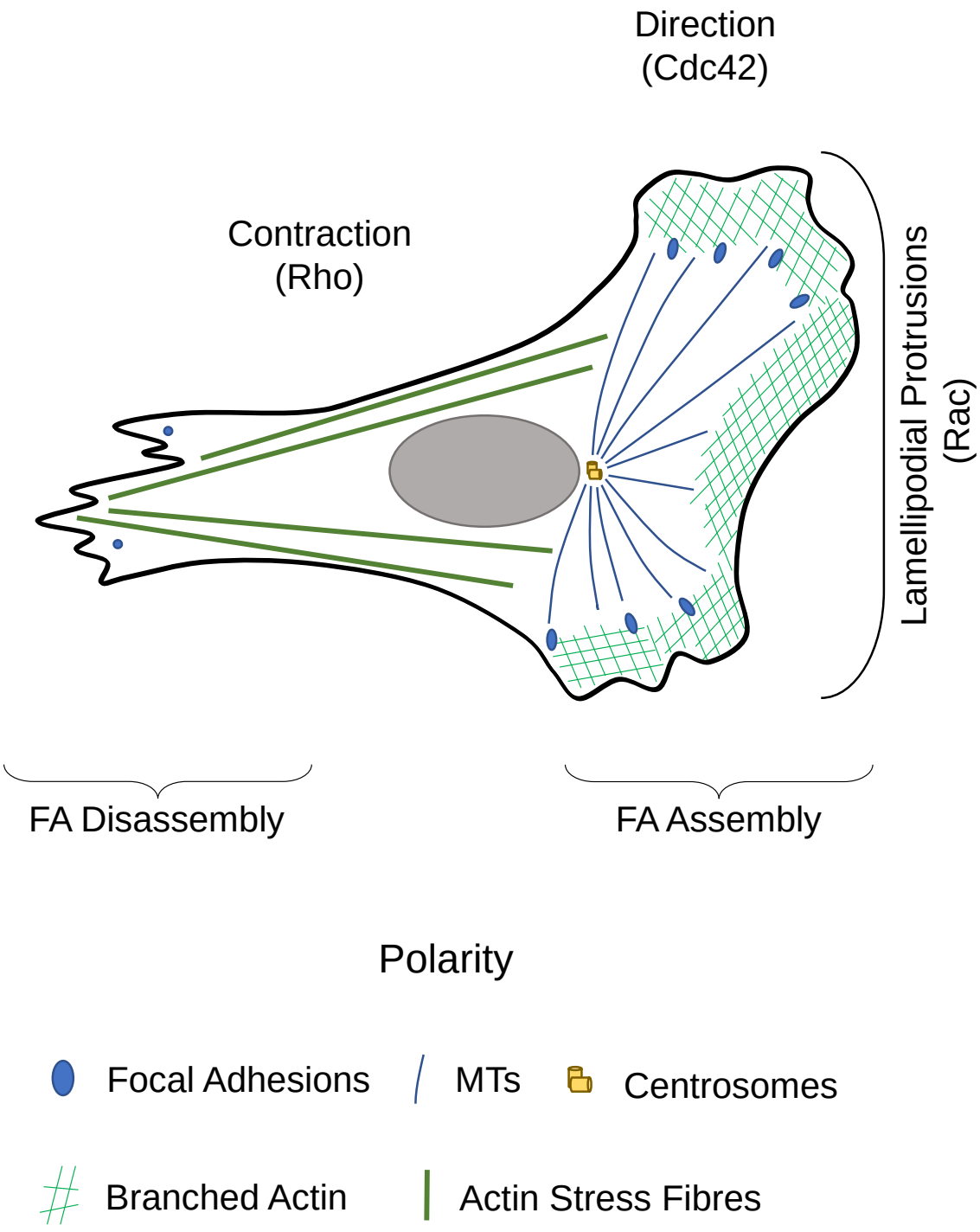

Figure 8 – Brief schematic overview of cell migration and the main GTPases involved. Lamellipodium formation from branched actin filaments at the leading edge of the cell, and indeed cell directionality, is dictated via the activity of Rac and Cdc42 GTPases. Just behind this leading edge new focal adhesions are assembled, allowing tension to be exerted on the ECM to pull the cell forward. Contraction of the cell body via actin stress fibres and myosin is orchestrated by Rho proteins, while microtubules are important in triggering disassembly of focal adhesions at the cell rear to avoid cell shearing. Adapted from Ridley et al., 2003.

from a number of receptors, such as receptor tyrosine kinases (RTKs), G protein-coupled receptors (GPCRs) and cytokine receptors, linking them to adhesion, proliferation and survival (Buday and Downward, 2008; Vigil et al., 2010). Humans possess three distinct Ras genes which encode four distinct proteins, namely H-Ras, N-ras and two K-ras isoforms (4A and 4B). Each of the membrane-localised Ras proteins exhibit differential localisation within the cell (Prior et al., 2003), likely due to disparity in the short hypervariable region, involved in membrane anchoring, upstream of the C-terminus of the protein, which leads to structural differences (ten Klooster and Hordijk, 2007). H- and N-ras are both localised at the plasma membrane and the Golgi, and can also be observed in lipid rafts, whereas K-ras localises predominantly to disordered regions of the plasma membrane (Hancock, 2003). In accordance with their subcellular compartmentalisation, alongside the structural differences and a variety of PTMs, Ras isoforms have different functions within the cell, and will partake in distinct cellular pathways (Shah et al., 2018). Mutations in small GTPases have been shown to be driving forces in a number of cancers, such mutations can render them constitutively active, removing the close regulation exerted on cellular processes such as differentiation, proliferation and migration (Alan and Lundquist, 2013). Not surprisingly, due to their pivotal roles in cell proliferation and adhesion, mutations in Ras genes are very common in the development and progression of cancers, with *RAS* being the most frequently mutated oncogene, detected in around 30% of human cancers (Stephen et al., 2014; Shah et al., 2018).

Another small GTPase within the 19-member Ras subfamily (Caron, 2003), known as Rap1, was initially identified, and dubbed K-rev, as an antagonist of Ras by its ability to normalise the phenotype observed in fibroblasts transformed with *KRAS* (Kitayama et al., 1989). This was later linked to competition for the Raf1 Ras target by Rap1 (Bos, 1998), with Rap1 binding to a Ras-binding region on Raf1 but not eliciting its activation (Cook et al., 1993; Takai et al., 2001). Predictably, constitutively active Rap1 mutants (such as RAP1V12) attenuate ERK activation through interference in the activation of c-Raf by Ras (Cook et al., 1993; Hu et al., 1997). There are in fact, two distinct Rap proteins, Rap1 and Rap2, which share only 60% sequence identity owing to large variations in their C-terminal regions (Takai et al., 2001), which potentially facilitate differences in localisation and activation (Caron, 2003). Each of these proteins consist of a pair of isoforms (Rap1A and Rap1B; Rap2A and Rap2B) which share 90-95% identity in their sequence, differing only by a few residues (Takai et al., 2001). The most is known about the functions of Rap1, while Rap2 remains more mysterious. Much like Ras, Rap1 proteins are activated in response to upstream signals from RTKs or GPCRs activated by cytokines or

chemokines (Bos et al., 2001; Shah et al., 2018). Both Ras and Rap proteins share a highly similar effector domain, along with the consensus sequences responsible for GTPase activity and interaction with GTP and GDP (Takai et al., 2001); however, they are resident within distinct activator and effector pathways, with Rap1 having a host of independent functions aside from its antagonistic interaction with Ras (Raaijmakers and Bos, 2001). Indeed, Rap1 is now recognised as a key regulator of multiple signalling pathways (Takai et al., 2001), along with many aspects of cell adhesion and motility (Bos, 2005), making it pertinent in cancer development and metastasis.

In tissues, including epithelia, cells adhere to both the ECM, through integrins, and to one another via cadherin-rich AJs, processes in which Rap1 has been shown to be involved (Boettner and Van Aelst, 2009). Recycling and affinity of integrins associated with the actin cytoskeleton has been shown to be under the regulation of Rap1 (Retta et al., 2006). This regulation may occur directly through spatial distribution or indirectly via modulation of cytoskeleton dynamics (Caron et al., 2003; Katagiri et al., 2003; Bos, 2005). Rap1 has been linked to the distribution of adherens junctions around the apical circumference of *Drosophila* epithelial cells, with Rap1 mutant cells displaying one-sided localisation of adherens junction components, suggesting that Rap1 is important for epithelial integrity and mobility (Knox and Brown, 2002). Alongside the regulation of stable adhesions, Rap1 has also been linked to the formation of early adhesions near the leading edge during cell migration, which lead to integrin clustering and the formation of focal adhesions against which force can be exerted during cell migration (Lagarrigue et al., 2015).

Direct mutations in the Rap1 protein are rarely reported in cancer (Gyan et al., 2005), in contrast to the prevalence of Ras mutations, however, increased and aberrant activation of Rap1 in human breast epithelial cells has been linked to development and progression of malignancies (Itoh et al., 2007). This may occur via transcriptional modulation or deletion of genes encoding the GEFs and GAPs which act specifically on Rap1. Regarding the project discussed here, modulation of the putative tumour suppressor gene (TSG) Rap1GAP, the principle GTPase activator

for Rap1, has been observed in multiple cancers including endometrial (Tamate et al., 2017) and pancreatic cancers (Zhang et al., 2006). Increased migration and invasiveness has been seen in human colon cancer cell lines when Rap1GAP is depleted (Tsygankova et al., 2013), and tumours exhibiting epigenetic silencing or loss of heterozygosity of the *RAP1GAP* gene are linked to increased metastatic dissemination and poorer prognoses (Mitra et al., 2008; Yang et al., 2017).

1.7. Development and Progression of Cancer

As a term, ‘cancer’, encompasses a group of around 200 distinct diseases, which may affect almost any area within the body of multicellular organisms (Gatenby et al., 2010). As a collective, cancers constitute the second leading cause of death worldwide, surpassed only by heart disease, however, this is predicted to change in the near future (Yancik, 2005). Despite being a collection of individual diseases, cancers share a kinship in their mode of pathogenesis, which is rooted in the accumulation of genetic mutations in single, or small groups, of cells within a specific organ or tissue which disconnect them from regulatory mechanisms (Hanahan and Weinberg, 2011). Mutated cells then proceed to grow outside of the normal homeostatic control that serves to regulate organ and tissue size, resulting in a large mass, known as a tumour, which may cause functional disruption within the organ or tissue concerned. Throughout their progression cancers become a self-fulfilling prophecy of mutations, gaining increasing numbers of abnormalities until, in the terminal stages of disease progression, cells from tumours invade into the surrounding tissue and spread to other organs and systems, in a process termed metastasis (Fimognari and Hrelia, 2007). This process, often linked to EMT processes described in the previous section, is associated with 90% of cancer mortality (Spano et al., 2012; Gandalovičová et al, 2017).

A major obstacle facing the quest to reduce cancer incidence and mortality is unpicking the wide range of underlying biological mechanisms, which are herculean

in their complexity, and therefore, despite an equally herculean effort, these processes are not yet fully resolved. However, as more mechanisms are unwoven an increasing number of targeted treatments are being designed to specifically kill cancer cells while leaving healthy cells unharmed via the disruption of disease-specific pathways or processes.

The cellular basis for cancer development was originally hypothesised in the early 20th century by Theodor Boveri, who was coincidentally the first to observe the centrosome as the master of chromosome segregation (Doxsey, 1998). Boveri hypothesised, in a monograph co-authored with, and posthumously translated by, his wife, and fellow biologist, Marcella O'Grady, that cancer arose from chromosomal abnormalities, as previously described by pathologist David von Hansemann, and uncontrolled cell divisions. Boveri proposed the existence of two sets of genes, one to elicit cell division, and another to prevent it in the absence of certain stimuli (Manchester, 1995), referred to as oncogenes and tumour suppressor gene (TSGs) respectively. The first specific examples of these genes were not identified until the latter part of the 20th century as the available experimental toolbox began to expand, countless others have since been identified. Largely, oncogenes are represented by genes intimately linked with stimulation of cell division, such as growth factors, however, in healthy cells these are known as proto-oncogenes (i.e. oncogenes that have not been activated). Conversely, TSGs encompass sets of regulatory genes which act to detect and deal with DNA damage and cellular stress, either by inciting repair of the damage, or initiating apoptosis if the issue cannot be resolved. During carcinogenesis, proto-oncogenes typically acquire 'activating' gain-of-function mutations, and the resulting oncogenes drive abnormal cell division. In order for aberrant division to proceed without being detected and halted by TSGs, the regulatory TSG genes must concurrently be subject to loss-of-function mutations, or undergo transcriptional silencing by epigenetic modification (Lee and Muller, 2010). A combination of these mutations, approximately four to six in humans, but

considerably fewer in mice, are required for full neoplastic transformation. This process of cancer development may occur over a long timescale of months and even years (Hahn and Weinberg, 2002). In some tissues there may be, in the majority of cases, a particular chain of common mutations which contribute to known carcinogenic sequences. An example of such a process can be found in the adenoma-carcinoma sequence of colorectal cancer development, in which non-malignant polyps progress to invasive carcinomas through a select set of genetic changes (Leslie et al, 2002). The huge variety of mutations which may contribute to the development of any given cancer, and the additional complexity provided by large amounts of genetic heterogeneity, not only between, but, within any given tumour, makes pinning down a single targeted treatment for all cancers highly unlikely. As a result, many current cancer chemotherapies largely involve broadly cytotoxic compounds which indiscriminately eradicate both cancerous and healthy cells.

1.8. Cancer and the Cytoskeleton

While genes encoding components of the cellular cytoskeleton, or their regulatory genes, are not commonly included in the initial mutations which serve to initiate and promote cancer development, it has been suggested that cytoskeletal and motility proteins acquire mutations in the later stages of tumour progression (Shah et al., 2012). However, in cancers occurring in the intestinal epithelium, a principle driving mutation is often the adenomatous polyposis coli (APC) gene, a key component in the Wnt signalling pathway which also stabilises apico-basal MTs. Germ-line mutations in APC occur in both genetically predisposed and sporadic colon cancer, eliminating its normal function in the Wnt pathway, leading to increased proliferation and affecting association of APC with MTs (Smith et al., 1994). As such, mutations in the actual cytoskeletal monomers themselves are uncommon, while mutations in proteins known to regulate their dynamics can be linked to progression in certain cancers. Regardless of mutations, MTs, and indeed the other two

cytoskeletal subsystems, are important in cell division and also in cell invasion, a process that is key in metastasis.

1.9. Phytochemicals in Cancer Prevention and Treatment

As mentioned earlier in the text, much of the current chemotherapeutic repertoire relies on broadly cytotoxic compounds, save for a limited number of emerging targeted therapies for certain cancer types. The progenitor of these cytotoxic cancer chemotherapies was nitrogen mustard, derived from mustard gas; a vesicant chemical weapon used in WWI and II (DeVita and Chu, 2008), however, when used as a therapy, any benefit of nitrogen mustard was limited by its high toxicity. Subsequent trials of compounds like the anti-folate methotrexate were met with slightly more success, and there are currently numerous cytotoxic compounds in use in the clinic, often in conjunction with both surgery and radiotherapy. Many of these agents exploit the rapid division of cancer cells in comparison with many healthy somatic cells, generally via production of reactive oxygen species (ROS), interference with cellular replication and induction of programmed cell death, apoptosis, or necrosis (Sak, 2012). On the surface, this appears to be a viable strategy, however, even within individual tumours cancers are highly heterogeneous, much like a varied animal population, and some cells within the tumour are not affected by the given chemotherapy agent, which acts much like an evolutionary selection pressure to select cells resistant to the therapy. These persisting cells often have an increased self-renewal capacity, much like stem cells, and have been linked to the expression of certain markers, leading them to be known as cancer stem cells (CSCs; Alison et al., 2012). Indeed, it is becoming increasingly evident that a number of cancers originate from mutations in existing stem cells, which may automatically determine stemness in tumour cells (López-Lázaro, 2018). These CSCs are thought to be able to survive treatment, despite the tumour as a whole being reduced, and persist in a dormant state for months or years after remission, inevitably re-emerging

and repopulating a more aggressive, heterogenous, drug-resistant, tumour (Harless and Qui, 2006), in a manner analogous to how epithelial stem cells may repopulate a tissue with multiple cell types following damage. Indeed, it has been shown that intensifying this selection process with more extensive chemotherapy produces increasingly aggressive relapses due to the selection of the most drug-resistant cell for future clonal expansion.

Using cytotoxic compounds which affect rapidly cycling cells inevitably causes some collateral damage to healthy cells in the body which undergo rapid division, such as those in the gut and hair follicles. This leads to prominent detrimental side effects which materialise as both acute symptoms and also chronic conditions that can impact the life of long term survivors (Sak, 2012). Current treatment methods also do not reliably inhibit the process of metastasis, and clinically evident metastatic disease is often incurable (Harless and Qui, 2006), despite many agents partially targeting the metastatic ability of cancer cells (Sak, 2012), leading to later relapse of disease. As such, a therapeutic compound which can specifically and reliably inhibit metastasis is highly desirable, if difficult to obtain due to differential responses of separate tumours and metastases (Thejass and Kuttan, 2006), and the use of multiple modes of migration by cancer cells (Gandalovičová et al, 2017).

A large amount of effort has been dedicated to unravelling the innumerable underpinning mechanisms driving the stepwise development and progression of cancers with the aim of finding more specific therapies which specifically eradicate cancer cells while ideally leaving healthy cells unharmed. This work has given rise to drugs like imatinib, a specific inhibitor of the BCR-ABL fusion kinase produced by initiating mutations in chronic myeloid leukaemia (CML) which dramatically increased survival rates and reduced the incidence of disease relapse in patients over a 60-month period (Druker et al., 2006). Such drugs, targeted to specific sites on proteins crucial to cancer progression, while being able to produce far superior responses to chemotherapy, are also subject to resistance and aggressive relapse, and, owing to

their highly specific nature, are often only effective on a small number of cancer subtypes. The ideal ‘magic bullet’, if a parallel may be drawn to anibiotics, would be a drug that could distinguish cancerous cells of all types from healthy cells by targeting some common mechanism, such as cell cycle dysregulation. Unfortunately, taking into account the diversity of cancers and their complex mechanisms of origin, the existence of such a ‘magic bullet’ seems relatively unlikely, nonetheless certain compounds from plants have displayed toxicity towards cancer cells *in vitro*, and epidemiological studies have also linked these compounds to a reduction in incidence of many cancers.

Throughout history plants and other natural products have yielded medicinal compounds, and many modern medicines, such as aspirin, are derived from natural plant products (Schmidt et al., 2008). To date the large repertoire of biologically active compounds produced by plants, known as phytochemicals, has yet to be fully explored, and research into their medical potential is ongoing. One such group under investigation are the isothiocyanates (ITCs), sulphur-containing compounds generated by enzymatic processing of secondary metabolites known as glucosinolates (Guo et al., 2014). These ITCs are characterised by their –N=C=S group, the central carbon of which is highly electrophilic, that mediates the biological effects of SFN by reacting with nucleophilic targets in the cell (Zhang, 2004). This project will primarily focus on one member, SFN (1-isothiocyanato-(4R)-(methylsulfinyl) butane), which is derived in considerable amounts from cruciferous vegetables within the *Brassicaceae* family, such as broccoli, brussels sprouts and cabbage, and in certain salad crops, including watercress and rocket. In recent years, epidemiological studies indicating that diets rich in crucifers are associated with a protective effect against cancers, including gastrointestinal cancers (Clarke et al., 2008), have led to SFN attracting considerable attention as a potential anti-cancer compound.

1.10. Sulforaphane as a Future Cancer Therapy

Plants generate a number of secondary metabolites, and in recent years a number of these have been investigated for their effect on cancer cells. Glucosinolates are one such group of secondary metabolites that have attracted a level of interest. Hydrolysis of glucosinolates leads to the generation of SFN, and indeed other ITCs; a process which is mediated by myrosinase (thioglucoside glucohydrolase) enzymes (Andréasson et al., 2001; Rangkadilok et al., 2002). Glucosinolates accumulate in plant cells where they are generally segregated from myrosinase enzymes on an intracellular level, within vacuoles, or on an intercellular level where enzyme and substrate are present in different cell types (Koroleva et al., 2010). Myrosinase enzymes and their glucosinolate subtrates become mixed in the event of plant tissue damage, through chewing or cooking (Vaughn and Berhow, 2005), or through a transport mechanism (Andréasson et al., 2001). This glucosinolate-myrosinase system most likely evolved as a defence by plants against insects, to which nitriles and ITCs are toxic, and possibly certain pathogens (Rask et al., 2000). A number of ITCs generated by this system, such as SFN have been found to hold beneficial bioactivities, yet others, such as SFN-nitrile are seemingly inactive (Basten et al., 2002).

Glucosinolate molecules consist of two moieties, a common glycone element along with a variable amino-acid derived aglycone side chain, the latter of which is most important in determination of the properties of the ITCs generated (Juge et al., 2007). Over 120 distinct glucosinolates have been identified across sixteen families of dicotyledonous angiosperms (Fahey et al., 2001), however, not all of these glucosinolates occur in edible plants, and even less are present in considerable amounts in cruciferous vegetables (Fahey et al., 2001; Juge et al. 2007). One glucosinolate present in relatively high quantities in cruciferous vegetables is glucoraphanin (4-methylsulfinylbutyl glucosinolate), the specific precursor of SFN. In broccoli, glucoraphanin accounts for over 50% of the total glucosinolate content

(Brown et al., 2002; Martinez-Villaluenga et al., 2010), hence why broccoli alone has been linked to dietary reduction of cancer risk, in addition to diets rich in crucifers as a whole. Once these plants are cooked and consumed, the myrosinase and glucoraphanin are mixed to produce sulforaphane (Fig.9), which is rapidly absorbed by cells of the gut where it is conjugated to glutathione (GSH) by glutathione transferases. Residual glucoraphanin present in the plant that was not hydrolysed as a result of cooking or chewing, or indeed was not converted due to heat induced denaturation of myrosinase, may still be converted into bioavailable SFN by certain species in the microbiota which express their own endogenous myrosinases (Juge et al., 2007). However, these myrosinases expressed by the human microflora are not as effective at hydrolysing glucosinolates as plant myrosinases, and if the latter are inactivated by too much heat during cooking then significantly less ITCs will be produced, as determined by measurement of ITC metabolites in urine (Getahun et al., 1999; Zhang, 2004).

From molecular studies, it has been indicated that sulforaphane can target cancers at each stage of their development, from initiation through promotion to progression and metastasis. Sulforaphane was primarily identified as a suppressor of tumour initiation in the late 1980s due to its induction of phase 2 enzymes, including NAD(P)H:quinone oxidoreductase (NQO1) and glutathione S-transferase in the Hepa 1c1c7 murine hepatoma cell line (Prochaska and Santamaria, 1988; Zhang and Tang, 2007). Phase 2 enzymes act to protect cells against cancer by detoxifying carcinogens and enabling their removal from the body (Clarke et al., 2008). Additionally, it has been shown that sulforaphane modulates Phase 1 enzymes, including selected cytochrome P-450 (CYP) enzymes which may activate certain pro-carcinogens via processing of exogenous and endogenous compounds (Zhang and Tang, 2007). A commonality to phase 2 genes, and many other genes involved in protection of cells against environmental stressors, is the presence of one or more cis-acting antioxidant response elements (AREs) in their 5’ flanking regions,

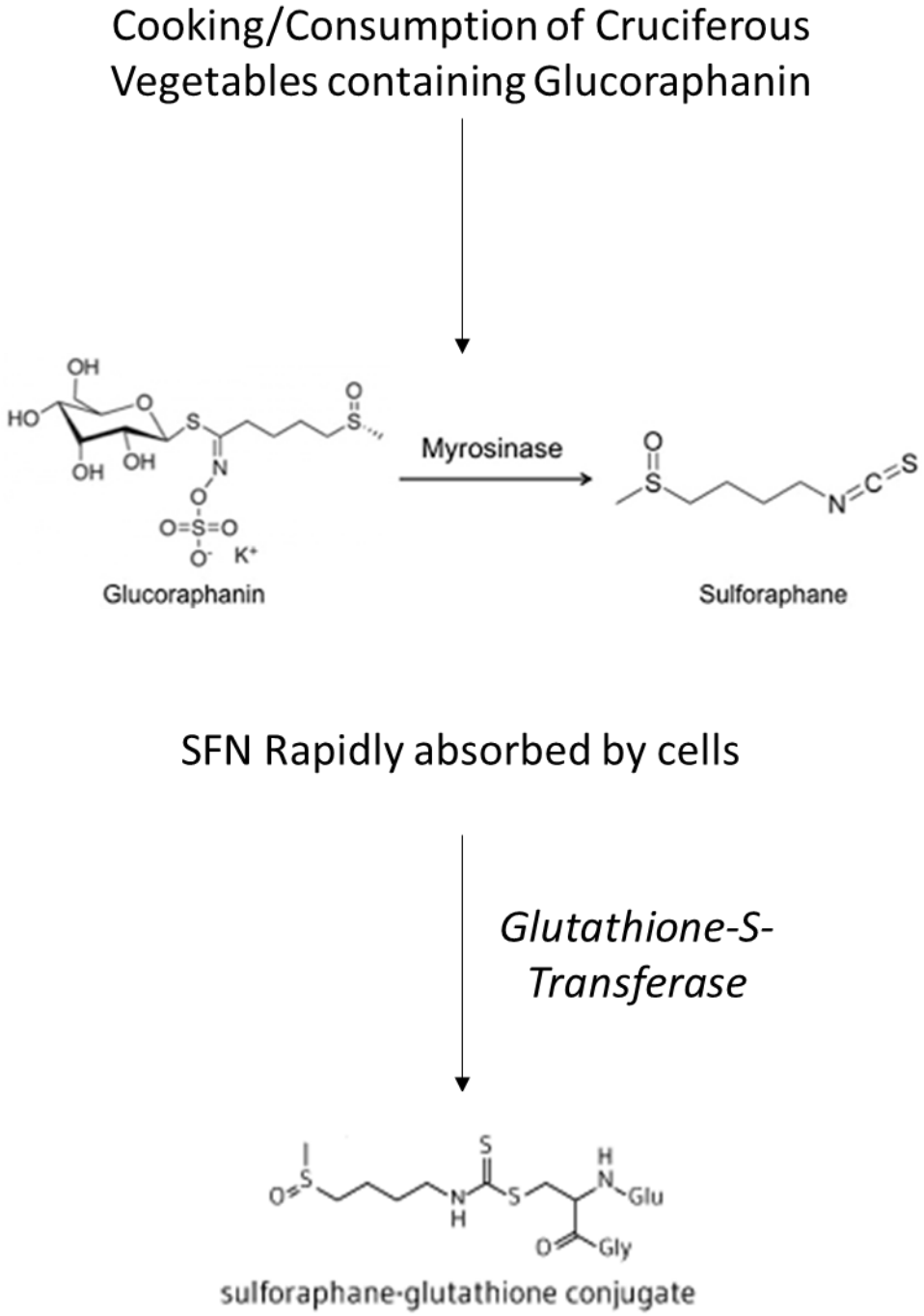

Figure 9 – SFN is produced from a glucoraphanin precursor by myrosinase enzymes. When plant cells are cooked or broken open by chewing, myrosinase enzymes are mixed with the glucoraphanin glucosinolates within the cells, where they convert this precursor into SFN. In the gut this is readily absorbed by cells before most of it is conjugated to glutathione within the cell by glutathione-S-transferase. Adapted from Juge et al., 2007

which can orchestrate coordinated induction of these genes via nuclear factor erythroid 2-related factor 2 (Nrf2), the key ARE activator (Zhang and Tang, 2007). Normally, Nrf2 is bound to Kelch-like ECH-associated protein 1 (Keap1) in the cytoplasm and targeted for proteosomal degradation, however, in response to an inducer, or in the presence of SFN which may modify of key cysteine residues within Keap1 (Dinkova-Kostova et al., 2017), Nrf2 is released and translocates to the nucleus where it activates genes possessing AREs (Zhang and Tang, 2007). Antioxidant activity of sulforaphane has also been linked to protection of the lens against H_2O_2-induced cataract formation (Liu et al., 2013), improved outcomes following cerebral (Yu et al., 2017) and myocardial reperfusion injury (Yunpeng et al., 2016) and in attenuation of cerebral vasospasm following subarachnoid haemorrhage (Zhao et al., 2016).

Following acquisition of an initiating mutation, aberrant activation or inactivation of genes involved in differentiation, apoptosis and the cell cycle occurs to allow initiated cells to survive and proliferate, a process termed tumour promotion. Research has shown that SFN can supress promoting events and remove initiated cells from a tissue in a dose and cell-type-dependent manner (Clarke et al., 2008). A marked effect of SFN is cell cycle arrest (Singh et al., 2004), generally at G_2/M, which has been shown to be transient after short (6hr) periods of exposure and irreversible following longer periods (>12hr) in colon cancer cells possessing wild-type p53 (Pappa et al., 2007). Arrest at G_1 (Shen et al., 2006) and G_1/S (Chiao et al., 2002; Wang et al., 2004b) has also been observed following SFN treatment. Relatively high doses of SFN have also been shown to have pro-apoptotic activity towards both pre-malignant and malignant cells (Fig.10). This effect was first reported in colon cancer cells at 15 and 50μM SFN concentrations (Gamet-Payrastre et al, 1998; Gamet-Payrastre et al., 2000; Pledgie-Tracy et al., 2007), and has been linked to concomitant activation of multiple pro-apoptotic pathways, including ROS generation, DNA-damage response and caspase-2-JNK pathways (Rudolf et al., 2009). In

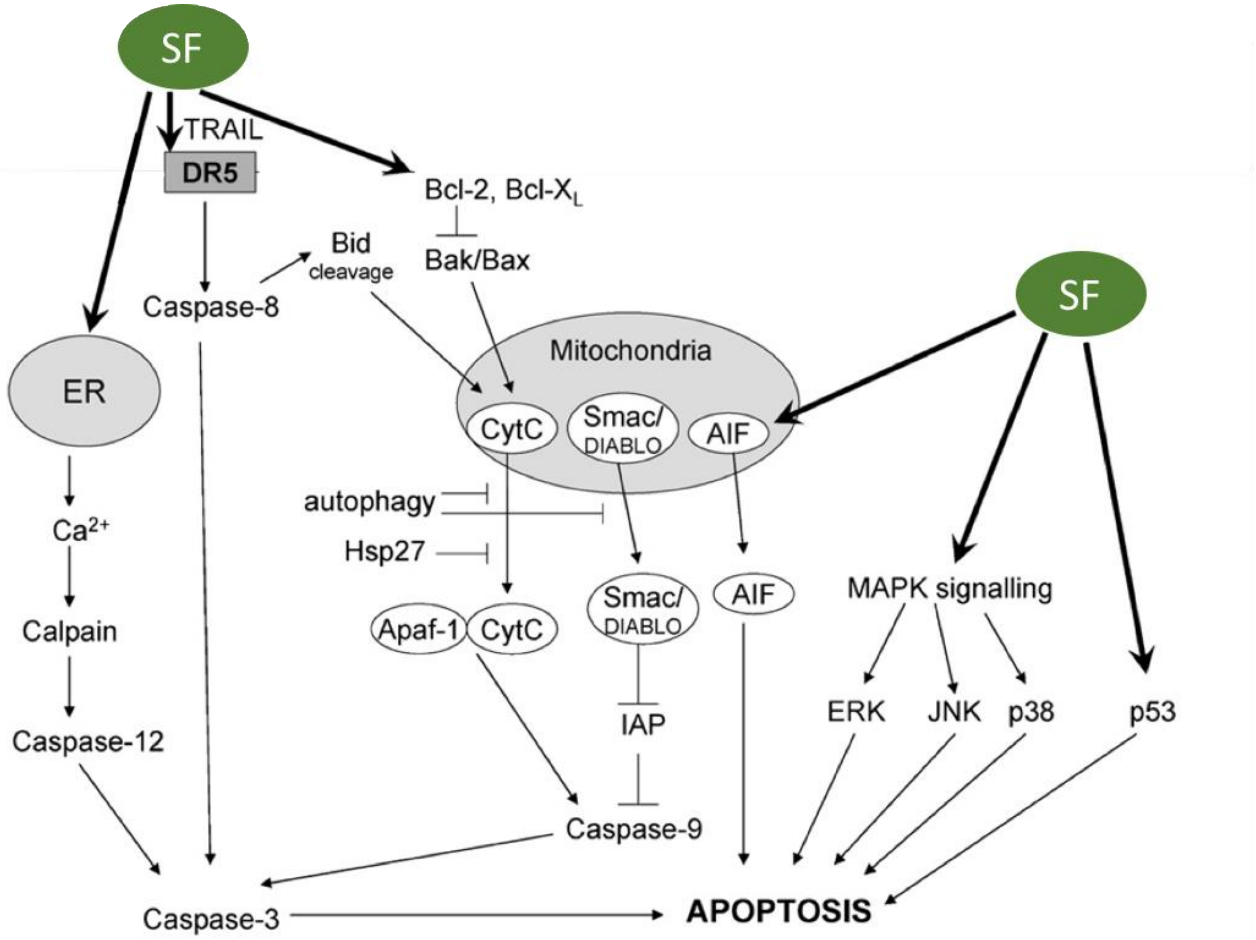

Figure 10 – The multiple targets of SFN on both intrinsic and extrinsic pathways within the cell to induce apoptosis. The apoptotic components shown in this schematic have all been highlighted as having altered expression or shown increased activation/inactivation following SFN treatment. Evidence has suggested that SFN may act to initiate multiple modes of apoptosis simultaneously. Adapted from Juge et al., 2007.

addition, inhibition of NF-κB by SFN (Moon et al., 2009) leads to suppression of prosurvival signals, tipping the balance of signalling in the cell towards apoptosis. It has also been suggested that sulforaphane can supress angiogenesis *in vitro* and *in vivo*, a process vital in the harnessing of a blood supply by developing tumours (Jackson et al., 2007).

A large-scale trial of SFN has yet to be published, however, smaller clinical studies have indicated that oral doses of 200μM SFN are detectable in healthy breast tissue at concentrations or around 2pM/mg of tissue within 2hr of ingestion, with blood plasma concentrations reaching almost 100μM (Cornblatt et al., 2007). Nonetheless, a number of *in vivo* preclinical evaluations of SFN have been performed in mice using both chemical and genetic models of cancer development. For example, 7,12-dimethylbenz[a]anthracene (DMBA)-induced mammary tumour (Zhang et al., 1994) and benzo[a]pyrene induced forestomach tumour formation (Fahey et al., 2002) was inhibited by SFN in rodent models. In addition, polyp formation in ApcMin/+ mice, predisposed to formation of adenomas, was reduced following dietary supplementation of SFN (Hu et al., 2006). Combination of *in vivo* and *in vitro* data yields heavy indication that SFN is a potential chemopreventive and chemotherapeutic agent. However, there are still unknown molecular effects of SFN, particularly effects on the MT cytoskeleton, and this project, using *in vitro* cell models aims to contribute to this field of knowledge with the aim of progressing the journey of SFN towards clinical use. SFN has also shown potential as a therapeutic compound in diseases characterised by mutated protein aggregation, such as Huntington's (Brokowska et al., 2016) and prion diseases (Lee et al., 2014), where it may reduce aggregated protein levels, potentially via autophagy induction.

Despite a large volume of literature focusing on SFN, relatively little of this has focused on the MT cytoskeleton, with a select number of publications indicating that SFN disrupts dynamic instability and inhibits MT polymerisation (Jackson and

Singletary, 2004; Jackson et al., 2007; Azarenko et al., 2008) and inhibits the MT-specific deacetylase HDAC6 (Hubbert et al., 2002; Myzak et al., 2006; Gibbs et al., 2009). To date a comprehensive exploration of the effects of SFN on MTs and associated proteins is yet to be conducted. The proposed project aims to provide a more detailed picture of the effect of SFN on MT composition, dynamics and associated proteins, with the hypothesis that SFN can stabilise MTs in cells and through this exert anti-cancer effects on cell polarity and migration.

Chapter Two

Materials and methods

2.1. Cell culture

To determine if any effects of SFN were common to all epithelial cells, or specific to certain tissue types, a range of immortalised epithelial cell lines were selected for experiments, including those representing carcinoma of the breast (MCF-7, MDA-MB-231), pancreas (Panc-1) and colon (TC7; details in Table 1). Non-tumorigenic ARPE-19 cells were also used for investigations against a non-cancerous background, as these cells are derived from healthy retinas. Cell lines were cultured in 75cm^2 cell culture flasks (T75; Nunc) in high glucose Dulbecco's modified eagle medium (DMEM, Gibco) supplemented with 10% foetal bovine serum (FBS), 1% L-glutamine, 100U/ml Penicillin and 0.1mg/ml streptomycin (subsequently referred to as complete medium). Cells were incubated at 37°C in a humid atmosphere consisting of 95% air and 5% CO_2.

Cells were thawed from frozen seeds into 25cm^2 flasks (T25; Nunc) and allowed to settle and proliferate for 1-3 days before being moved to T75 flasks and passaged twice a week. Prior to passaging, reagents were pre-warmed in a 37°C water bath for 30min. Firstly, old culture medium was aspirated and discarded before the cell monolayer was briefly washed with 2ml 0.25% Trypsin/0.02% Ethylenediaminetetraacetic acid (EDTA; Gibco). Cells were subsequently detached from the flask base through the addition of 3ml fresh Trypsin/EDTA and incubation for 5-10min until all cells had detached. Trypsin was neutralised by adding an equal volume of complete medium and this mixture was repeatedly aspirated in the flask to obtain a single-cell suspension. The cell suspension was then centrifuged at 1000RPM for 5min to obtain a loose cell pellet. The supernatant was discarded before cells were resuspended in fresh medium and diluted into a total of 10ml in sterile T75 flasks at a ratio appropriate to allow cells to reach 80-90% confluency prior to the next passage. In between passages culture medium was changed every 2-3 days. To avoid confounding phenotypic changes, thawed seeds were not maintained in culture for more than 3 months, at which point they were discarded and another low passage stock was removed from the freezer.

2.2. Cell Seeding

For immunolabelling experiments cells were seeded onto glass coverslips (VWR International), that had been sterilised at 180°C for 4hr prior to use, in 3cm plastic petri dishes and incubated for at least 24hr prior to use in immunofluorescence procedures. Flat bottom plastic multiwell plates (Nunc) were used for scratch wound (24-well) and viability assays (96-well).

Table 1 – Cell line details and medium requirements of immortalised *Homo sapien* cancer cell lines from breast, pancreas and colon origin.

Cell Line	Species	Tissue of Origin	Medium	Source
ARPE-19	*Homo sapien*	Retina	DMEM/F-12 nutrient mixture 10% FBS 1% L-Glutamine 100U/ml Penicillin 0.1mg/ml streptomycin 0.1% Gentamycin	American Type Culture Collection
Caco2/TC7	*Homo sapien*	Colon adenocarcinoma	DMEM High Glucose 10% FBS 1% L-Glutamine 100U/ml Penicillin 0.1mg/ml streptomycin	Gift from Dr M. Winterbone, Institute of Food Research, Norwich Research Park, NR4 7UG
Capan-1	*Homo sapien*	Pancreas (metastatic site from liver cancer)	DMEM High Glucose 10% FBS 1% L-Glutamine 100U/ml Penicillin 0.1mg/ml streptomycin	American Type Culture Collection
MCF-7	*Homo sapien*	Breast	DMEM High Glucose 10% FBS 1% L-Glutamine 100U/ml Penicillin 0.1mg/ml streptomycin	American Type Culture Collection
MDA-MB-231	*Homo sapien*	Breast	DMEM High Glucose 10% FBS 1% L-Glutamine 100U/ml Penicillin 0.1mg/ml streptomycin	American Type Culture Collection
Panc-1 (Clone 3)	*Homo sapien*	Pancreas	DMEM High Glucose 10% FBS 1% L-Glutamine 100U/ml Penicillin 0.1mg/ml streptomycin	High EB2 expressing clone isolated by J. Gadsby

In preparation for seeding cells were trypsinised, pelleted and resuspended in complete medium (as described in 3.1.) before being counted using a haemocytometer and seeded according to requirements on an experimental basis.

2.3. Sulforaphane Treatment of Cells

High purity R,S-Sulforaphane (LKT Labs) was diluted upon receipt in 1.41ml Dimethyl Sulfoxide (DMSO) to give a 100mM stock solution which was stored as 10μl aliquots at -20°C. Seeded cells were allowed to adhere to the culture surface before the medium was removed and replaced with complete medium containing SFN at known concentrations. The DMSO concentration was maintained at 0.05% in each condition by dilution of the 100mM SFN stock into working stocks, of which 0.5μl was added per ml of medium (Table 2). Alongside these sulforaphane treatments both untreated and DMSO vehicle controls (0.5μl DMSO/ml) were performed. Cells were incubated with sulforaphane for 24 or 48hr before analysis.

Table 2 – Details of dilutions of 100mM R,S-Sulforaphane in DMSO for addition to cell culture medium.

Working Stock	100mM Stock	DMSO	Total Volume	Final Concentration
4mM	0.4μl	9.6μl	10μl	2μM
10mM	1μl	9μl	10μl	5μM
20mM	2μl	8μl	10μl	10μM
30mM	3μl	7μl	10μl	15μM
40mM	4μl	6μl	10μl	20μM
60mM	6μl	4μl	10μl	20μM

2.4. Immunolabelling of 2D Monolayer Cultures

For immunolabelling experiments, cells were seeded (as described in 2.2.) at concentrations of between 1 $x10^3$ and 1.5 $x10^5$ depending on the required confluency. Once ready for labelling, cells were removed from the incubator, medium was discarded and cells were fixed with ice cold -20°C methanol in the freezer at -20°C for 5min. Once fixed, the methanol was discarded and cells were briefly washed 3 times with phosphate buffered saline (PBS) substituted with 1% goat serum (GS). Cells were then incubated for 30min at RT in a blocking solution of PBS 10% GS. Glass coverslips were then placed cell side down onto 48μl primary antibody diluted in PBS 1% GS (dilutions shown in Table 3) and incubated at RT for 1hr under an opaque cover.

Coverslips then underwent 6 5min washes in PBS 1% GS before being placed onto 48μl aliquots of secondary antibody (Table 4), again cell side down, and incubated at RT under an opaque cover for 30min.

Table 3 – Primary antibodies used in immunolabelling procedures. Including details of manufacturers, species and dilution used.

Target	Species	Dilution	Manufacturer
α-Tubulin	Rabbit	1:100	Abcam
Acetylated Tubulin	Mouse	1:200	Sigma
Actin	Mouse	1:200	Abcam
EB1	Mouse	1:500	BD
EB2	Rat		Abcam
Rap1GAP	Rabbit	1:250	Abcam
Rap1GAP	Mouse	1:250	Santa Cruz
YL1/2 (tubulin)	Rat	1:150	Thermo

Table 4 – Secondary antibodies used in immunolabelling procedures, including details of fluorophores, manufacturer and dilution.

Target Species	Species	Dilution	Fluorophore
Mouse	Goat	1:1000	Alexa 488
Rabbit	Goat	1:1000	Alexa 488
Rabbit	Goat	1:1000	Alexa 647
Rat	Goat	1:1000	Alexa 488
Rat	Goat	1:1000	Alexa 647

Following this, cells were washed once in PBS 1% GS for 10min before nuclei were stained using a 1:1000 solution of 4',6-diamidino-2-phenylindole (DAPI) diluted in PBS for 10min. Following a two further 10min washes in PBS coverslips were mounted in hydromount cell side up on microscope slides with a coverslip on top. After allowing 24hr for the hydromount to set cells were imaged using a Zeiss Axioplan 2ie widefield microscope at x20 and x63 with auto exposure.

When using Phalloidin conjugated to Alexa Fluor488 to label for actin a PHEMO fix was used, as this paraformaldehyde-based fixation method creates cross-links between proteins and preserves actin filaments. Firstly, the ingredients for 2X PHEMO buffer (Table 5) were mixed in 30ml ddH_2O, with 10M KOH added until the solution was clear. The buffer was then adjusted to pH 6.9 and 10ml was

retained to make PHEMO fix (Table 6). The remaining buffer was made into a 1X solution by adding 32ml ddH_2O and 8ml DMSO. PHEMO fix was made by adding 10ml dissolved 4% paraformaldehyde (PFA; with two drops of 10M NaOH added to encourage PFA into solution at 70°C) with 10ml PHEMO buffer before adding the remaining ingredients in Table 6. Both solutions were kept in a 37°C water bath until use. When cells were ready to be fixed they were washed with PBS pre-warmed to 37°C before being fixed with PHEMO fix solution for 10min at 37°C. Cell layers then underwent two 10min washes with PHEMO buffer solution before being washed with PBS for 5min at RT. Cells were then taken through the standard immunolabelling procedure from the 10% GS block stage as detailed above.

Table 5 – Ingredients for 2X PHEMO Buffer

Concentration	Ingredient	Formula Weight	Final Amount
68mM	PIPES	302.4	2.056g
25mM	HEPES	238.3	0.596g
15mM	EGTA	380.4	0.571g
3mM	$MgCl_2$	95.2	0.029g

Table 6 – Composition of PHEMO fix solution

Concentration	Ingredient	Final Amount
3.7%	Paraformaldehyde	0.74g
0.05%	Glutaldehyde	40μl
0.5%	Triton x100	100μl

2.5. Viability Assays

To assess any reduction in cell viability caused by sulforaphane cells were plated in triplicate for each condition at a density of $1x10^4$ cells/well in a flat-bottomed 96 well plate and left to settle for 24hr. Following this time complete medium containing the relevant concentrations of DMSO or SFN (5, 10, 20 and 30μM) was added and cells were incubated with SFN for 24hr. PrestoBlue® Cell Viability Reagent (Invitrogen) was diluted 1:10 in complete medium as per manufacturer's instructions and absorbance was read at both 570 and 600nm after 1 and 2hr.

Following this the 600nm values were subtracted from the 570nm values and statistical significance was assessed via one-way ANOVA ($P<0.05$).

2.6. Scratch Wound Assays

Epithelial cell lines, MDCKII and Panc-1, were trypsinised and diluted to $1x10^6$ cells/ml before 70μl of this cell suspension was seeded into each side of a 2 Well silicone culture insert (Ibidi) placed into the wells of a 24-well plate. Cells were incubated for 24-48 hours to reach confluency before the insert was removed, to leave a neat cell free space between two patches of confluent cells. Cells were then briefly washed with pre-warmed DMEM before being dosed with DMEM containing set doses of SFN. Plates were then placed in an incubator linked to a Zeiss Axiovert widefield microscope, allowed to acclimatise for 30min to prevent loss of focus, and automatically imaged at set positions in each well for 16hr. Brightfield images were captured using a 5X objective every 2min for the first hour and every 20min for the remaining 15hr. The cell-free area in each condition was manually measured using ImageJ and calculated as a percentage of closure over time. One-way ANOVA analysis of average percentage closure was performed to determine statistical differences between control and treated conditions. To obtain data on individual cell velocities and distances the manual tracking plugin on ImageJ was used to track 16 cells from each condition in Panc-1 assays (8 cells from each of two separate experiments) and 3 cells from each treatment of MDCKII cells. Statistical significances between the mean measurements for each condition were assessed using two-tailed t-tests assuming unequal variance.

In a variation of this assay, cells were seeded and grown to confluence as described above before cell division was blocked via addition of 2mM Thymidine for 17hr, which would remove much of the effects of cell division from the wound closure. Wounds were then made with a pipette tip, and cell layers were dosed with SFN along with 2mM Thymidine to maintain the block and imaged at intervals as previously discussed.

2.7. Scratch Wound Immunolabelling

Further to the time-lapse images of scratch wounds, fixed, immunolabelled scratch wounds were also employed to assess the localisation of proteins at the scratch frontier. Cells were seeded onto glass coverslips and allowed to grow to confluency. A scratch was then made manually in the layer using a P200 pipette tip before loose cells were rinsed off through two brief DMEM washes. Media containing

doses of SFN equivalent to the time lapse experiments was then added over the coverslips. These were then incubated for 17hr to allow partial wound closure before cells were fixed and stained in the same way as described in section 2.4.

2.8. Centrosome Positioning Analysis

Scratch wounds, set up as per 2.7., were labelled for α- and γ-tubulin, with the nuclei stained using DAPI as per the protocol in 2.4. and widefield fluorescence images of cells at the leading front of the wound were taken. Using ImageJ, lines were drawn on these images through the centre of the nucleus perpendicular to the cells apparent direction of movement, as indicated by lamellipodial projections. Using these lines, the centrosome could be scored as being at the front or rear side of the nucleus depending on whether it was present in front of the line, nearest the cell-free area, or behind the line, nearest the rest of the cell monolayer, respectively. Scoring of 50 cells per condition (DMSO, 10 and 15μM SFN) was performed and this was expressed as a percentage of cells with their centrosome in front of the nucleus.

2.9. Western Blotting

Cell lines were grown to 70-80% confluency in T75 flasks before being dosed with SFN for 24hr. Following this, cells were removed from the incubator and old medium was discarded before the cell layer was washed once with 5ml ice cold PBS. 250μl of lysis buffer plus protease inhibitor cocktail diluted 1:100 as per manufacturer's instructions (Thermo Fisher Scientific) was then added over the cell layer before incubating on ice for 15min. A cell scraper was used to disrupt and collect the cell layer at the bottom of the flask before a further 15min incubation on ice. Lysate was then collected into a 1.5ml Eppendorf and centrifuged at 13,000RPM (Eppendorf 5430) for 10min at 4°C. The lysate supernatant was retained for quantification and western blotting, it was stored at -20°C when required.

Protein lysates were quantified using the Pierce BCA protein assay kit (Thermo Fisher Scientific) as per manufacturer's instructions before known amounts of proteins were mixed with loading buffer (plus 10% β-mercaptoethanol) and water to give a total well volume of 25μl. Samples were then boiled at 95°C for 1min before being stored on ice until use. Samples were loaded alongside PageRuler™ Plus Prestained protein ladder (Thermo Fisher Scientific) into the wells of an SDS-PAGE gel (10% polyacrylamide separation gel, 5% stacking gel) and run at 120V for approximately 1hr 45min until the blue loading dye had run off of the edge of the gel.

Protein bands were transferred to a nitrocellulose membrane by means of a semi-dry transfer at 15V for 35min before being blocked in 5% milk in PBS plus 0.1% Tween 20 (PBST) overnight at 4°C with constant rocking. The following day blots were warmed to RT slowly while rocking before primary antibodies, diluted in PBST 1% milk as per Table 7, were substituted for the blocking solution and blots were incubated at 4°C overnight while rocking.

Table 7 – Primary antibodies used for western blotting

Target	Species	Dilution	Manufacturer
α-Tubulin	Rabbit	1:1000	Abcam
Acetylated Tubulin	Mouse	1:2000	Sigma
Actin	Rabbit	1:1000	Abcam
Hsp70	Mouse	1:5000	Abcam
Rap1A	Mouse	1:200	Thermo
Rap1GAP	Rabbit	1:10,000	Abcam

Table 8 – Secondary antibodies used for western blotting procedures, including details of dilution and fluorophores

Target Species	Dilution	Fluorophore Details	Manufacturer
Rabbit	1:50,000	680 (Red)	Li-Cor
Mouse	1:50,000	790 (Green)	Li-Cor

Once the blots had once again reached RT following overnight incubation, blots were washed three times (5min per wash) in PBST 1% milk. Secondary antibodies conjugated to fluorophores were diluted in PBST 1% milk 0.1% SDS as per Table 8 before being incubated for 90min on the rocker at RT. Following this, blots were washed twice in PBST 1% milk and once in PBS (5min per wash) before being imaged on an Odyssey fluorescence scanner (Li-Cor).

Chapter Three

Sulforaphane and Cell Migration

3.1. Introduction

Cell Migration is a fundamental process in multicellular organisms, playing pivotal roles in development, adult homeostasis and, when improperly regulated, in disease processes. The process of metastasis, dissemination of solid tumours leading to establishment of secondary growths at distant sites in the body, is one of the core hallmark capabilities of cancers (Hanahan and Weinberg, 2000), and is linked to 90% of cancer deaths (Gandalovičová et al., 2017). Logically, metastasis is primarily fuelled by the ability of cells to invade into the surrounding ECM and enter nearby vasculature. While existing chemotherapeutics do, to an extent, have anti-metastatic effects, there is as yet no drug which reliably, and specifically, inhibits the invasion and dissemination of tumour cells. However, in a recent paper Gandalovičová and colleagues (2017) proposed that there should be more focus on the search for so-called 'migrastatic' drugs which could suppress the ability of cancer cells to invade away from a tumour. Recently, SFN has been shown to reduce the metastatic capabilities of cancer cells (Roy et al., 2015), and may in part represent a migrastatic candidate, in addition to its many other effects on the cell cycle and resistance to oxidative stress (Juge et al., 2007). Reorganisation and control of the cellular cytoskeleton, generally under the direction of small GTPases, is crucial in migration both in 2D and 3D environments, and therefore, any effects of SFN on the cytoskeleton, which may subsequently impact on cell motility, were investigated using immunolabelling techniques and scratch wound assays.

In a 2D context, cell migration is a complex, multistep process involving a number of signalling cascades, small GTPases and cytoskeletal rearrangement. In the 3D environment found *in vivo*, metastatic dissemination takes on additional layers of complexity, with cells needing to coordinate the formation of metastasis-specific F-actin-rich invadopodia and distant adhesion formation with chemotactic and contractile activities in order to migrate through the stromal ECM and enter the vasculature (Bravo-Cordero et al., 2012). The innumerable molecules involved in this

process cannot be fully discussed here, however, certain key groups of molecules, and their roles in cancer metastasis, will be subsequently discussed.

The action of small GTPases, including the ubiquitously expressed Rho family GTPases, Cdc42, Rac and Rho which are involved in protrusion formation, directionality and contractility respectively has been well investigated *in vitro* (Raftopoulou and Hall, 2004). Aberrations in the expression or function of these proteins, or indeed in their activating GEFs or inactivating GAPs, impact greatly on cancer progression. For example, expression of the Rho subfamily member RhoC is frequently increased in malignancies, where it correlates with metastasis (Clark et al., 2000), subsequent modulation of RhoC to diminish its action can impair metastasis (Xing et al., 2015). Similar effects are observed following modulation of aberrant Cdc42 using micro-RNAs or small-molecule Cdc42 inhibitors (Shi et al., 2018). The importance of GTPases in metastasis seems to extend principally to alterations in their expression via transcriptional or translational mechanisms, as gain-of-function mutations in Rho coding sequences are distinctly rare, restricted mainly to certain gastric carcinoma subsets (Kakiuchi et al., 2014).

Once initial contacts with the ECM have been established, integrins cluster on the cell surface and their cytoplasmic domains act as scaffolds for cells to assemble focal adhesions (FAs), complex assemblies of adaptor, scaffold and signalling proteins on the inner plasma membrane which form a link between the actin cytoskeleton and the ECM to allow the exertion of tension for cell body movement during migration (Nagano et al., 2012). Initially the activated integrins recruit focal adhesion kinase (FAK) and paxillin to create naïve adhesions which are then matured by binding of additional proteins including talin and the type III intermediate filament protein vimentin (Liu et al., 2015). Numerous signalling proteins also get recruited to FAs for transmission of ECM-derived input into proliferation, survival and migration pathways (Mitra et al., 2005; Stoker, 2005; McDonald et al., 2008). In order to continue progression through the matrix, FAs must, once they are

no longer needed, be disassembled. It has been shown that MTs play a key role in this process, with repeated targeting of MTs to FAs, particularly in regions of FA disassembly, being observed with live imaging techniques (Kaverina et al., 1999; Rid et al., 2005). As such it appears that contact from MTs acts to trigger the disassembly of FAs, linking the dynamics of these two entities, further reinforced by the observed stabilisation of FAs following treatment with the MT depolymerising agent Nocodazole and their subsequent disassembly following its removal from cells (Ezratty et al., 2005; Ezratty et al., 2009). During FA disassembly, the clustered integrins are internalised via endocytosis and the actin-ECM connection is severed (Ezratty et al., 2005; Nagano et al., 2012). Disassembly of FAs is particularly important at the rear of the cell, to prevent tension generated against FAs behind the leading edge from shearing the cell in half.

Modulation of MT dynamic instability is also important in cell migration, with +TIP proteins and tubulin PTMs allowing for fine tuning of microtubule activity during cell migration. The master +TIP, EB1, which as described earlier tracks GTP-bound MT plus ends autonomously via its N-terminal CH domain, binds across four tubulin monomers in a nucleotide-dependent manner (Maurer et al., 2012). This interaction, although much higher in affinity compared to the interaction with GDP tubulin, has rapid binding/unbinding kinetics (Bieling et al., 2007). With their C-terminal EB homology domain proteins in the EB family can recruit a whole host of other +TIP proteins, which contain either CAP-Gly domains or SxIP motifs, that in turn have marked effects on the dynamics of MTs (Komarova et al., 2002). Differential recruitment of these proteins leads to disparaging effects on MT dynamics, and these effects are thought to depend almost entirely on EB1, which acts as the hub of +TIP complexes, meaning that if EB1 expression or function is disturbed it has drastic knock on effects in terms of MT behaviour and function (Bush and Brunner, 2004; Komarova et al., 2009). Oncogenic roles for EB1 have been suggested in breast cancer, where its upregulated expression, observed in both human tissue samples

and cell lines, has been linked to higher histological grades of tumours and increased incidence of lymph node metastasis. Furthermore, knockdown of EB1 expression has been shown to reduce cancer cell proliferation, while forced overexpression has a promoting effect (Dong et al., 2010). Similar upregulation of EB1, consistent with the hallmark loss of EB1 binding partner APC, has also been identified in colorectal carcinogenesis. It is thought that through EB1 upregulation, control of chromosome alignment and microtubule stabilisation via interaction with APC is potentially lost, leading to dysregulated proliferation and chromosomal instability. Depending on the APC status of colorectal cancer cell lines, knockdown of EB1 could diminish the cancerous phenotype. Interestingly, upregulation of EB1 was also reported in the histologically normal tissues surrounding the pre-malignant tissue, perhaps indicating a predisposition to malignancy (Stypula-Cyrus et al., 2014). Potentially, as the aforementioned results indicate, modulating the EBs, particularly EB1, via therapeutic intervention may reduce the invasiveness of tumour cells and lead to reduced cell proliferation.

As outlined previously, acetylation of MTs occurs on Lysine 40 of α-tubulin, a residue positioned on the luminal face, i.e. inside the tubule (Hammond et al., 2008). Acetylation, generally occurs on polymerised MTs, while deacetylation is generally rapidly performed on depolymerised tubulin (Aldana-Masangkay and Sakamoto, 2011). In mammals, tubulin acetylation levels are generally governed by the opposing actions of the acetylase α-tubulin acetyltransferase (ATAT1) and the MT-Specific histone deacetylase-6 (HDAC6; Li and Yang, 2015). Despite generally being associated with stabilised MTs, it has been indicated that metastatic breast cancer cells exhibit high levels of tubulin acetylation, particularly in cell protrusions. Further to this, proteomic analysis of patient specimens indicated that increased acetylation was associated with more aggressive behaviours in basal-like breast cancers, with a tendency towards disease progression in patients with high acetylation levels (Boggs

et al., 2014). In line with these observations, relatively high expression of HDAC6 has been shown to be correlated with reduced disease progression and better survival rates in breast cancer (Zhang et al., 2004). However, HDAC6 overexpression has also been identified in the development and progression of a number of other cancers, including acute myeloid leukaemia (AML), and its expression in cells seems to be required to facilitate hallmark anchorage-independent proliferation following Ras transformation of cells (Aldana-Masangkay and Sakamoto, 2011).

The ITC SFN has been reported to exert a number of effects inside cells, and principle among these investigated effects is the ability of SFN to induce phase I and II detoxification enzymes and shield cells from oxidative stress. A comparatively small volume of work has focused on the effects of SFN on migration and the filaments of the cellular cytoskeleton. Combined with its other chemopreventive and cytotoxic effects, further evidence of the effects of SFN on cell migration and the cytoskeleton would increase its attractiveness as an anticancer agent, as it could facilitate its prevention of metastasis.

Inhibition of migration by SFN has been reported in smooth muscle cells, and this was linked to its reduction of matrix metalloproteinase-9 (MMP-9) activity through Ras and RhoA modulation (Hung et al., 2013). This could be a clinically relevant observation, as invading cells secrete proteolytic enzymes including the MMPs at their leading front which enables remodelling of the ECM to make a path for the cell (Chang and Werb, 2001). However, it must be noted that, through a process known as mesenchymal-to-amoeboid transition (MAT), cancer cells may invade into tissues via protease-independent amoeboid migration, as opposed to mesenchymal invasion, which is protease-dependent (Gandalovičová et al., 2017). However, as there is a limited, but potentially expandable, pool of evidence to suggest that SFN exerts effects on both MT (Jackson et al., 2007; Azarenko et al., 2008) and actin (Hung et al., 2013) filaments, possibly via acting on TNFα in the case of actin, it could target cell migration through modulation of cytoskeletal remodelling.

In cells, SFN has been shown, in a similar way to current MTAs, to affect microtubule dynamic instability, rather than the levels of tubulin in cells. At a concentration of 15μM, SFN has been shown to supress dynamic instability of MTs in MCF-7 breast cancer cells expressing GFP-tagged α-tubulin, with microtubules observed in time lapse imaging of treated cells displaying fewer length changes, either growth or shortening, than MTs in control cells based on analysis of between 25 and 30 MTs per condition (Azarenko et al., 2008). In bovine aortic endothelial (BAE) cells 15μM SFN appeared to cause MT depolymerisation and induction of apoptosis, with a suppression of angiogenesis by SFN also observed via matrigel plug assays in mice (Jackson et al., 2007). Similar effects on MT polymerisation have also been observed in mouse mammary carcinoma cell lines (Jackson and Singletary, 2004). Microtubule depolymerisation has also been observed in the hepatocellular carcinoma HepG2 cell line at a dose of 40μM, which in physiological contexts is relatively high (Pocasap et al., 2018). Sensitivity to SFN varies between cell lines, so the precise effect of SFN on MTs is still relatively unclear, due to existing studies being carried out in different cell lines at different dose ranges, which would have different effects. In MCF-7 it has been reported that doses as low as 5μM SFN can significantly affect MT growth and shortening rates, however, this effect becomes more significant as doses increase to 15μM (Azarenko et al., 2008).

Despite this inconsistency there is evidence to indicate that SFN, and other ITCs, can covalently bind to tubulin and other proteins in the cell. This binding to proteins by ITCs reflects the onset of cell cycle arrest and apoptosis, indicating that SFN most likely exerts its effects via covalent protein binding and modification, with MALDI-TOF/TOF analysis of ITC binding to tubulin suggesting that cysteine 303 is the principle target. Additonal evidence from circular dichroism analysis, in which circularly polarised light is used to assess protein secondary structure, indicates that colvalent binding of benzyl-ITC (BITC), also found in cruciferous vegetables, induces

measurable changes in secondary structure, potentially decreasing the α-helical content of tubulin or inciting aggregation. Investigation of the tertiary structure via fluorometry also indicated global changes in protein folding (Mi et al., 2008).

Tubulin PTMs may also be modified by SFN, which has been shown to inhibit HDACs, including evidence that it inactivates the MT specific HDAC6 thereby reducing its ability to acetylate α-tubulin (Gibbs et al., 2009).

In this chapter results of investigations into cell migration and cytoskeletal networks in cells treated with SFN will be presented. These investigations are important due to the integral role of cell migration in cancer metastasis and mortality. Limited evidence has been published indicating that SFN exerts some, potentially anticancer, effects on the cellular cytoskeleton and cell migration. In the interest of revealing more about these potential effects, and therefore the possiblility that SFN may reduce metastasis, these effects were investigated through indirect immunofluorescence and scratch wound studies.

3.2. Results

3.2.1. Modulation of cell viability by 24hr SFN treatment

The literature suggests that different cell lines originating from various organs and tissues in the body may differ in their sensitivity to SFN in terms of its effects on cell cycle progression and apoptotic initiation. Therefore, the cancerous epithelial cell lines used in these experiments were, following 24hr exposure to doses of SFN ranging from 5-30μM, assayed for changes in viability using Presto Blue.

As expected, SFN appeared to show a dose-dependent reduction in viability in MCF-7, MDA-MB-231, Panc-1 and TC7 cell lines (Fig. 11). However, although a decline in viability is apparent from doses around 10μM, viability is only significantly reduced at 20 and 30μM ($p= 0.002$ and 0.004 respectively) in MCF-7 cells (Fig. 11A) and at 20 ($p=0.032$), but not 30μM in TC7 cells (Fig. 11B). In both MDA-MB-231 and

Panc-1 cell lines there was a decline in viability, although this is not significant, as can be seen in the charts presented in Fig. 11C-D.

These results were used to determine that 5μM SFN would be an appropriate 'low' dose while 10 and 15μM would be used as 'high' doses for future experiments, as although viability was reduced at these doses it was not substantial enough to hinder the experiments.

3.2.2. Indirect immunolabelling of MTs and EB1 in cancerous and non-cancerous cell lines

Localisation of the master +TIP EB1 was investigated using indirect immunofluorescence following treatment of breast cancer cell lines MCF-7 and MDA-MB-231 with SFN for 24 or 48hr, and following 24hr treatment for pancreatic Panc-1 $EB2^{Hi}$, retinal ARPE-19 and colorectal TC7 cell lines. For each condition, 15 cells were imaged, with figures being composed from representative cells. In MCF-7 cells labelled for EB1 and MTs following 24 (Fig. 12) and 48hr (Fig. 13) incubation with 5 and 10μM SFN, EB1 was present in untreated and treated MCF-7 cells in characteristic comets at the plus ends of MTs, where GTP-tubulin concentration is highest. However, these comets appear to be visibly shortened compared to WT cells in MCF-7 cells after incubation with 10μM SFN for 24 and 48hr (Fig. 14). Treatment with 5μM SFN appears to have a visibly intermediary effect after both 24 (Fig. 12D-F), and 48hr (Fig. 13D-F). Similar experiments were performed in MDA-MB-231 cells following 24 (Fig. 15) and 48hr (Fig. 16) exposure to 5 and 10μM SFN. In this cell line, derived from a more aggressive cancer, 5μM SFN seems to have little effect on EB1 comet size after 24hr (Fig. 15D-F). However, following 24hr incubation with 10μM SFN (Fig. 15G-I) comets in MDA-MB-231 do appear shortened, yet this affect is not observed at 48hr (Fig. 16D-F; Fig. 17). Shortening of comets also seems apparent in Panc-1 cells incubated with 10 and

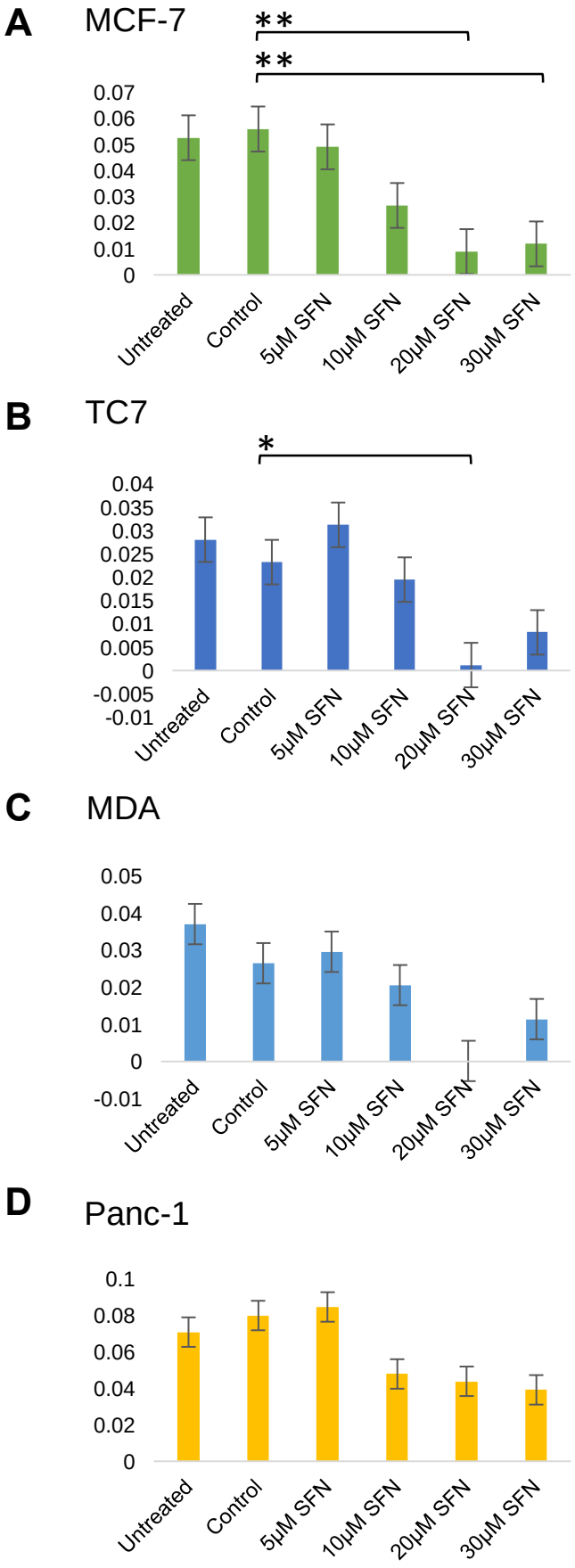

Figure 11 – 24hr treatment with sulforaphane reduces viability in a dose-dependent manner in both breast and colon cancer cell lines. MCF-7 cells treated with 20μM and 30μM SFN show a significant decrease in viability when compared to DMSO controls (A; p=0.002 and 0.004 respectively). Like MCF-7 cells, TC7 colon cells did show significant loss of viability at 20μM SFN (p=0.032) but not at 30μM (B). Although reductions in viability at these doses were observed in MDA and Panc-1 ($EB2^{Hi}$) cells (C,D) these were not statistically significant.

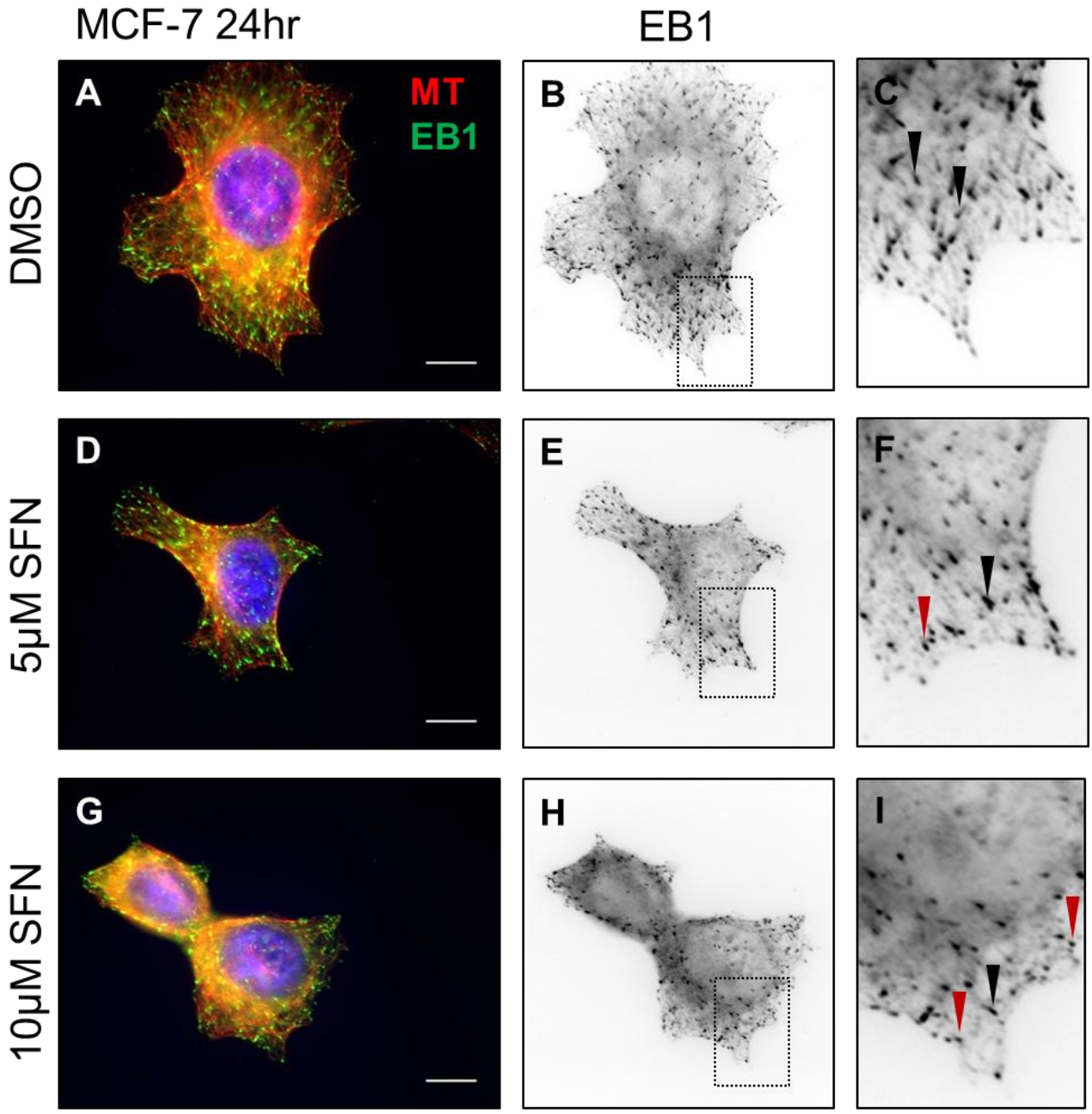

Figure 12 – Reduced size of EB1 comets in MCF-7 cells following 24hr exposure to 5 and 10μM SFN. In DMSO treated control cells EB1 associates with MT plus-ends in a comet-like distribution (A.B), with an extended tail (C, black arrows). Following 24hr exposure to 10μM SFN (G) many EB1 comets appear shorter (H) with many appearing as dots (I, red arrows), while a few still remain as elongated comets (black arrow). Treatment for 24hr with 5μM SFN (D, E) has an intermediate effect, with some EB1 comets still retaining their elongated shape (F, black arrows) while others appear shortened (red arrows). Scale bars = 10μm. Images taken by O. Hodges (Undergraduate Student). Images representative of 20 cells per condition.

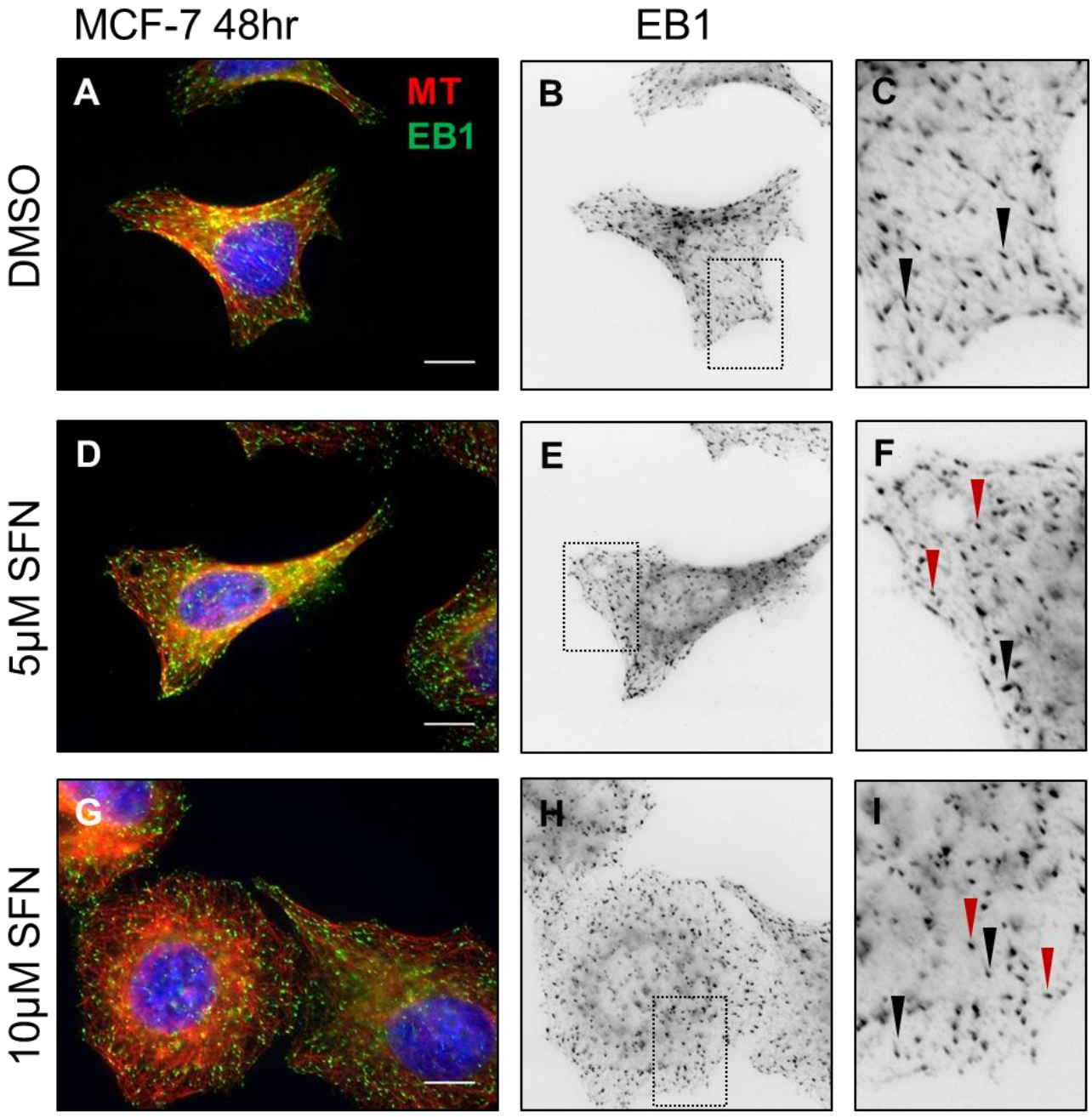

Figure 13 – Reduced size of EB1 comets in MCF-7 cells following 48hr SFN exposure. As with 24hr treatment DMSO treated control cells display distinct elongated EB1 comets associated with MT plus-ends (A-C; black arrows). Following 48hr exposure to10μM SFN (G) most EB1 comets appear shortened (H), appearing as dots (I, red arrows), while very few comets possess an elongated tail (I, black arrows). Treatment for 48hr with 5μM SFN (D, E) has an intermediate effect, with a larger number of EB1 comets still retaining their elongated shape (F, black arrows) while others appear shortened (red arrows). Scale bars = 10μm. Images taken by O. Hodges. Images representative of 20 cells per condition.

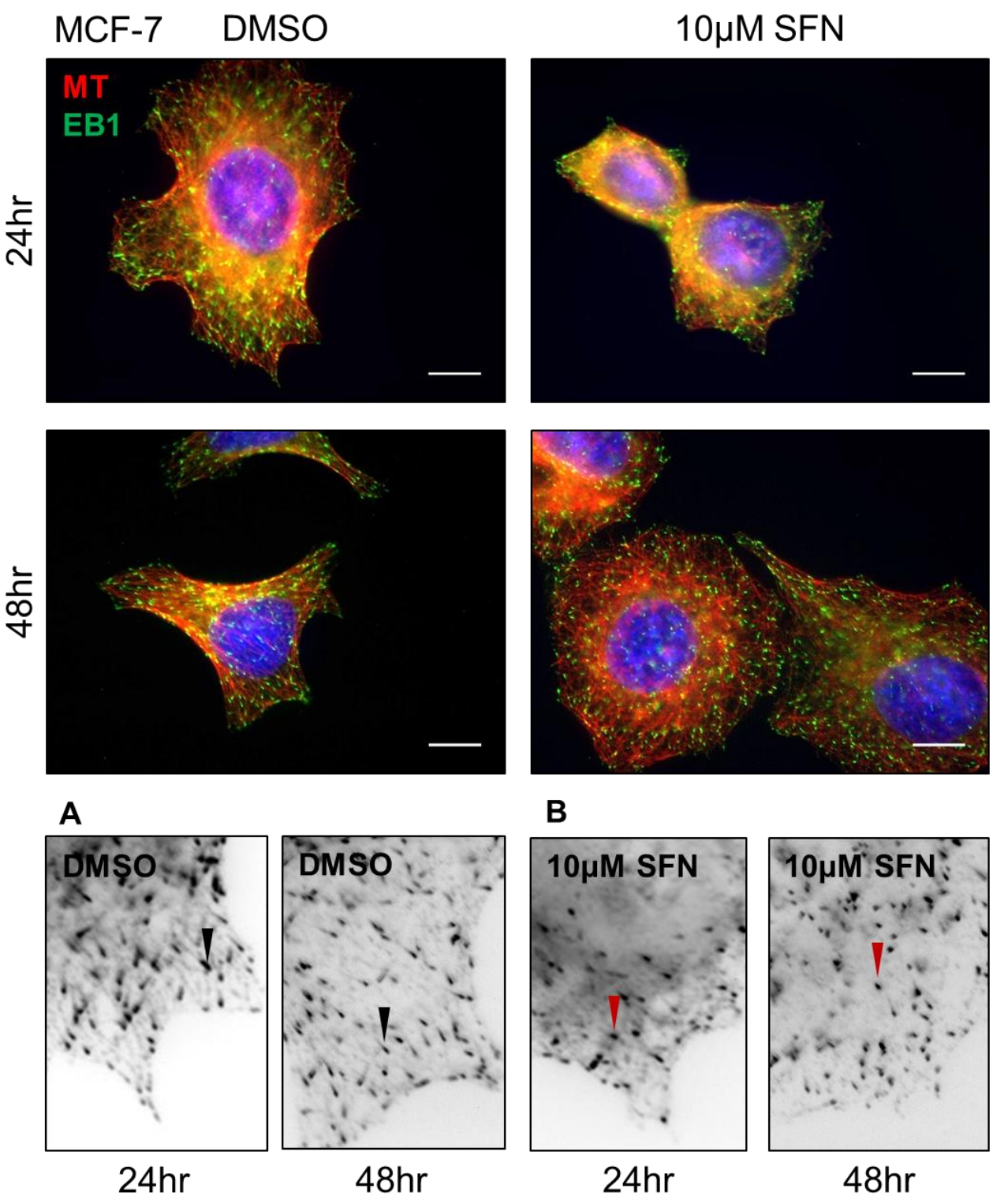

Figure 14 – Direct comparison between MCF-7 cells exposed to 10μM SFN for 24 and 48hr. In both DMSO and SFN treated cells EB1 continues to specifically associate with the plus-ends of MTs. However, in comparison to vehicle controls, in which EB1 comets are typically elongated (A; exemplified by black arrows) EB1 comets still appear shortened following 24hr treatment and remain so after 48hr exposure to SFN (B, red arrows). Scale bars = 10μm, images representative of 20 cells per condition.

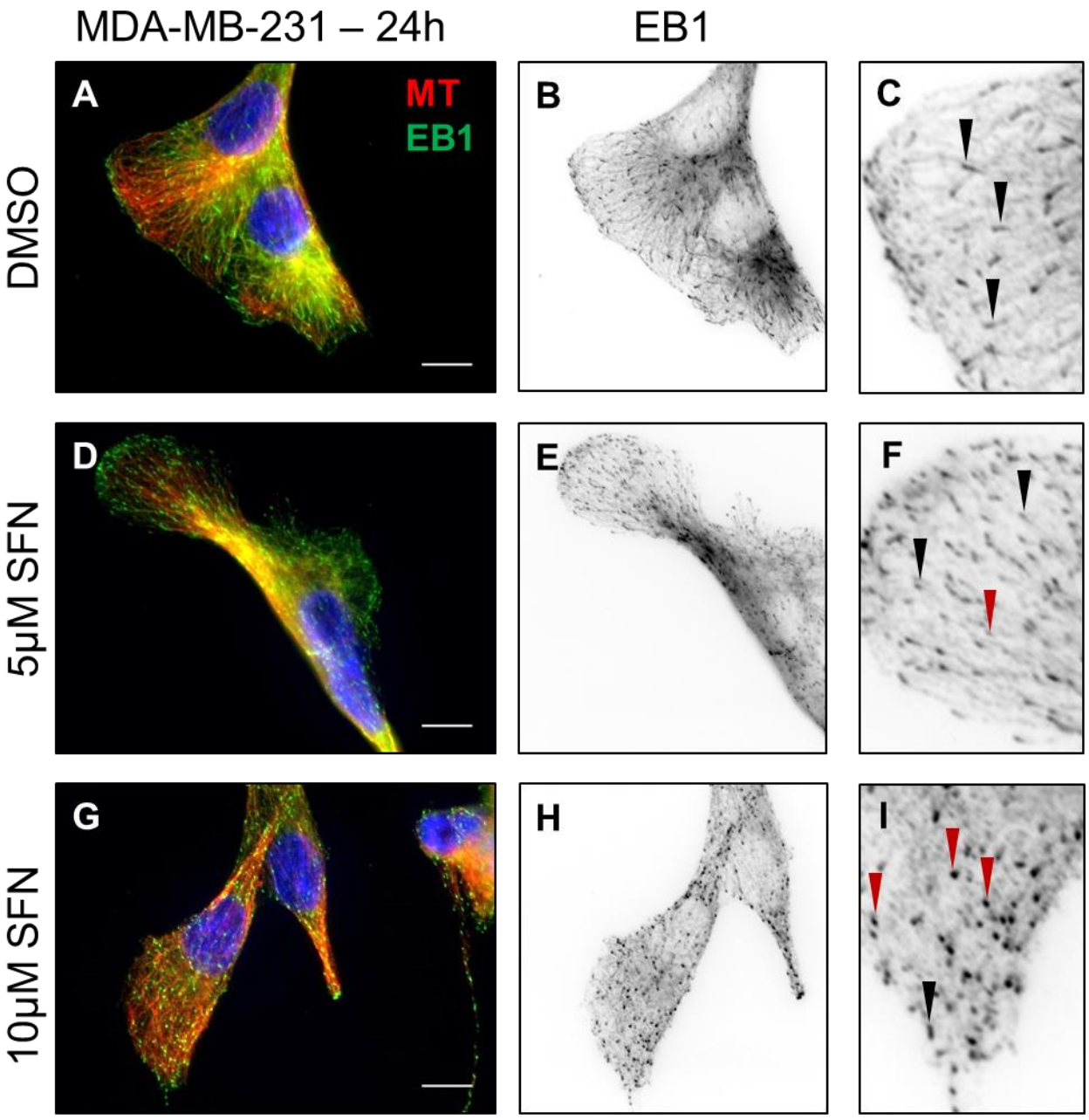

Figure 15 – Reduced size of EB1 comets in MDA-MB-231 cells following 24hr SFN exposure. In DMSO treated controls, as with MCF-7 cells, EB1 associates with MT plus-ends (A) in a comet-like distribution (B), displaying the characteristic elongated tail (C, black arrows). Following exposure to 10μM SFN for 24hr (G) many EB1 comets appear shortened (H) with many appearing dot-like (I, red arrows), while few remain as elongated comets (black arrow). Treatment for 24hr with 5μM SFN (D, E) has a less prominent effect, with some EB1 comets still retaining their elongated shape (F, black arrows) while others appear as dots (red arrows). Scale bars = 10μm. Images taken by O. Hodges. Images representative of 20 cells per condition.

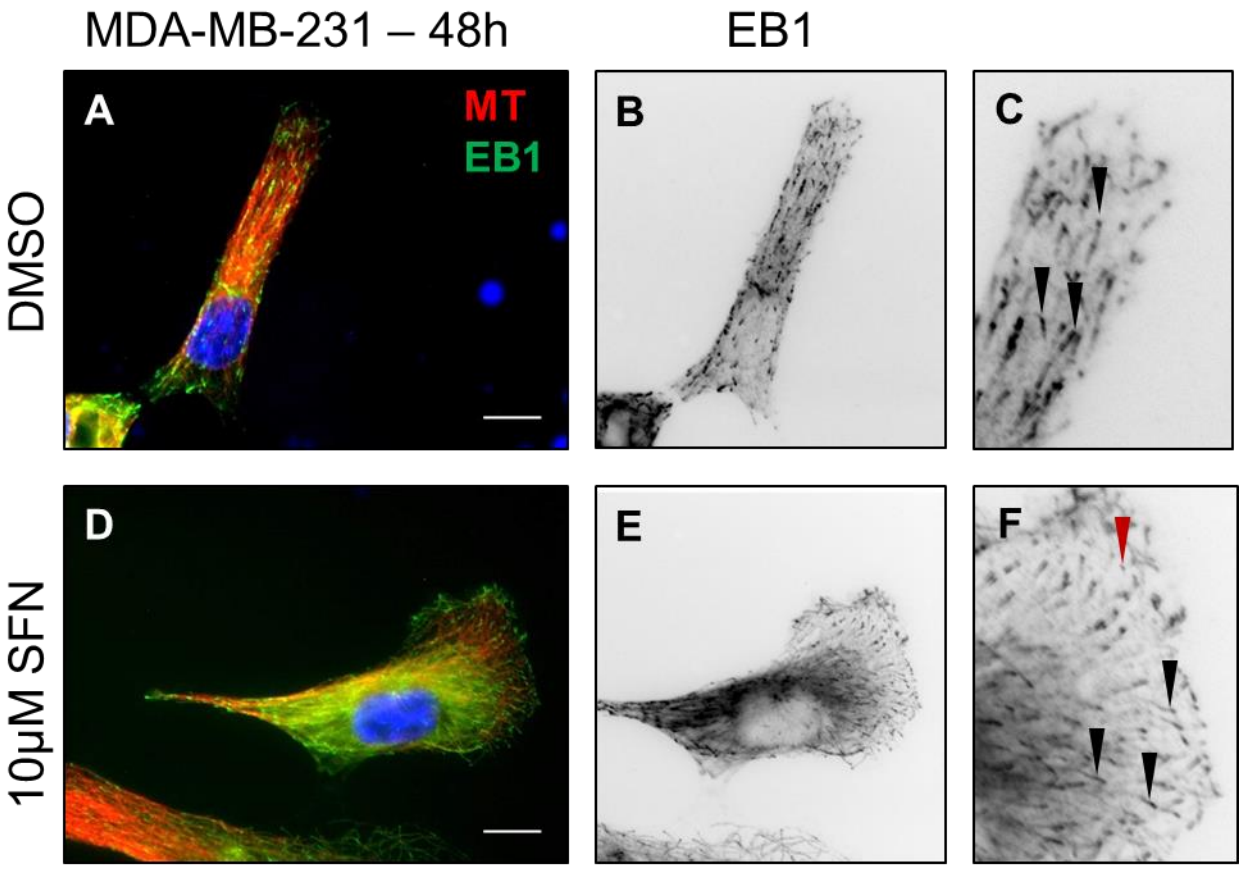

Figure 16 – EB1 comets do not appear to be shortened in MDA-MB-231 cells following 48hr exposure to 10μM SFN. In vehicle controls following 48hr, as with 24hr exposure, EB1 associates with MT plus-ends (A,B) in a comet-like distribution, displaying the characteristic elongated tail (C, black arrows). Following exposure to 10μM SFN for 48hr (G,H) many EB1 comets appear elongated (black arrows) as in vehicle controls, while very few exhibit the dot-like appearance (red arrow) as seen in 24hr treatments. (NB: 5μM SFN treatment was performed, however, at the imaging stage no cells could be found on these slides). Scale bars = 10μm. Images taken by O. Hodges. Images representative of 20 cells per condition.

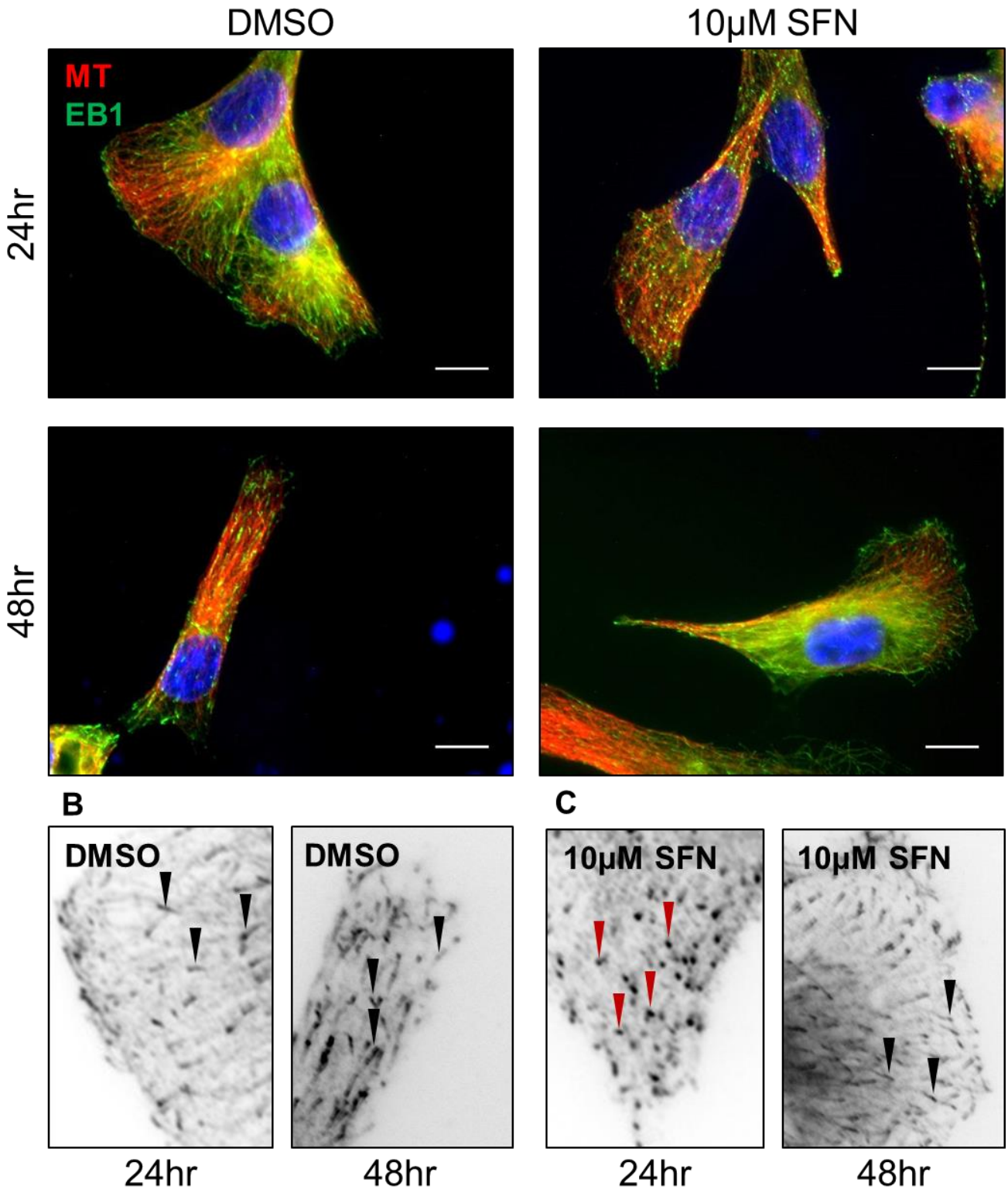

Figure 17 – Direct comparison between MDA-MB-231 cells exposed to SFN for 24 and 48hr. In both DMSO and SFN treated cells EB1 continues to specifically associate with the plus-ends of MTs (A). When compared to vehicle controls, in which EB1 comets are typically elongated (B; black arrows) EB1 comets appear shortened following 24hr treatment with 10μM SFN, as with MCF-7 cells (C; red arrows). However, following 48hr treatment most EB1 comets display the typical elongated shape (C; black arrows). Scale bars = 10μm, images representative of 20 cells per condition.

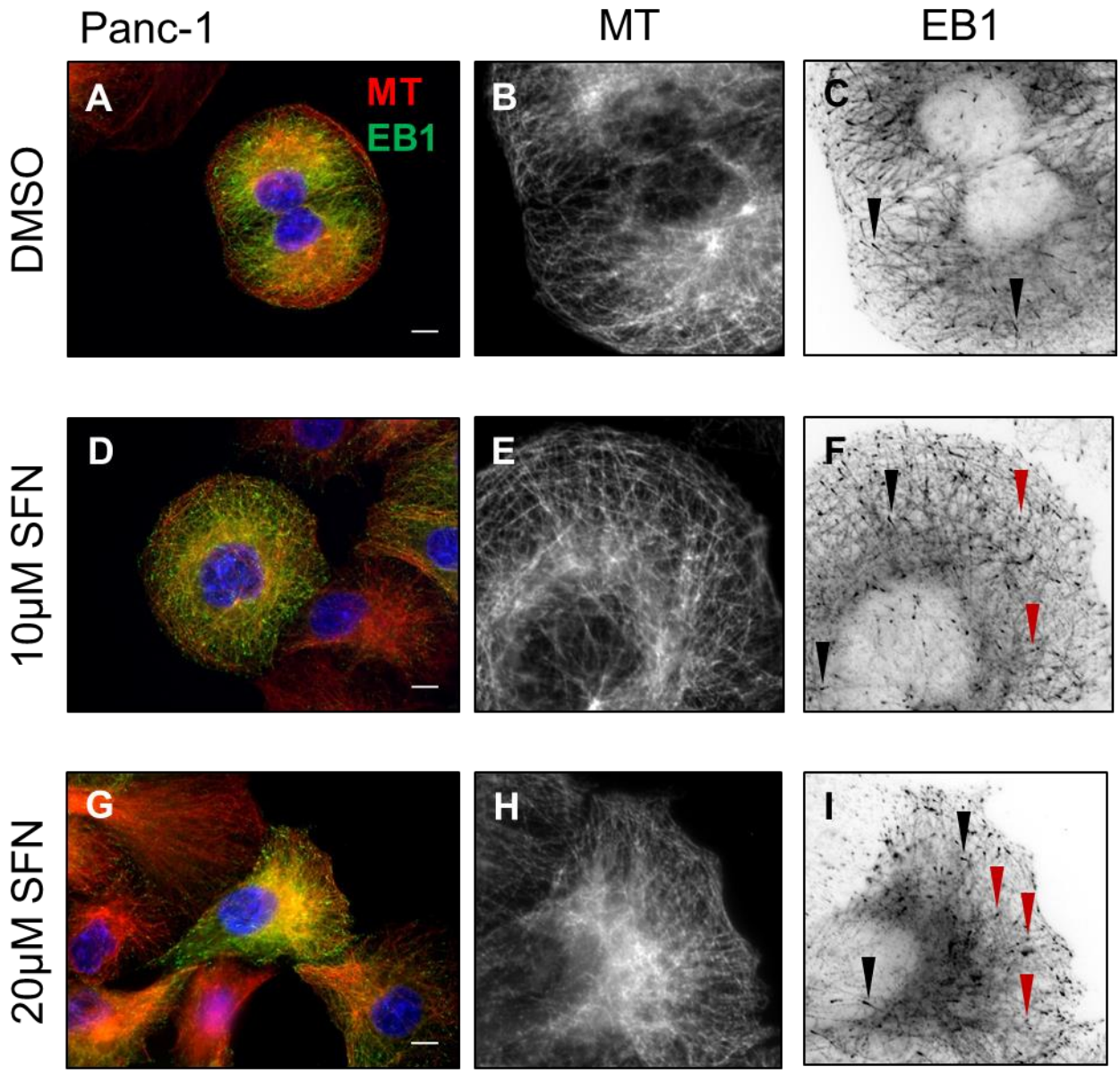

Figure 18 – Shortening of EB1 comets in Panc-1 cells following 24hr treatment with 10μM SFN. As with both breast cancer cell lines, in DMSO treated Panc-1 cells EB1 is present as elongated comets, and also appears to localise along the MT lattice further than in other cell lines (A, C; black arrows). Following treatment with 10 (D-F) and 20μM (G-I) SFN many EB comets appear shortened (F, I; red arrows), while some do retain their elongated structure (Black arrows). Additionally the MT networks in treated Panc-1 appear disorganised (B, E, H), although this may be due to high EB2 expression in these cells. Scale bars = 10μm, images representative of 20 cells per condition.

20μM SFN for 24hr (Fig. 18), but the effect is less prominent at 10μM (Fig. 18D-F). However, this effect does not seem to occur in all cell lines tested. No Shortening of EB1 comets was observed in ARPE-19 retinal pigment cells following 24hr incubation with either 5 or 10μM SFN (Fig. 19). There also appears to be no obvious shortening of comets in the TC7 colorectal cell line (Fig. 20A-F), although it appears that EB1 tends to localise further along MTs in these cells compared to the breast cancer cell lines (Fig. 20G-J).

Ideally, to quantify this effect comet analysis should have been performed, to count the average number of comets in cells and measure their length. From this the significance of the effect of SFN on comet length could be determined. However, the images captured from these experiments were not of fixed exposure, which would be required for this analysis, therefore these experiments would need to be repeated in the future to capture fixed exposure images of EB1 comets.

3.2.3. Acetylated tubulin in cancer cell lines

Indirect immunofluorescence indicates that levels of acetylated tubulin in both breast cancer cell lines, MCF7 (Fig. 21) and MDA-MB-231 (Fig. 22), do not greatly change following treatment with 5, 10 or 20μM SFN for 24hr. Localisation of acetylated tubulin labelling appears largely unchanged following treatment of cells. No discernible effect was seen in Panc-1 cells labelled for acetylated tubulin following 24hr incubation with 10μM SFN (Fig. 23A-D). To confirm this, protein levels of α-tubulin and acetylated tubulin in cell lysates would need to be quantified via western blotting, or via measuring the fluorescence intensity from immunolabelled cells, following 24hr treatment of cells with SFN. Western blotting was performed on cell lysates from another pancreatic cell line, Capan-1, and this did not appear to show any changes in either α-tubulin and acetylated tubulin levels (Fig. 23E-F). However, as seen with the EB1 comets there may be differences between cell types so lysates from the other cell lines would need to be used for western blotting to verify these immunofluorescence experiments.

3.2.4. Scratch wound assays to investigate cell migration following SFN treatment

Ibidi well inserts were used to create a cell free area which was imaged every 2min for 1hr in an attempt to pinpoint the beginnings of the effect of SFN, then every 20min for a further 16hr to ensure wound closure was observed. Manual measurement of wound closure using ImageJ indicated that in the case of MDCK II cells 10 and 15μM SFN significantly reduce percentage closure (20.07% and 13.45%

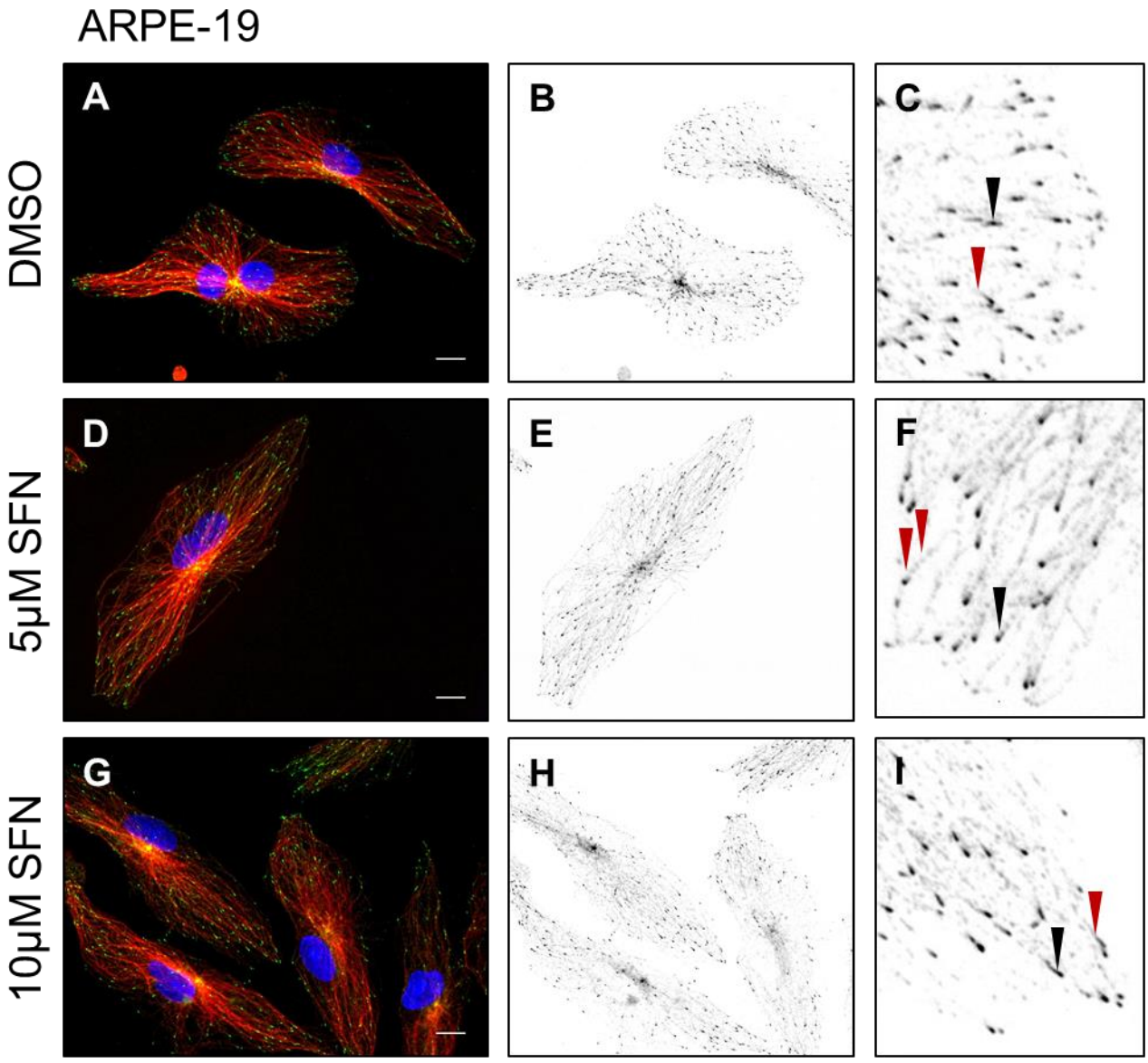

Figure 19 – EB1 comets appear unchanged in ARPE-19 cells following 24hr treatment with 5 and 10μM SFN. ARPE-19 cells were incubated with 5 and 10μM SFN for 24hr and labelled for MTs and EB1 (A,D,G), which was present in comets at the plus ends of MTs. Comets in control cells were elongated (B,C; black arrows), as were those in treated cells (E,F,H,I; black arrows), unlike the shortened comets seen in breast cancer cell lines. As in Panc-1 cells, there does appear to be more EB1 along the lattice in ARPE-19 cells then in breast cancer cell lines (C,F,I; red arrows) Scale bars = 10μm, images representative of 20 cells per condition.

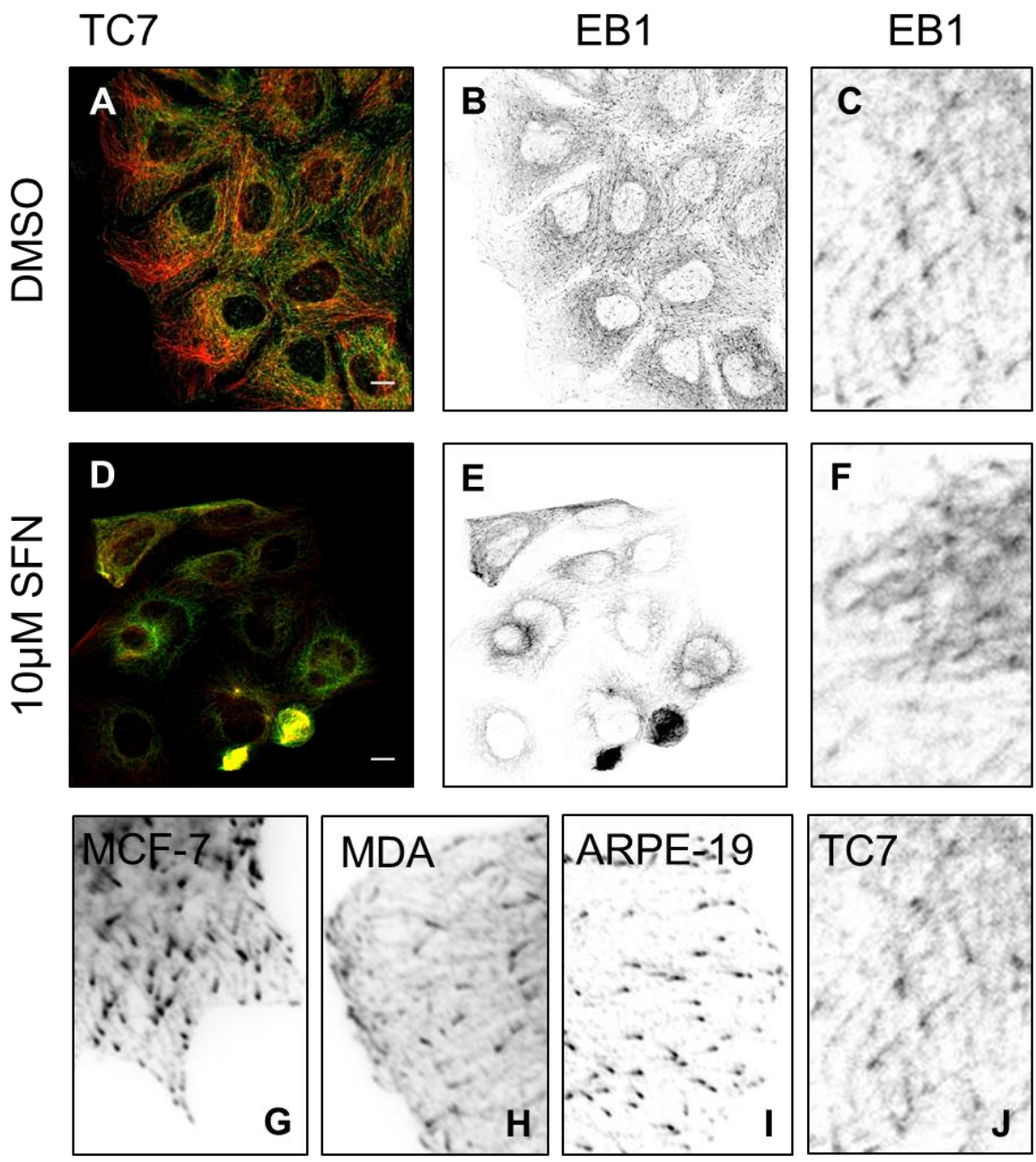

Figure 20 – EB1 comets in TC7 cells appear largely unchanged following 24hr treatment with 10μM SFN. TC7 cells were incubated with 10μM SFN for 24hr and labelled for MTs and EB1 (A,D,) Comets in control cells were elongated (B,C), as were those in treated cells (E,F), unlike the shortened comets seen in breast cancer cell lines. The EB1 protein was present in comets at the plus ends of MTs, however these appeared to be spread further along the MT lattice in both control and treated cells than in other cell lines subjected to similar experiments, which tended to have concentrated comets with less EB1 along the lattice (G-J). Scale bars = 10μm, images representative of 20 cells per condition.

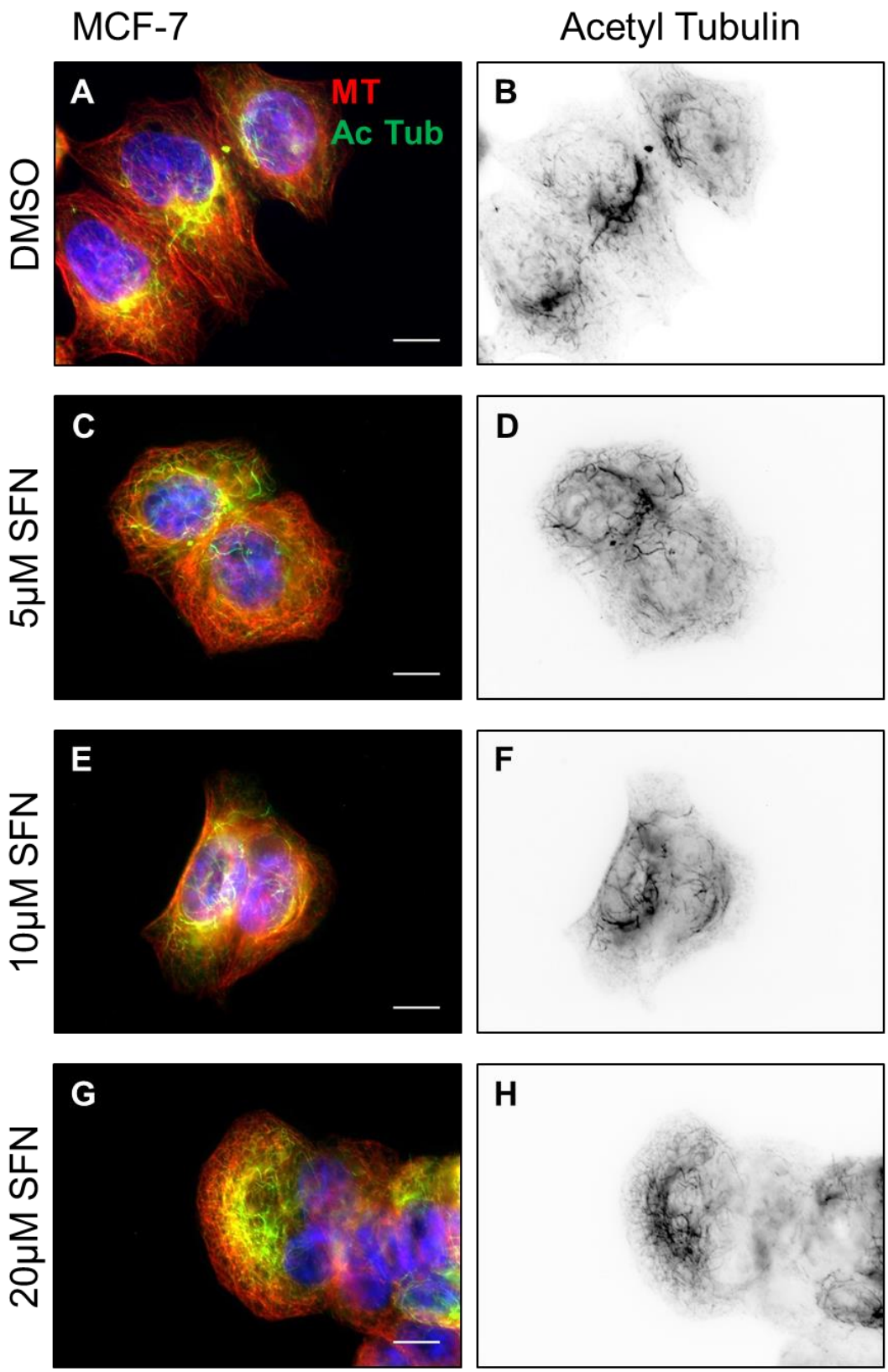

Figure 21 - Acetylated tubulin levels in MCF7 cells appear unchanged after 24hr dose with 5, 10 and 20μM SFN. In DMSO treated cells acetylation largely occurs along more stable MTs around the nucleus, as peripheral MTs are more dynamic. This is largely similar in cells treated with 5, 10 and 20μM SFN, with the main area of acetylation focused around the nucleus (B, D, F, H). Scale bars = 10μm. Images taken by O. Hodges. Images representative of 20 cells per condition.

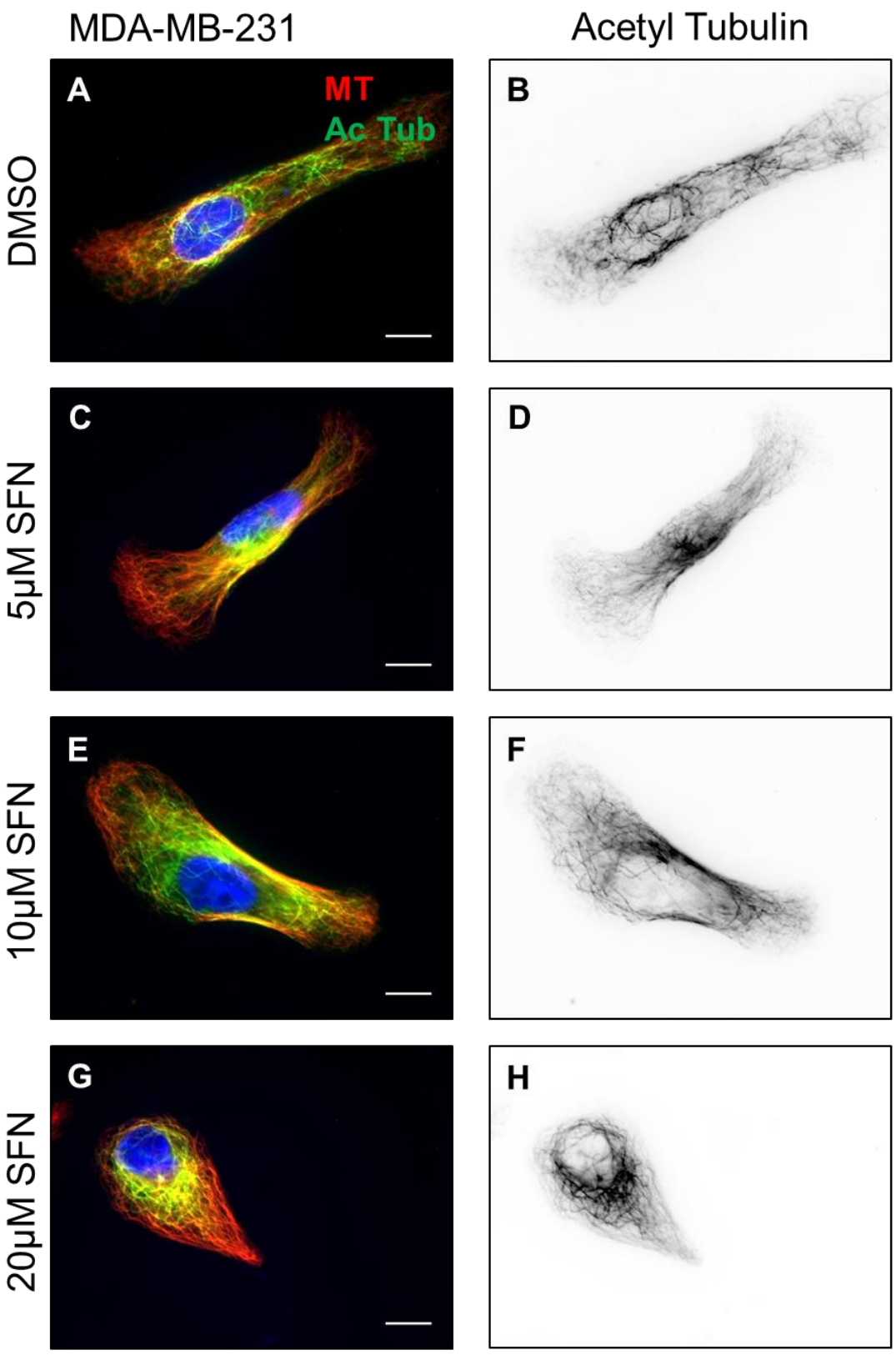

Figure 22 - Acetylated tubulin levels in MDA-MB-231 cells appear unchanged after 24hr dose with SFN. In DMSO treated controls, as with MCF-7 cells, acetylation largely occurs along more stable MTs around the nucleus, however, acetylation seems to extend further towards the periphery in MDA-MB-231 cells than in MCF-7s, even in controls. Acetylation patterns are largely unchanged in cells treated with 5, 10 and 20μM SFN (B, D, F, H). Scale bars = 10μm. Images taken by O. Hodges. Images representative of 20 cells per condition.

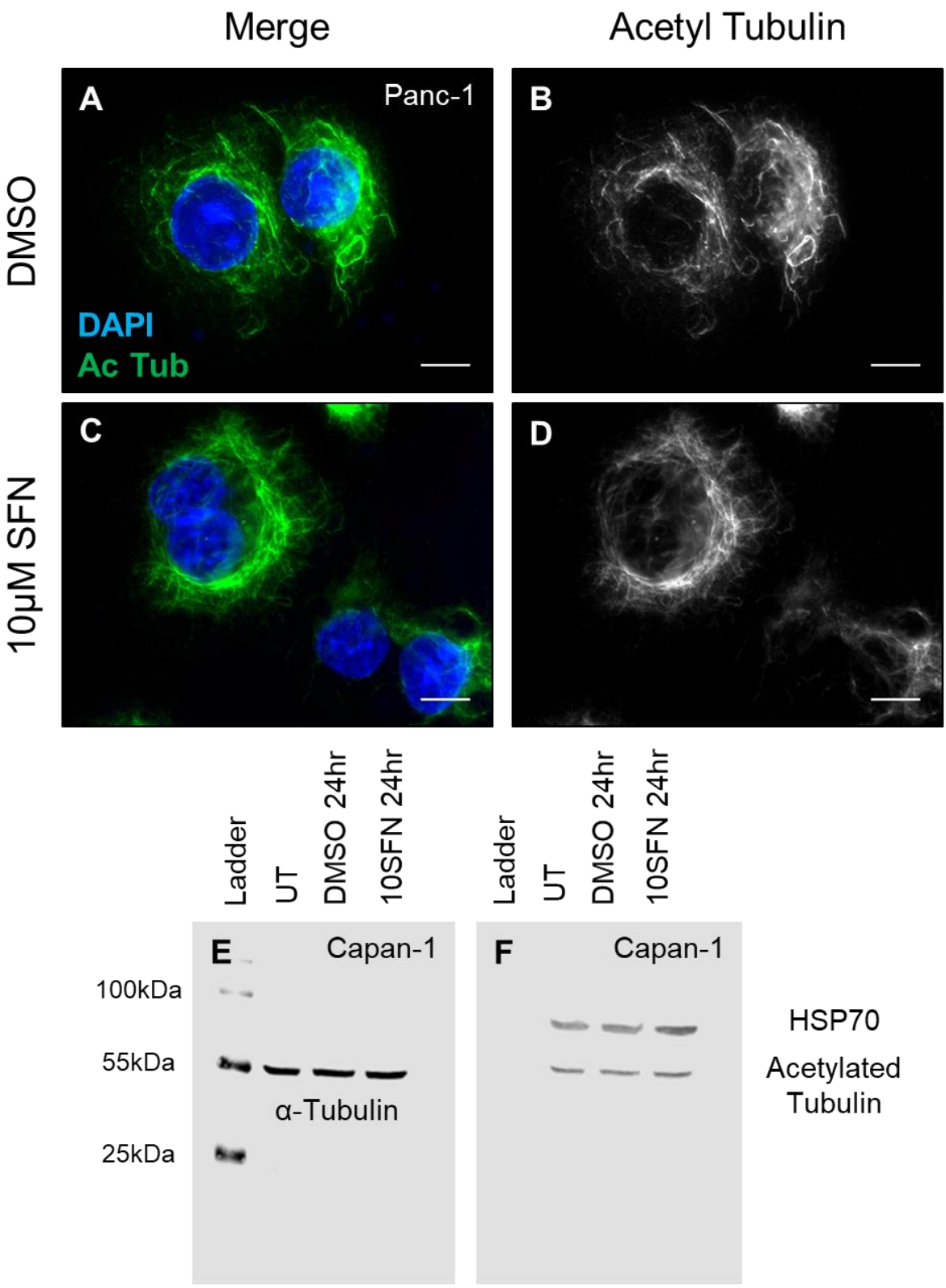

Figure 23 – Acetylated tubulin levels in Panc-1 cells following 24hr treatment with 10μM SFN. Acetylated tubulin in Panc-1 cells is found largely distributed close to the nuclear region in the middle of the cells (A,C). Distribution and levels of acetylated tubulin appear relatively unchanged by 24hr exposure to 10μM SFN (B,D). Western blotting in another pancreatic cell line, Capan-1, did not appear to indicate any changes in levels of α-tubulin (E) or acetylated tubulin despite consistent loading indicated by HSP70 housekeeper protein (F). Scale bars = 10μm. Images representative of 20 cells per condition.

closure respectively; p=<0.001) compared to untreated (88.94% closure) and DMSO vehicle control cells (79.03% closure; Fig. 24).

In similar wound closure experiments with Panc-1 cells (Fig. 25) SFN seemed to have a less pronounced effect, yet cell layers treated with 10 and 15μM SFN exhibited significantly reduced closure (47.65% and 47.32%, p=0.040 and 0.047, respectively) compared to the DMSO vehicle control (62.57%), but not untreated wounds (58.44%). It should be noted that there was no significant difference between the untreated and DMSO control conditions.

Plotting the percentage closure from 20min intervals throughout the first 8hr period of closure, before control wounds in the MDCKII condition almost completely close, shows the rate of closure of both MDCKII and Panc-1 wounds (Fig. 26). From these graphs, the highly significant change in closure in MDCKII cells can be seen (Fig. 26A), with both 10 and 15μM SFN rates diverging from as early as 20min into the experiment. Rates of closure in Panc-1 cells, where the effect of SFN is less significant, do not diverge as soon, with the significantly different DMSO and treated rates only beginning to diverge around the 200min timepoint.

To assess if these observed effects were in part due to the proven inhibition of cell proliferation by SFN, and toxicity as measured by Presto blue assays (Fig. 11), cell layers were treated with 2mM Thymidine for 16hr prior to insert removal, which would induce cells to collect in the G1/S phase of the cell cycle, and therefore prevent cell division. This block on division was maintained during live imaging with continued incubation with 2mM thymidine. Despite removing the contribution of cell division, it still appears that 10 and 15μM SFN reduce the percentage closure of wounds (Fig. 27), however, only one repeat of this experiment was conducted, with less than 3 replicates in each condition so the significance of these differences cannot be calculated at this time. Further repeats of these assays would be required to confirm that SFN is still effective in reducing wound closure in the presence of Thymidine.

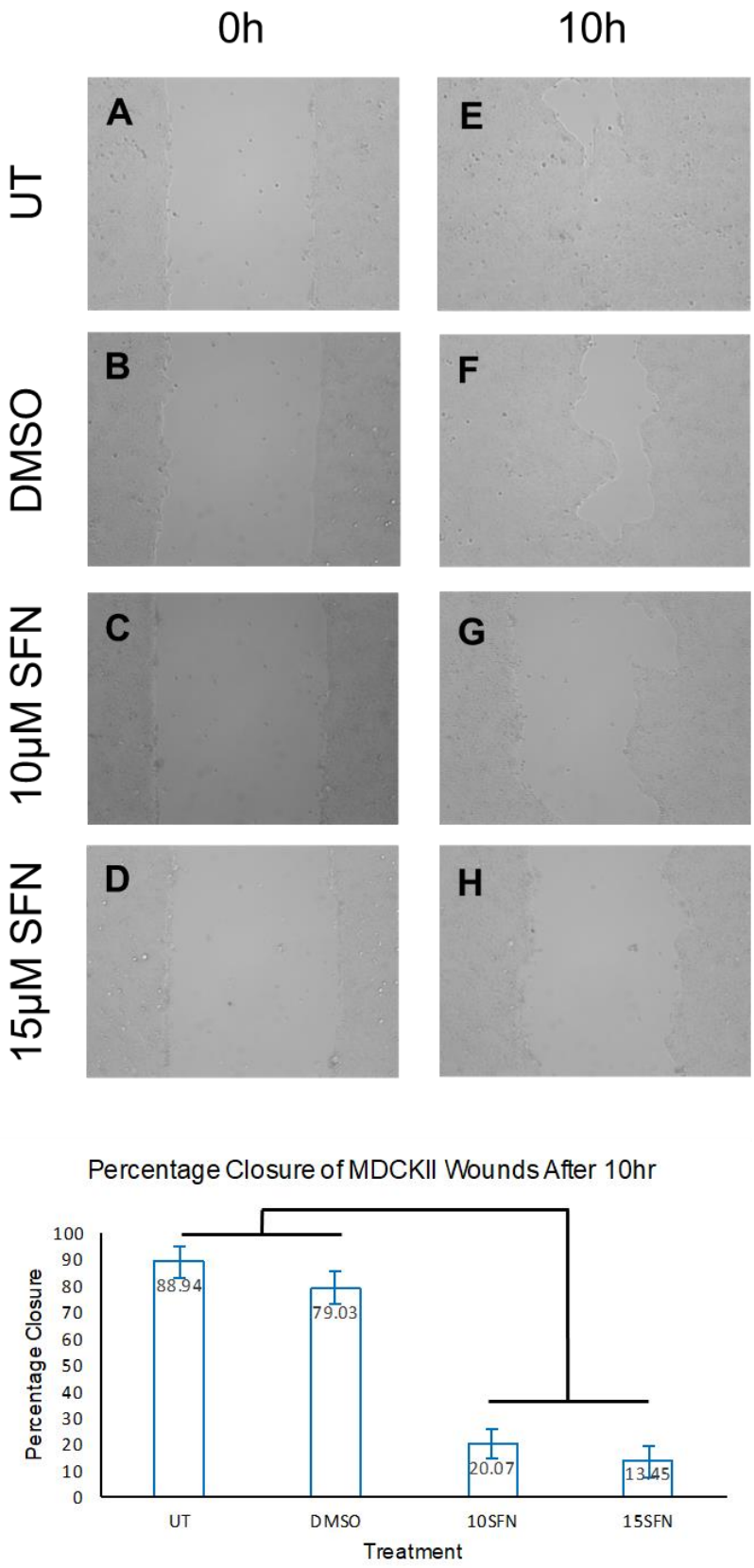

Figure 24 – Percentage closure of MDCKII wounds over 10hr is significantly reduced by the presence of 10 and 15µM SFN. Over 10hr, closure of wounds made in MDCKII cell layers imaged at 5x magnification (A-D) is very significantly reduced by the presence of both 10 and 15µM SFN (G,H; p=<0.001), compared to both DMSO and UT controls. SFN treated wounds are still left relatively open compared to control wounds which are almost completely closed.

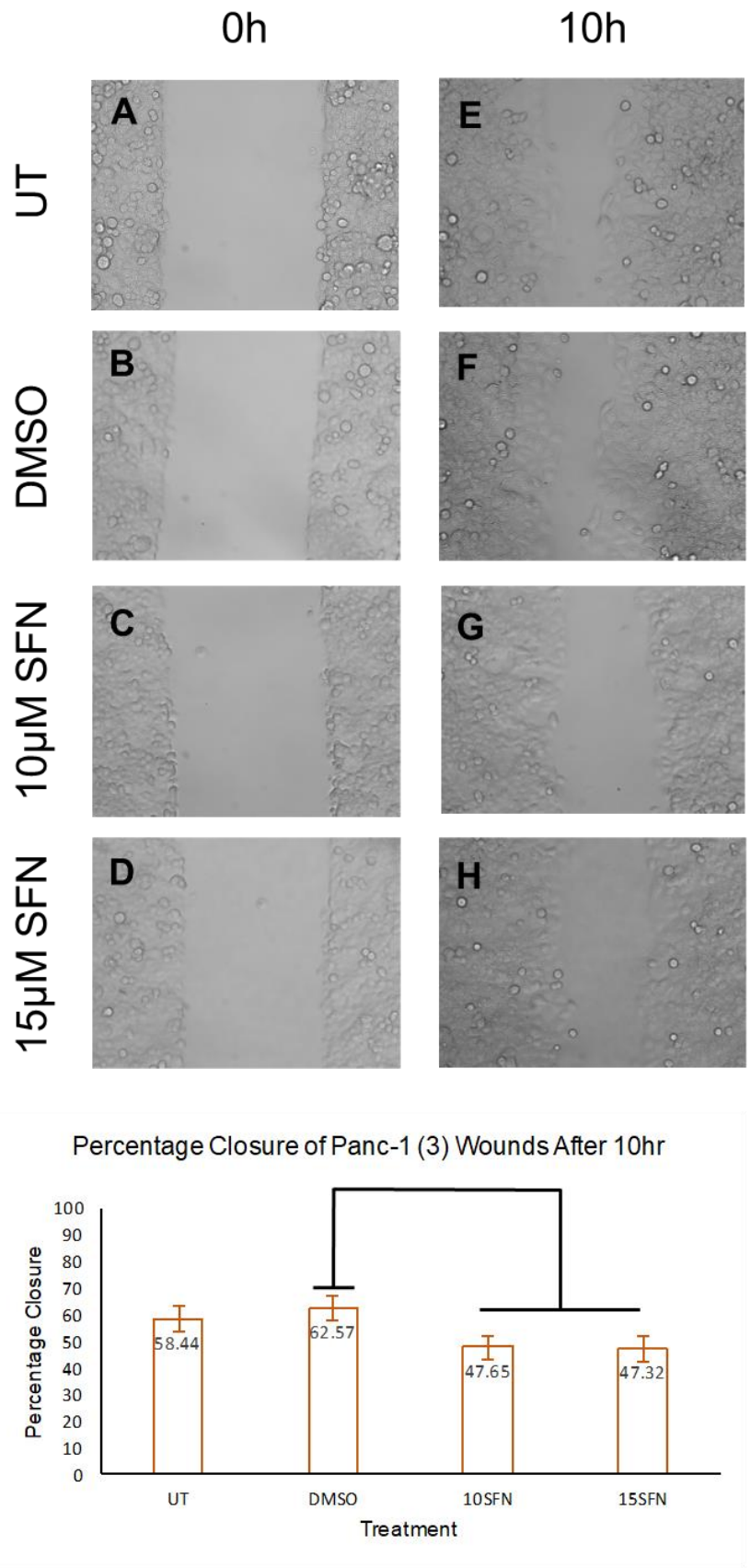

Figure 25 – Percentage closure of Panc-1 wounds over 10hr is significantly reduced by 10 and 15μM SFN. Percentage closure on Panc-1 wounds imaged at 5x magnification (A-D) was significantly reduced in the presence of 10 and 15μM SFN (G,H, p=0.040 and 0.047 respectively) over 10hr compared to DMSO (F;), but not to UT control cells (E; p=0.108 and 0.124 for 10 and 15μM SFN respectively).

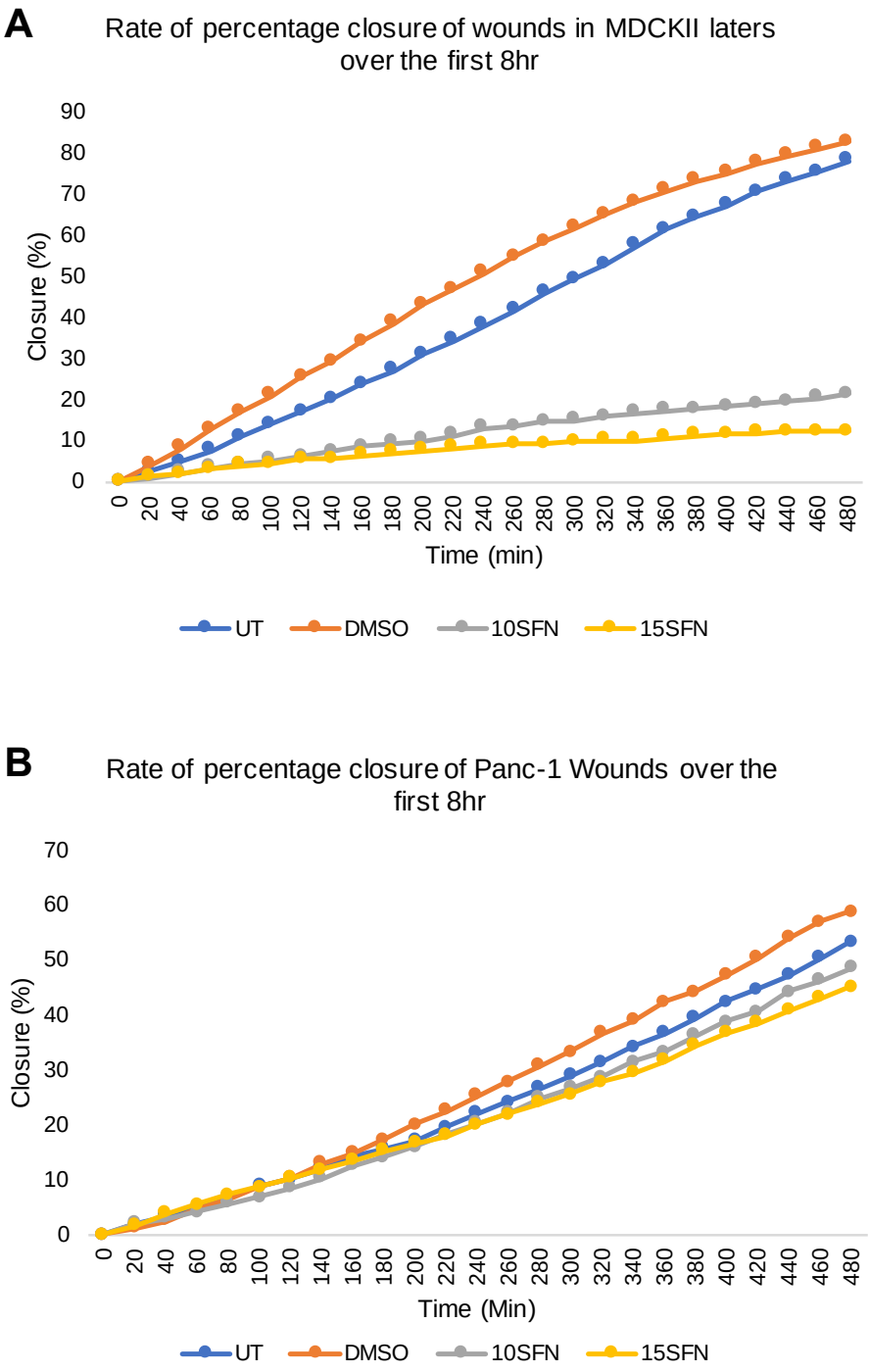

Figure 26 – Rate of wound closure in MDCKII and Panc-1 layers over the first 8hr. Measurements of percentage closure at 20min intervals indicates that in MDCKII cells the effect of SFN is noticeable after around an hour (A). The effect in Panc-1 cells is less prominent (B), and less significant as shown in Fig. 25, however, the rates appear to noticeably diverge between 180 and 200min.

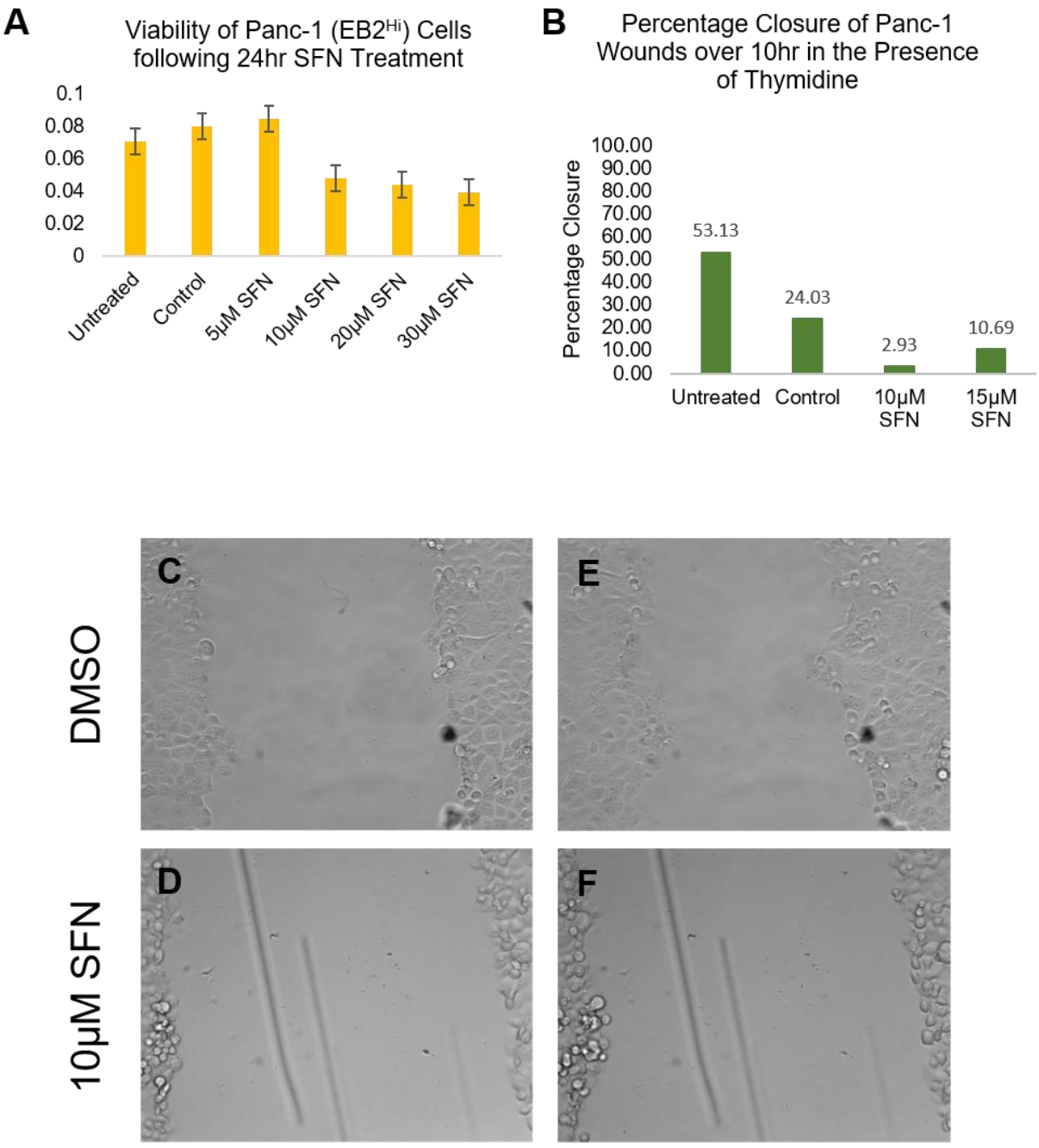

Figure 27 – Wound closure is still slowed by SFN even in the presence of the mitotic block Thymidine. Viability of Panc-1 cells with high EB2 (EB2^{Hi}) is affected, although not statistically significantly, by treatment with SFN (A), so a wound closure assay was performed on cells that had been treated with thymidine to block mitosis, thus eliminating any effects of SFN on cell proliferation from the assay. The results of this seemed to indicate that there was still an effect on percentage closure by both 10 and 15μM SFN (B). Cells were treated with thymidine for 17hr prior to wounding (C,D), and although these wounds appeared to close less over 10hr than those not treated with thymidine, there does appear to be increased closure of the DMSO control wound over the 10 μM SFN condition (E,F).

3.2.5. Distance, directionality and centrosome positioning in the closing scratch wound

Using the time-lapse videos recorded of Panc-1 wound closure between 1hr and 10hr during scratch wound closure, in which images were taken every 20min, 16 cells from each condition, based on recordings from two separate experiments, were individually manually tracked using the manual tracking plugin on ImageJ, which can give quantitative data on velocity and distance travelled as well as an idea of the directionality of cells migrating into the wound. Using the longer videos enabled lengthier tracks to be recorded, and a clearer representation of maintained directional migration of cells. The average distance travelled by cells between 1hr and 10hr of the recording is reduced by SFN treatment from around 30μm in UT and DMSO controls to approximately 24μm in both 10μM and 15μM conditions (Fig. 28A). Correspondingly this is accompanied by a reduction in cell velocity, from an average of 0.54μm/sec and 0.44μm/sec respectively in UT and DMSO controls to 0.24μm/sec and 0.28μm/sec in 10μM and 15μM SFN conditions (Fig. 28B). Overlaying these tracks onto the images, so the paths taken can be seen over time, does not seem to show any loss of directionality in cells treated with SFN, cells in all conditions appear to migrate in a relatively linear and persistent manner towards the cell-free area (Fig. 29), their velocity, and therefore total distance, is just reduced.

Due to the close-packed nature of MDCKII cell layers manually tracking individual cells was challenging. Based on tracking of three cells per condition (Fig. 30), from the same experiment, a reduction in both average total distance travelled (Fig. 30A) and average velocity (Fig. 30B) can be seen in 10μM and 15μM SFN conditions compared to control cells. This analysis also seems to indicate that UT MDCKII cells have a faster rate of migration, with the average velocity of MDCKII cells almost twice that of UT Panc-1 cells (1.01μm/sec and 0.55μm/sec respectively; Fig. 30C).

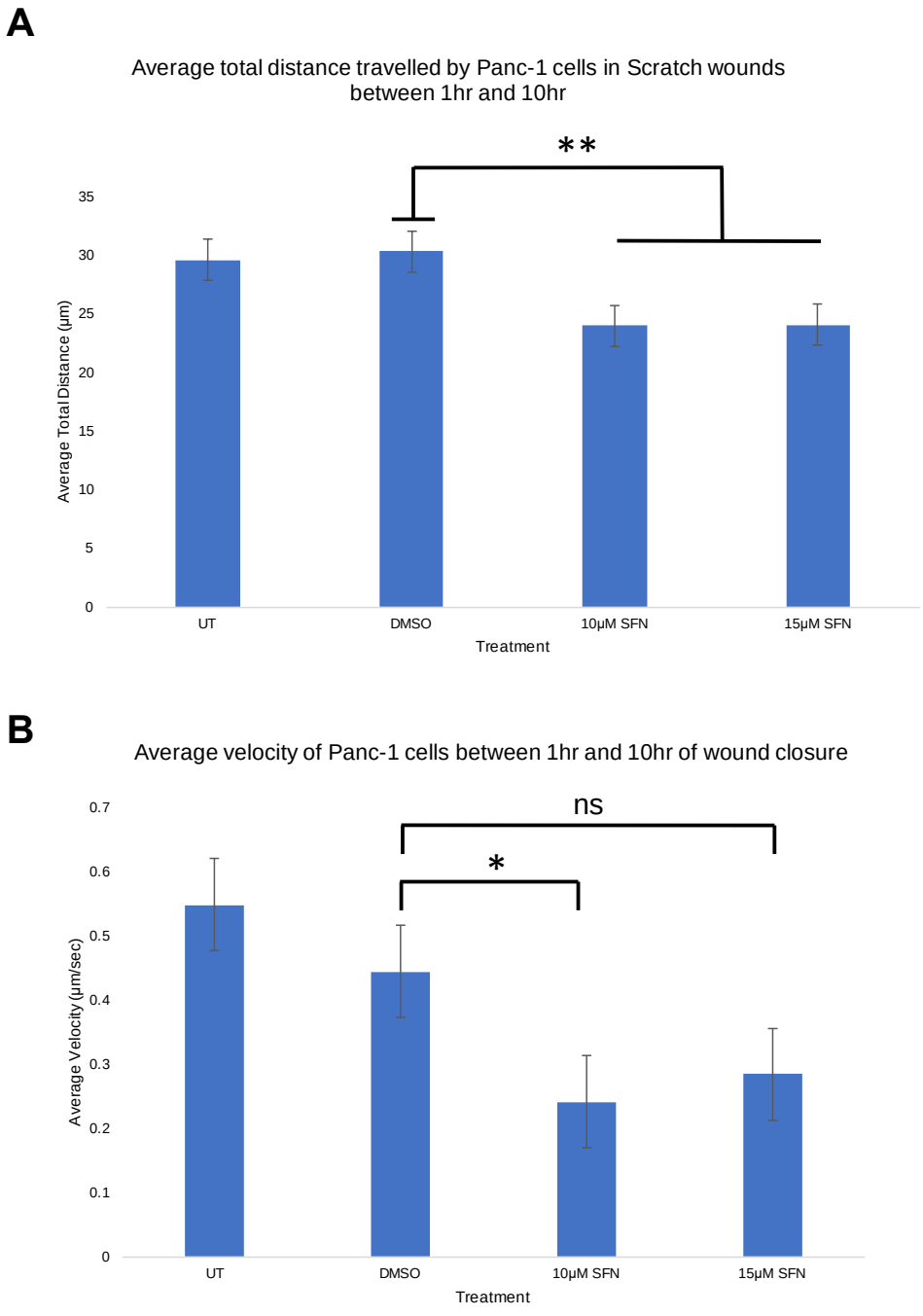

Figure 28 – Average total distance travelled and velocity of Panc-1 cells between 1 and 10hr of wound closure. Manual tracking of cells at the leading edge of wounds as they move into the cell free area indicates that there is a significant reduction in the total distance travelled by cells into the cell-free area (A) following treatment with 10 and 15µM SFN (p=0.005 in both doses). This is also reflected in a reduction in velocity (B) of cells in wounds exposed to 10µM SFN (p=0.019), however, at 15µM SFN this reduction is not significant (p=0.088). Results based on tracking data from 16 cells per condition.

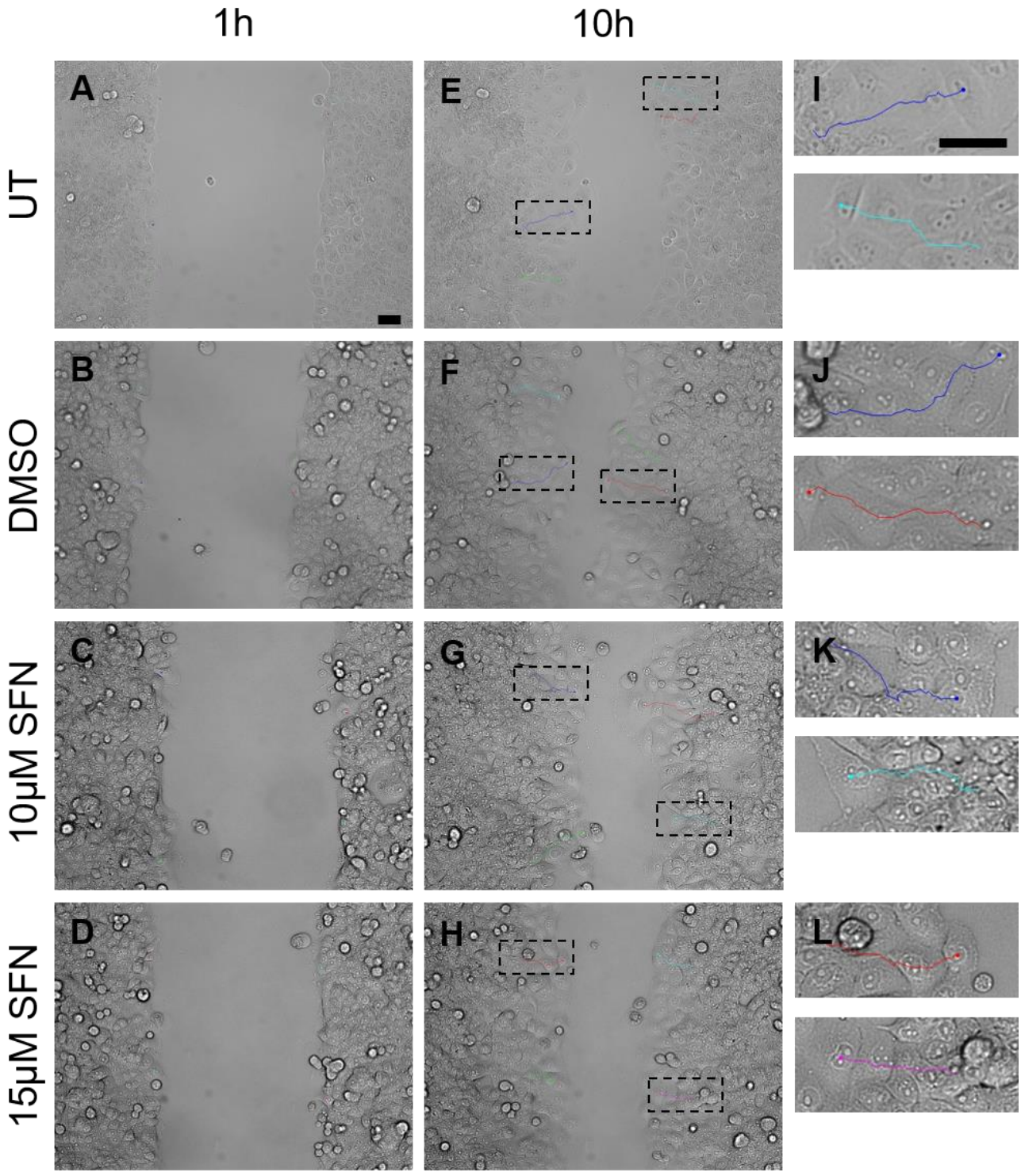

Figure 29 – Manual tracking to show directionality of cells moving into the cell-free area. Overlay of four manual tracking recordings per condition, selected from 16 recorded per sample. Ffrom the starting point (A-D) to the final point (E-H), appear to show that directionality is not noticeably affected by SFN treatment in Panc-1 cells. Cells migrate in a fairly linear and persistent manner towards the cell free area, and tend not to deviate largely from this path (I-L). Scale bars = 30μm

A Average distance travelled by MDCKII cells between 1hr and 10hr of wound closure

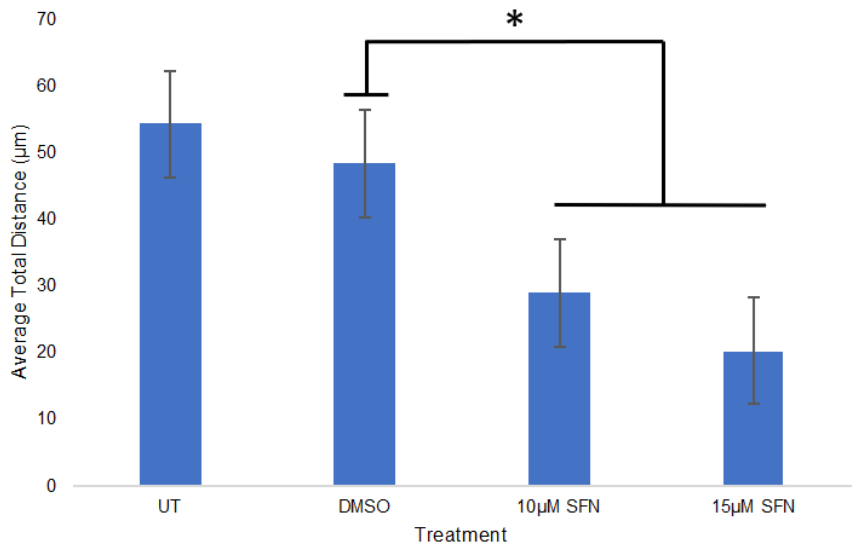

B Average velocity of MDCKII cells in the closing scratch wound between 1hr and 10hr

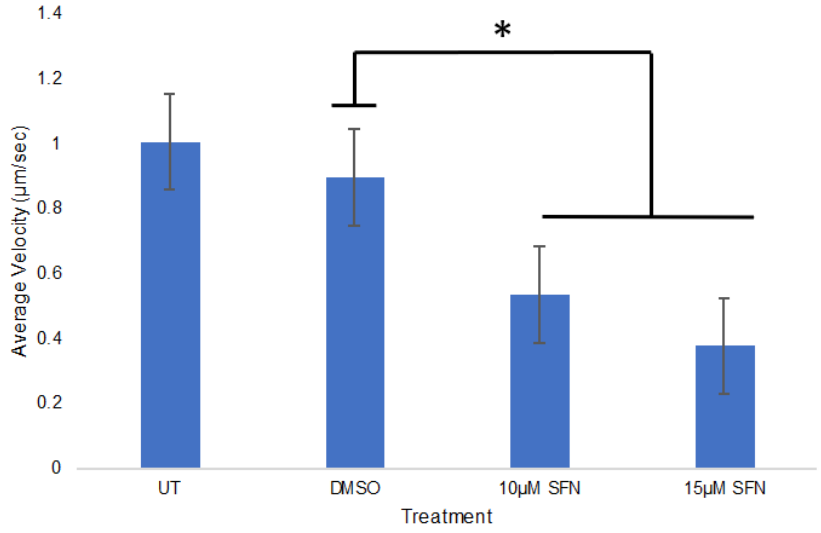

C	**Average Velocity of UT Cells (µm/sec)**
Panc-1	MDCKII
0.55	1.01

Figure 30 – Preliminary measurement of average total distance travelled and velocity of MDCKII cells between 1 and 10hr of wound closure. Manual tracking of cells at the leading edge of wounds as they move into the cell free area indicates that there is a significant reduction in the total distance travelled by MDCKII cells (A) into the cell-free area following exposure to 10 and 15µM SFN (p= 0.044 and p=0.013 respectively). This is also reflected in a significant reduction in velocity of cells (B) in wounds exposed to both 10 and 15µM SFN (also p= 0.044 and p=0.013 respectively). Comparing the velocity of untreated Panc-1 and MDCKII cells shows that MDCKII cells migrate almost twice as fast as Panc-1 cells in these conditions (C). Data based on 3 cells per condition.

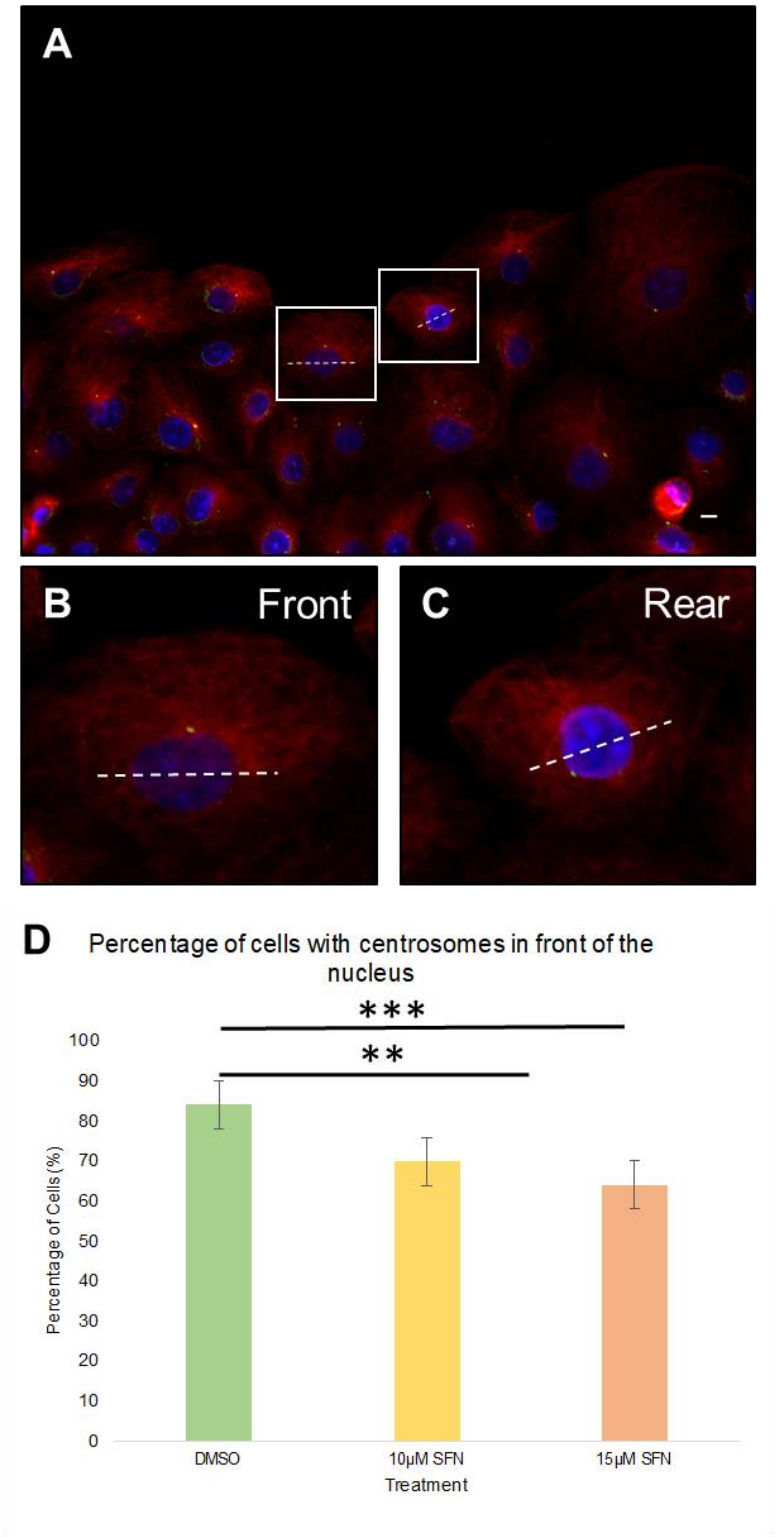

Figure 31 – The percentage of cells with the centrosome in front of the nucleus during cell migration is reduced following treatment with 10 and 15μM SFN. Centrosome position was scored in cells by drawing a line through the nucleus perpendicular to the direction of migration indicated by the lamellipodia (A). If the centrosome was in front of this line relative to cell direction it was scored as in front of the nucleus (B), while if it was behind this line that it was scored as being at the rear of the nucleus (C). Analysis of 50 cells per condition, with each full cell in the images taken was analysed, (D) indicates that treatment with both 10 and 15μM SFN significantly reduces the percentage of cells with their centrosome in front of the nucleus during migration ($p=0.001$ and $p=0.0003$ respectively).

This may explain the differences in SFN effects, as it could be more pronounced in cells that migrate faster prior to treatment.

Using scratch wound immunofluorescence labelling for α- and γ-tubulin, following 17hr of closure in the presence of SFN, the position of the centrosome in relation to the nucleus in cells was scored. By drawing a line across the centre of the nucleus perpendicular to the apparent direction of cell migration the centrosome could be scored as either in front or behind the nucleus (Fig. 31A-C). Scoring of centrosomes in 50 cells per condition indicates that the percentage of cells with their centrosomes in front of the nucleus is significantly reduced by both 10 ($p=0.001$) and 15μM SFN ($p=0.0003$). This change in centrosome positioning may have implications for the directionality of cell movement.

3.3 Discussion

Subjecting the cell lines used in these experiments to Presto Blue assays indicated that the best concentrations to represent low and high doses of SFN were 5μM for a low dose and 10-15μM for a high dose. These concentrations were then employed in the range of experiments used to investigate the effects of SFN on cell migration. The localisation of EB1 was assessed by indirect immunofluorescence in a range of immortalised epithelial cell lines, with comets in breast and pancreatic cancer cell lines appearing shortened following treatment with SFN over 24, and in the case of MCF7 cells, 48hr. The length of EB1 comets tends to reflect the rate of microtubule growth, as the faster monomers are being added to the plus end the larger the GTP cap will become. Therefore, the shortened EB1 comets seen following SFN treatment may reflect a reduction in MT growth rate, which was reported at a dose of 15μM in MCF7 cells by Azarenko and colleagues (2008). It may be that this reduction in velocity due to SFN is also occurring at doses as low as 5μM, where EB1 comets appear to start shortening. This would require quantification, possibly by

comet analysis, to determine if EB1 comets in treated cells are significantly shorter than those in controls. Further investigation via time lapse imaging to ascertain whether MT growth rates do begin to slow at 5μM doses would also corroborate this. It would also be pertinent to investigate why the comets are shortened, an effect which could be due to the reported structure changes in tubulin caused by covalent binding of SFN to Cys303 (Mi et al., 2008). This could affect tubulin polymerisation, as tubulin aggregation was reported following dosing of cells with more potent ITCs than SFN (Mi et al., 2008), or possibly alter the affinity of EB1 CH domains for tubulin.

It doesn't appear from the immunofluorescence studies that SFN has a large effect on levels of acetylation, which does not necessarily agree with previous reports of inhibition of HDAC6 by SFN. Western blot analysis of acetylated tubulin levels in another pancreatic cell line, Capan-1, did not appear to show any changes in acetylation either. However, due to potential variations between cell types quantification of acetylated tubulin via western blotting in Panc-1 cells and the two breast cancer cell lines would be required for confirmation of the immunofluorescence observations. Forced overexpression of HDAC6 in the cell lines used could be carried out, as overexpression of HDAC6 has been shown to override the inhibitory effect of SFN (Gibbs et al., 2009), and this may reverse the reduction in cell migration observed in scratch assays.

Scratch wound assays, in which percentage closure of a cell free area was calculated following live imaging experiments, showed significantly slower closure at 10 and 15μM SFN, particularly in MDCKII cells. Manual tracking of both Panc-1 and MDCKII cells at the forefront of the encroaching monolayers also indicated a reduction in both velocity and total distance travelled by cells exposed to 10 and 15μM SFN. Panc-1 cells appeared more resistant to the effects of SFN, however, this may reflect that they are also less susceptible to cell cycle arrest, and, as shown by cell tracking data, have a lower baseline speed of migration. Despite this, when

cell division was blocked using thymidine in Panc-1 cell layers there still appeared to be reduced closure in conditions treated with 10 and 15μM SFN. This indicates that the effect seen in MDCKII and Panc-1 cells is potentially mainly due to effects of SFN on cell migration, however, these experiments would need to be repeated with a thymidine block to determine this for certain. Reduction of cell migration in the presence of cell division inhibitors has been previously reported (Hung et al., 2013), and further investigation to determine the mechanism by which SFN reduces cell migration is required, although it is not illogical to suggest that reduction of microtubule dynamics by SFN, as shown by Azarenko and colleagues (2008), could contribute to this. There could also be an effect on the actin cytoskeleton which has not yet been thoroughly investigated, but it has been suggested that SFN reduces the amount of F-actin, possibly through TNFα (Hung et al., 2013).

Although tracking data did not seem to indicate a loss of directionality in cells during SFN treatment at 10 or 15μM, analysis of centrosome positioning in Panc-1 cells at the leading edge of the closing scratch wound using immunofluorescence indicated that doses of 10 and 15μM SFN significantly reduce the percentage of cells which have centrosomes positioned to the front of the nucleus. This would require further investigation, possibly using micro-patterned slides to influence cells to adopt front-to-rear polarity as in migration. Using these micro-patterns precise scoring of centrosome position relative to the nucleus would be possible as the direction of cells would be oriented by the patterns, whereas it is more subjective to determine direction based on lamellipodial protrusions in immunolabelled scratch wounds. The centrosome is not essential in itself for cell crawling in all cell types (Verhovsky et al., 1999), however centrosome positioning in front of the nucleus, behind the lamellipodium, has been shown to be important in cell directionality, and changes in direction of lamellipodial protrusions lead to reorientation of the centrosome which stabilises the direction of movement (Ueda et al., 1997). It is thought that the position

of the nucleus and centrosome in relation to migratory front-to-back polarity is important for MT nucleation and organelle positioning during migration. It has been shown that disruption of proper nuclear positioning slows the rate of migration in multiple cell types including fibroblasts (Gant Luxton and Gundersen, 2011).

It can be taken from these investigations that there most likely is an effect of SFN on the rate of wound closure in 2D layers, and that this is possibly linked to cell migration in particular, as opposed to effects on cell proliferation. Taking into account previous evidence provided indicating that SFN reduces migration of cells and affects MT dynamics, one would suggest that further work should focus on determining the effect of SFN on the dynamics of MTs at the leading edge of cells using live imaging and on the actin cytoskeleton, an aspect of SFN function that has not been properly investigated to date. Further upstream regulation of migration and adhesion formation by SFN, through modulation of the expression of the Rap1-specific GAP, Rap1GAP, may also have an effect on cell migration and play a role in the underlying mechanism behind the results discussed in this section. An investigation of the link between SFN and Rap1GAP expression will be discussed in the following chapter.

Chapter Four

Sulforaphane and Rap1GAP in Epithelial Cells

4.1. Introduction

Migration and invasion of cells may be modulated by other means aside from direct interaction with the cellular cytoskeleton. Instead, signalling proteins upstream of cytoskeletal and adhesion proteins may be modulated. Many of these upstream proteins are small GTPases or their regulatory proteins, GEFs and GAPs. A number of these proteins have been implicated in the migration and invasion of cancer cells during tumour progression, with some, the GTPases in particular, tending to increase invasion, while others, generally the inactivating GAPs, have been shown to act in a tumour supressing capacity.

The term small GTPase encompasses a wide range of proteins, sometimes also called small G proteins, which range from 21 to 30kD in size (Yang, 2002) which possess a conserved molecular switch mechanism facilitating cycling between active GTP-bound and inactive GDP-bound states (Mishra and Lambright, 2016). Small GTPases evolved with relatively low dissociation constants, and therefore slowly hydrolyse GTP at low turnover rates. As a result, two classes of regulatory proteins co-evolved with the small GTPases which can exchange GDP for GTP and accelerate hydrolysis. Exchange of GDP for GTP, mediated by GEFs, leads to conformational changes within the GTPase, which can then in turn be recognised by certain effector proteins, which would not recognise the inactive conformation. Accelerated hydrolysis of GTP, involving nucleophilic attack on the terminal γ phosphate and cleavage of the phospo-monoester bond, is facilitated by GAPs, and can increase the intrinsic hydrolysis rate by as much as 10^5-fold. In the case of RasGAPs this reaction is facilitated by an arginine finger which protrudes into the GTPase active site to stabilise the transition state of the hydrolysis reaction (Ahmadian et al., 1997).

Structurally, the Small GTPases share a core GTPase domain composed of 5 α-helices clustered around a six-stranded β-sheet (Vetter and Wittinghofer, 2001).

A total of five G-motifs are present in the sequence to coordinate with the nucleotide and an essential Mg^{2+} ion which facilitates high affinity binding to the nucleotide and hydrolytic activity (Bourne et al., 1991). The third of these, the DxxG motif, is generally followed by a glutamine residue which is important in catalysis (Mishra and Lambright, 2016). The N- and C- terminal domains extending out from the GTPase core display variation between and even within subfamilies, but these may include further motifs or structural features which confer further functionality, including those pertaining to subcellular localisation or effector specificity (Mishra and Lambright, 2016).

Activation of GTPases is connected to extracellular stimuli via GEFs, which once activated, generally by second messengers incited by a range of signalling events, act to weaken the affinity of the inactive protein for GDP, leading to its dissociation and replacement, generally with GTP due to higher intracellular concentrations of the triphosphate form (Zhang et al., 2017). Often GTPases are acted upon by multiple GEFs, which can in turn respond to different second messengers, functionally this allows fine tuning of the spatiotemporal activation, and therefore function, of GTPases, so certain stimuli will elicit activation of a given GTPase in particular intracellular compartments depending on the initial signalling input. The situation is similar in terms of GAPs, where there may be more than one GAP which can inactivate a certain GTPase.

In this chapter, results will focus principally on Rap1 and its specific GAP, Rap1GAP. As described earlier in the text, there are two loosely related rap families, Rap1 and Rap2, each comprising two closely related isoforms, A and B. Despite sharing approximately 50% sequence identity with Ras proteins, Rap1 proteins have a few key structural differences to the other members of the GTPase family. Contrary to the catalytic glutamine found in many GTPases, Rap GTPases possess a non-catalytic threonine in the same position (Mishra and Lambright, 2016). Correspondingly, Rap1GAP differs in its catalytic mechanism, as RapGAPs are not

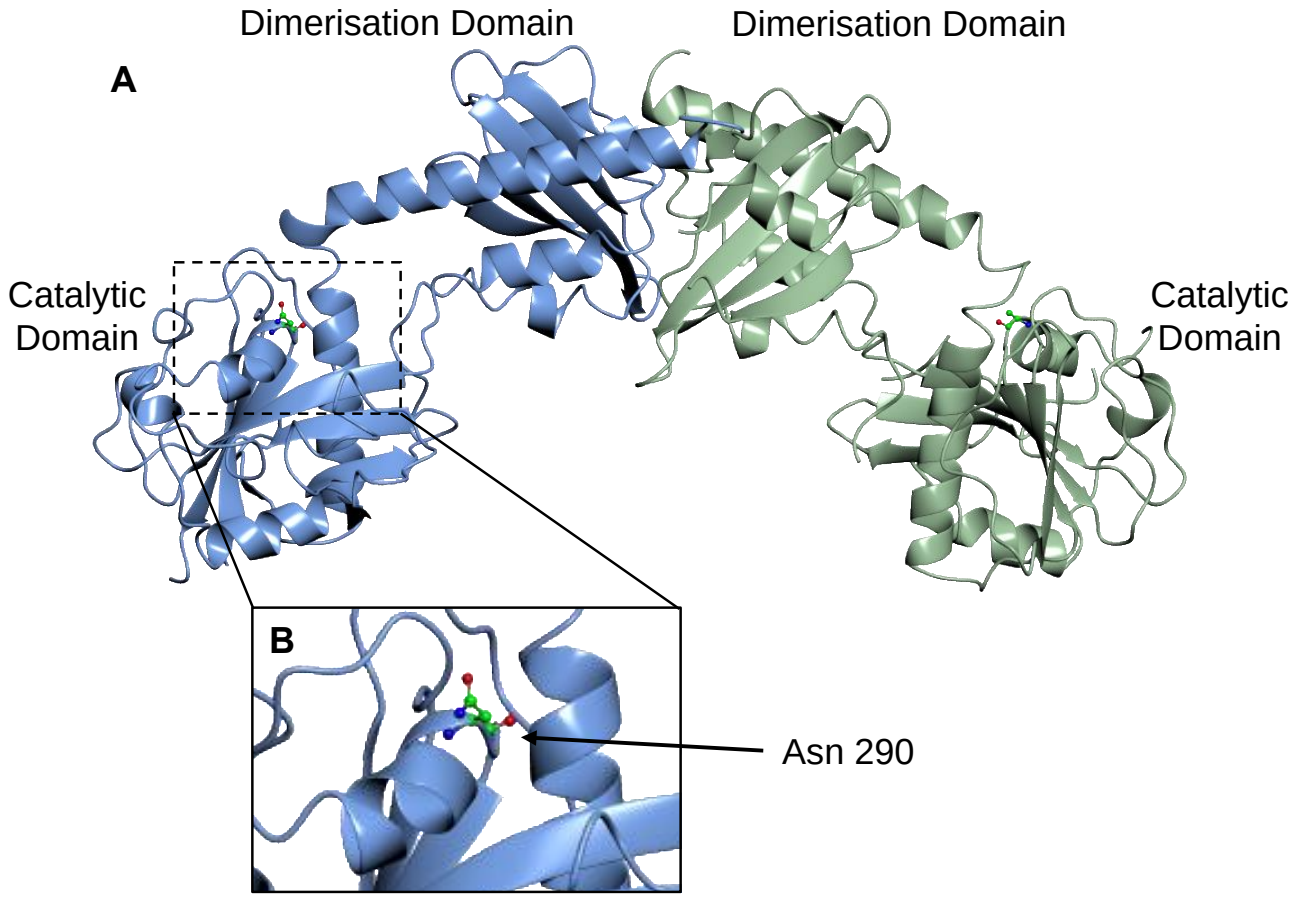

Figure 32 – Crystal structure of Rap1GAP to show the ball-and-stick representation of the catalytic asparagine thumb. Rap1GAP operates as a dimer, as shown by the blue and green monomers joined via the dimerization domains (A). Within the catalytic domain is Asn290, the catalytic asparagine, which is distinct to the consensus arginine finger found in other GAPs. Mutation of this residue leads to loss of Rap1GAP activity. Image generated using CCP4MG and PDB file 1SRQ (Deposited by Daumke et al., 2004)

related to other GAPs, therefore instead of a catalytic arginine, they offer a catalytic asparagine, dubbed an asparagine thumb (Fig. 32). Mutation of this catalytic asparagine, at position 290, completely ablates Rap1GAP activity on Rap1 proteins (Daumke et al., 2004). Due to their 95% sequence similarity, Rap1GAP is able to regulate the deactivation of both Rap1A and Rap1B isoforms (Zhang et al., 2006).

Expression changes in Rap1 have also been implicated in cancer development and progression. Rap1 has multiple roles in the cell, including the inside-out activation of integrins where integrins are activated by proteins within the cells, rather than by matrix proteins in the ECM (Bos, 2005). It is likely to be a key regulator of cell adhesion formation and maturation in epithelial cells via interactions with E-cadherins (Matthijs et al., 2006). Rap1 has also been shown to have a role in guiding the directionality of cells during migration. At their leading edge, cells possess a number of dynamic activated integrins which associate with actin filaments in small protrusions known as ‘sticky fingers’, which are key in the sensing of the surrounding ECM to guide migrating cells. Within these structures, activated Rap1 binds to a Ras association domain in Rap1-GTP-interacting adaptor molecule (RIAM; Zhang et al., 2014), to form a complex which localises to the plasma membrane via a pleckstrin homology domain in RIAM. Once at the membrane, the complex recruits talin to facilitate inside-out β-integrin activation (Wynne et al., 2012). Activated integrins can then be linked to the actin cytoskeleton through actin adaptor proteins (Fig 33; Lagarrigue et al., 2015). This complex has been shown to play a key role in integrin-mediated adhesion of T-cells and their homing to lymph nodes (Calderwood, 2015), and therapeutic targeting of this process may be a method to reduce tumour metastasis, which is largely dependent on integrin contacts with the ECM. The increase in invasive behaviour of cells seen following downregulation or loss of heterozygosity of Rap1GAP (Tsygankova et al., 2013) adds support to this notion, as when Rap1 activity is allowed to persist in cells they are better able to move through the ECM.

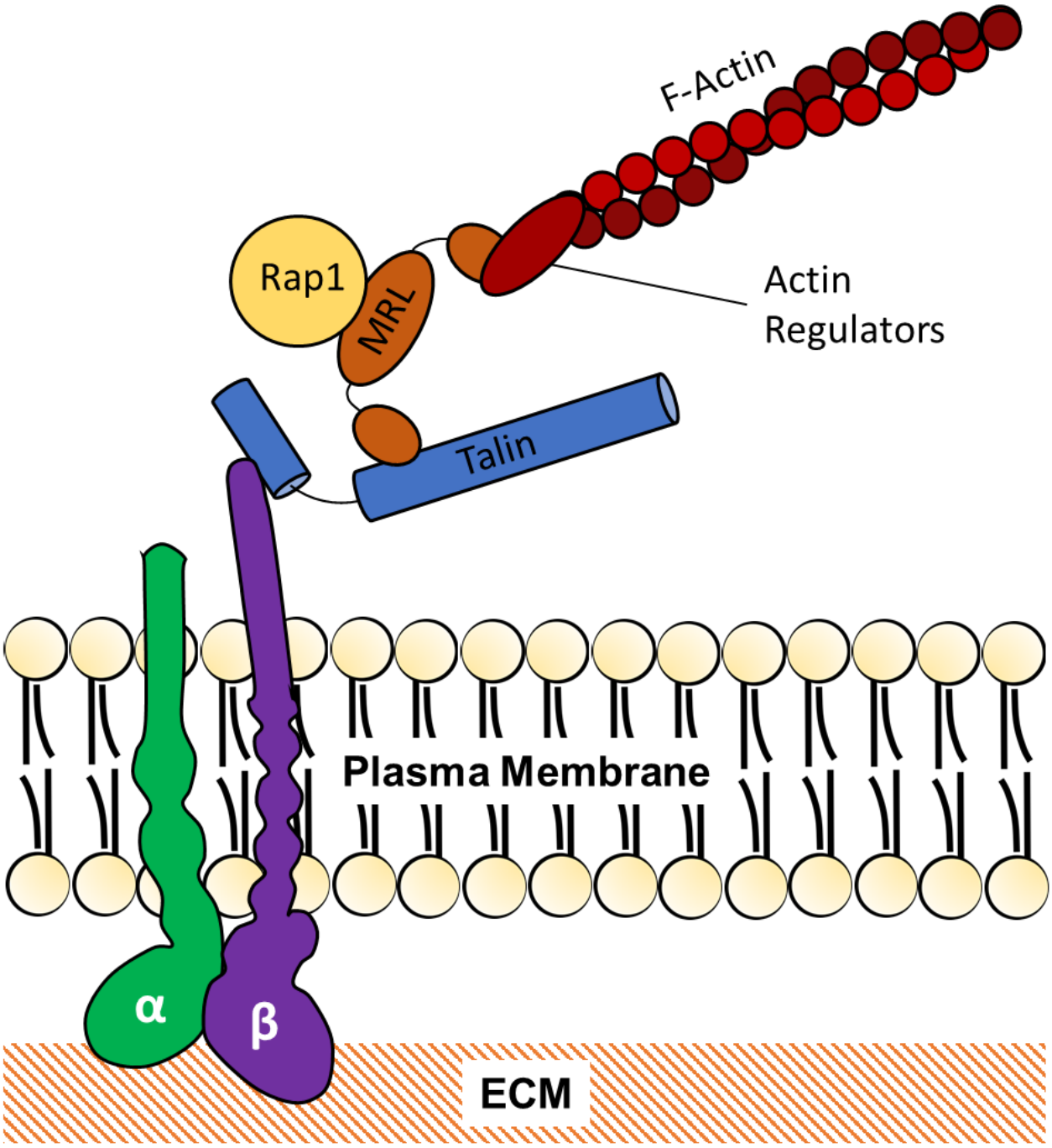

Figure 33 – Schematic of MRL, Talin, Integrin complexes which form at the tip of 'sticky fingers' during migration. At the leading edge of cells sticky fingers form form to guide migration, with complexes linking integrins to the actin cytoskeleton facilitating initial adhesions with the ECM. Actin filaments, via regulatory proteins, are linked to talin through the Mig-10/RIAM/Lamellipodin (MRL) family proteins RIAM or lamellipodin, denoted in this diagram as MRL. Complex formation is initiated by activated Rap1 binding to RIAM or other MRL proteins, which then localise to the plasma membran and recruit talin, which is a common protein involved in activation of many β integrins *in vitro*. Adapted from Lagarrigue et al., 2015

Previous microarray data obtained in the lab, indicated that Rap1GAP was the most upregulated transcript in Panc-1 EB2^{Hi} cells following 48hr treatment with SFN. This observation warranted further investigation due to Rap1GAP's reported role as a putative tumour suppressor in multiple cancer types. Immunohistochemical staining revealed a link between expression of Rap1GAP in resected tumour samples and better overall patient survival, especially if E-cadherin expression levels were also simultaneously high (Tamate et al., 2017). In renal cell carcinoma cell lines, it was shown that although Rap1GAP expression appeared to have no effect on migration, it was inversely correlated with invasion in matrigel, collagen or fibronectin-coated Boyden chambers, a behaviour that could be reduced by forced overexpression of Rap1GAP (Kim et al., 2012). In oropharyngeal squamous cell carcinoma cell lines, expression of Rap1GAP was shown to lead to a reduction in active Rap1 and downregulate ERK activation, leading to reduced proliferation in these cell lines compared to normal keratinocytes (Zhang et al., 2006). Due to this tumour-suppressive role for Rap1GAP it is often downregulated in cancers, for example by promoter hypermethylation (Kim et al., 2012). Allelic loss of Rap1GAP was reported in papillary thyroid cancers following histological analysis of tumour sections from patients (Nellore et al., 2009). This downregulation, both by loss of heterozygosity and promoter hypermethylation, was linked to the more aggressive forms of thyroid cancer (Zuo et al., 2010), and to increased invasion in colorectal cancer cell lines (Tsygankova et al., 2013) highlighting Rap1GAP's behaviour as a tumour suppressor gene.

4.2. Results

4.2.1. Rap1GAP is upregulated in Panc-1 cells following 24hr SFN treatment

Analysis using previously obtained microarray data (Alqurashi, unpublished) highlights Rap1GAP as the most upregulated gene in Panc-1 cells

A

Top hits in microarray following 48hr SFN Treatment			
Upregulated		**Downregulated**	
Gene	LogFC	Gene	LogFC
Rap1GAP	1.74	CD24	-1.68

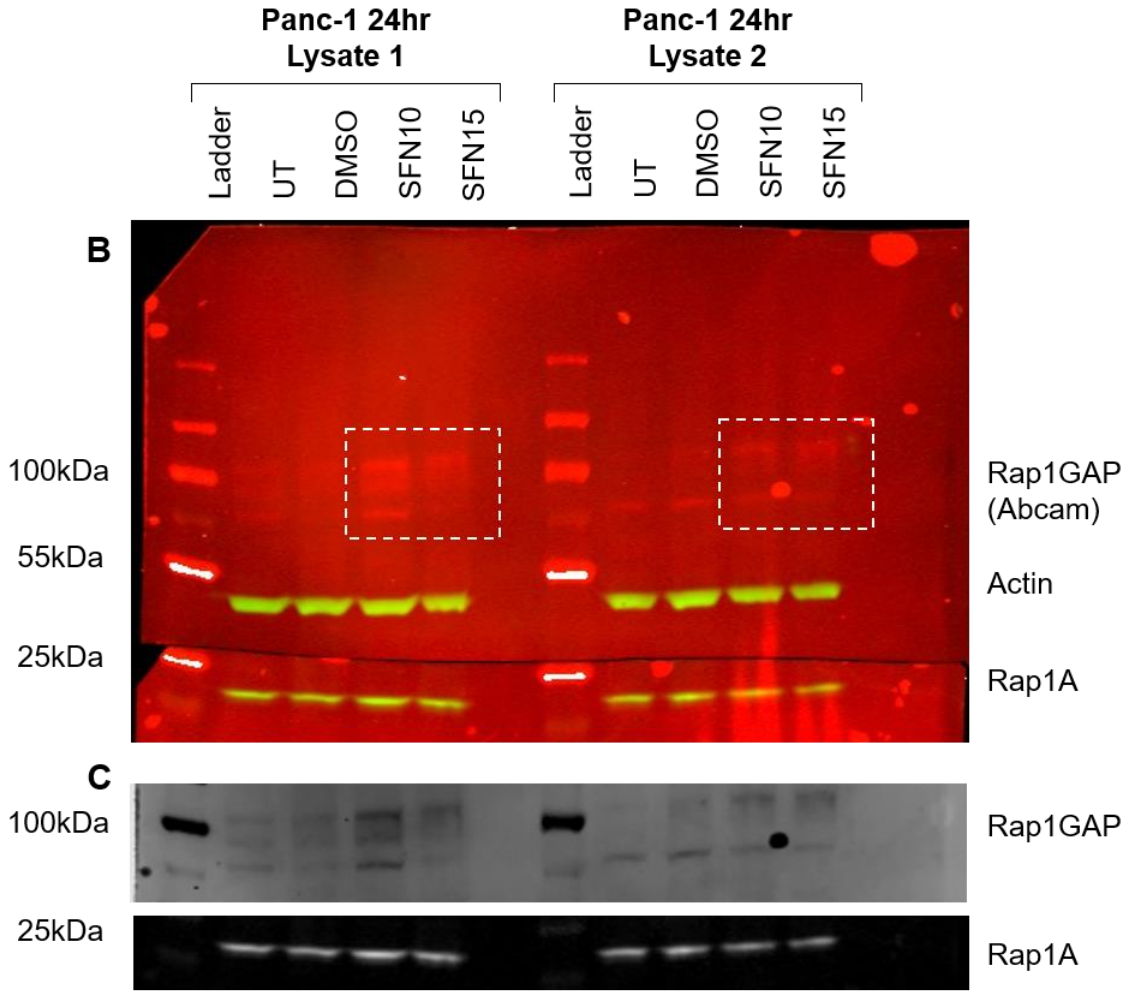

Figure 34 – Rap1GAP is upregulated at the RNA and protein level following treatment with SFN. Microarray analysis of RNA extracts from Panc-1 cells treated with 10μM SFN for 48hr indicated 986 significantly differentially expressed genes, (A) shows the top up- and down-regulated genes. Rap1GAP is the most upregulated gene in comparison to control cells, with a LogFC value of 1.74, which translates to an almost four-fold increase in expression in real terms. While the most down-regulated gene was the adhesion molecule, and CSC marker, CD24. Western blotting using whole cell lysates (B) also indicates that levels of Rap1GAP proteins increase in whole cell lysates following 24hr SFN treatment while Rap1A levels appear to be unchanged. This can be seen clearer in black and while images of the blots at around 100 and 25kDa.

following 48hr treatment with 10μM SFN (Fig. 34A), as indicated by the log fold-change (logFC). Interestingly, the most downregulated gene was the adhesion molecule, and reported marker of CSCs, cluster of differentiation 24 (CD24). No further investigation into the role of this downregulation in SFN treated Panc-1 cells was conducted due to time constraints, but it could be followed up in the future.

In order to confirm this at the protein level, western blotting of whole cell lysates collected from Panc-1 cells following 24hr treatment with SFN was performed. The blots indicate an upregulation of Rap1GAP protein in both 10 and 15μM SFN conditions compared to UT and DMSO vehicle controls. Rap1GAP appears as a triple band around 95kDa using the Abcam antibody (Y134), possibly reflecting different phosphorylation states of the protein, or perhaps low specificity of the antibody. The western blot also suggests that levels of the 21kDa Rap1A protein remain constant following SFN treatment (Fig. 34B-C).

Western blot analysis was also performed on lysates from MDA-MB-231 cells, in order to determine if Rap1GAP upregulation occured in another epithelial cell line from a different tissue. Interestingly, despite the highly metastatic background of MDA-MB-231 cells, originating from a triple-negative breast cancer metastasis, these cells appeared to express high levels of tumour suppressive Rap1GAP when compared to the Panc-1 cells (Fig. 35A), despite roughly similar levels of protein being loaded (59.25μg for Panc-1 and 50.86μg for MDA-MB-231). However, there does not seem to be any effect on expression of Rap1GAP by SFN in MDA-MB-231 cells (Fig. 35B).

4.2.2. Rap1GAP in epithelial cells

Immunofluorescence labelling of Panc-1 cells using the Abcam anti-Rap1GAP antibody indicated the presence of filamentous Rap1GAP networks, which did not directly co-localise with MTs, in a proportion of cells (Fig. 36). These filament

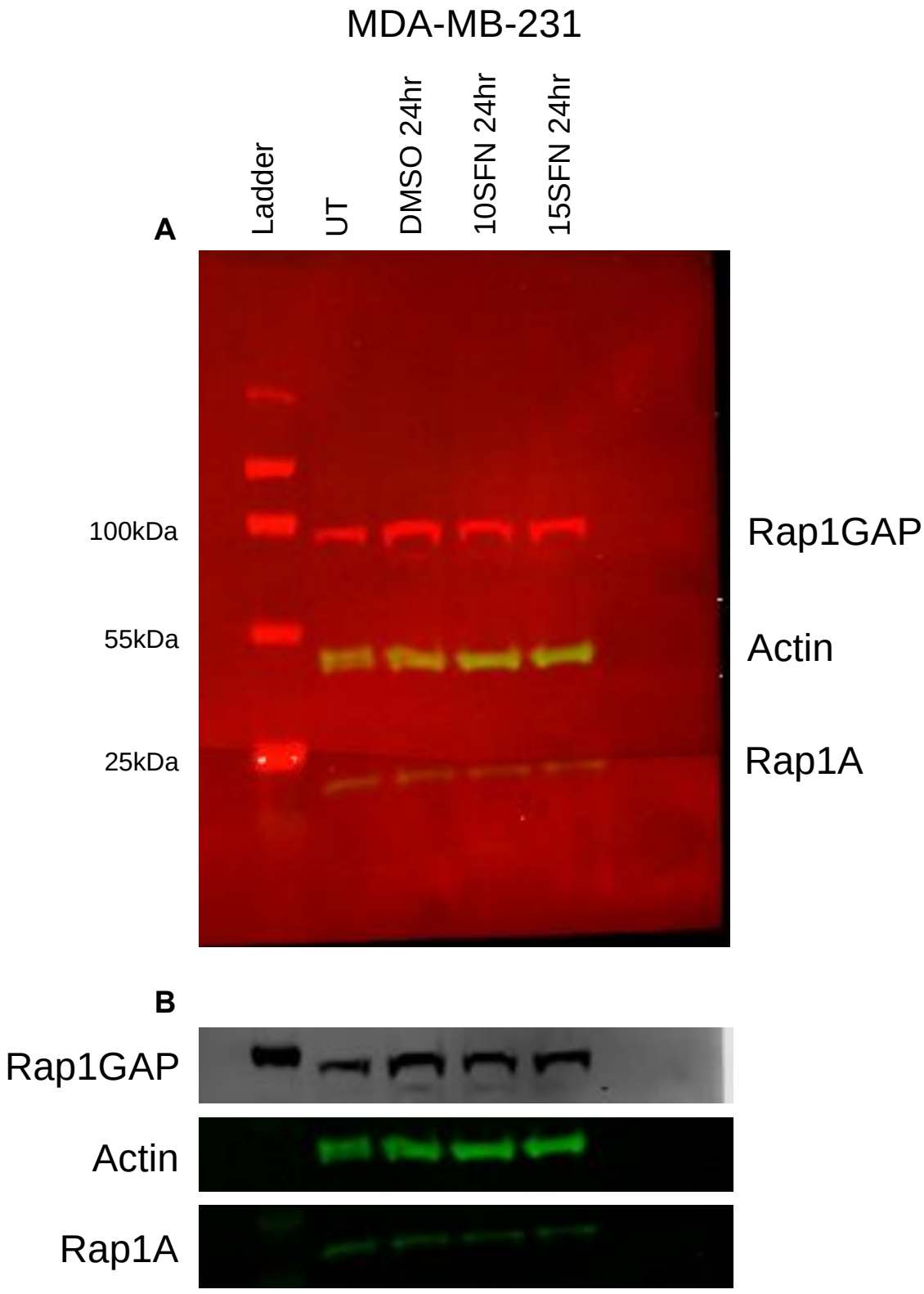

Figure 35 – MDA-MB-231 cells express high levels of Rap1GAP protein, but this is not upregulated by 10 or 15μM SFN. High levels of Rap1GAP, and low levels of Rap1A, are expressed in MDA-MB-231 triple negative breast cancer cells (A). However, SFN does not appear to lead to an upregulation of Rap1GAP protein at 10 or 15μM (B).

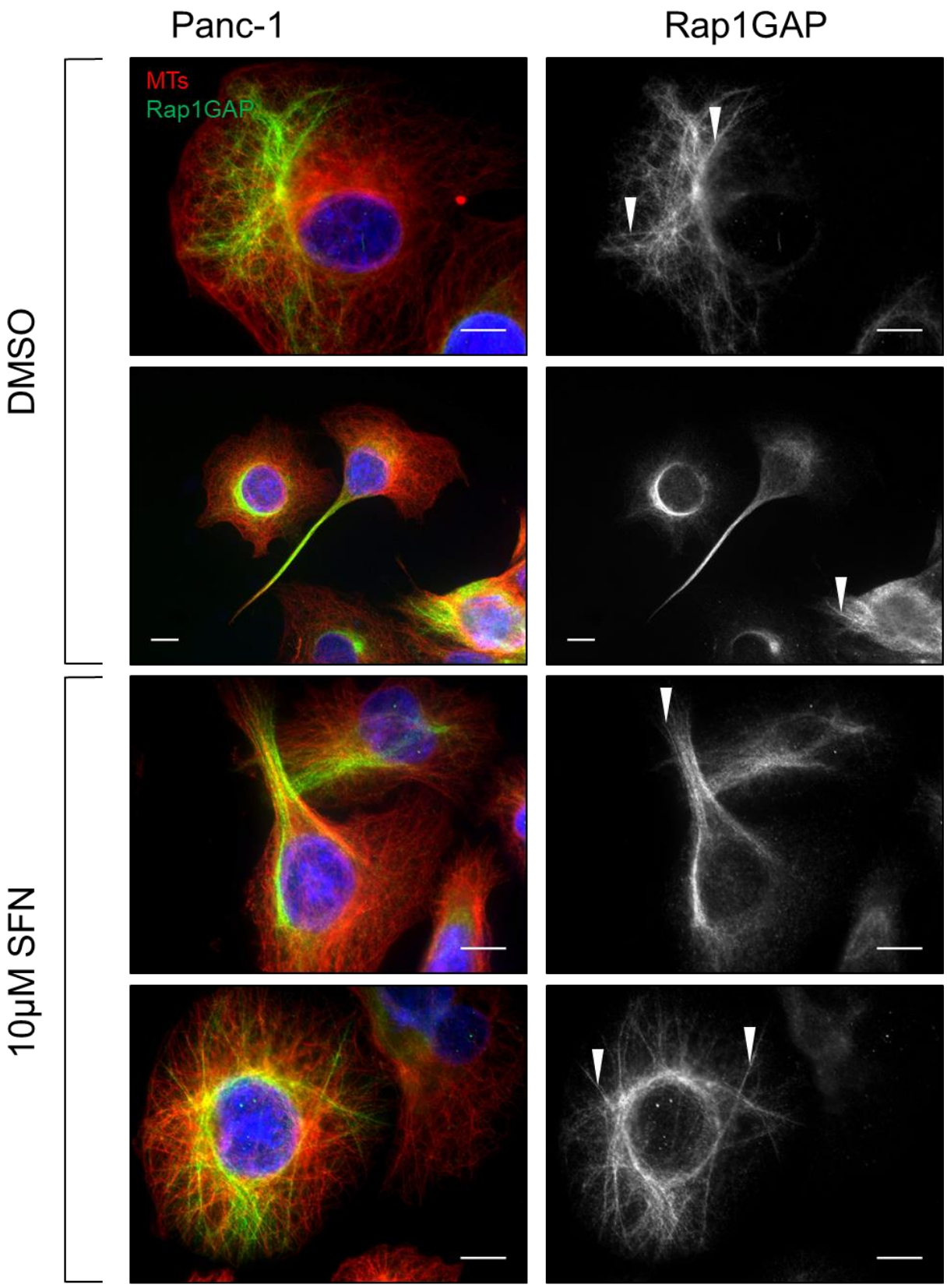

Figure 36 – Rap1GAP appears to be localised in filament-like networks within Panc-1 cells labelled using Abcam anti-Rap1GAP antibody. Networks (White arrows) were seen in a large number of both control and treated Panc-1 cells labelled with a Rap1GAP antibody purchased from Abcam. These networks do not seem to follow the patterns of the MT network. Scale bars = 10μm, images representative of 15 cells per condition.

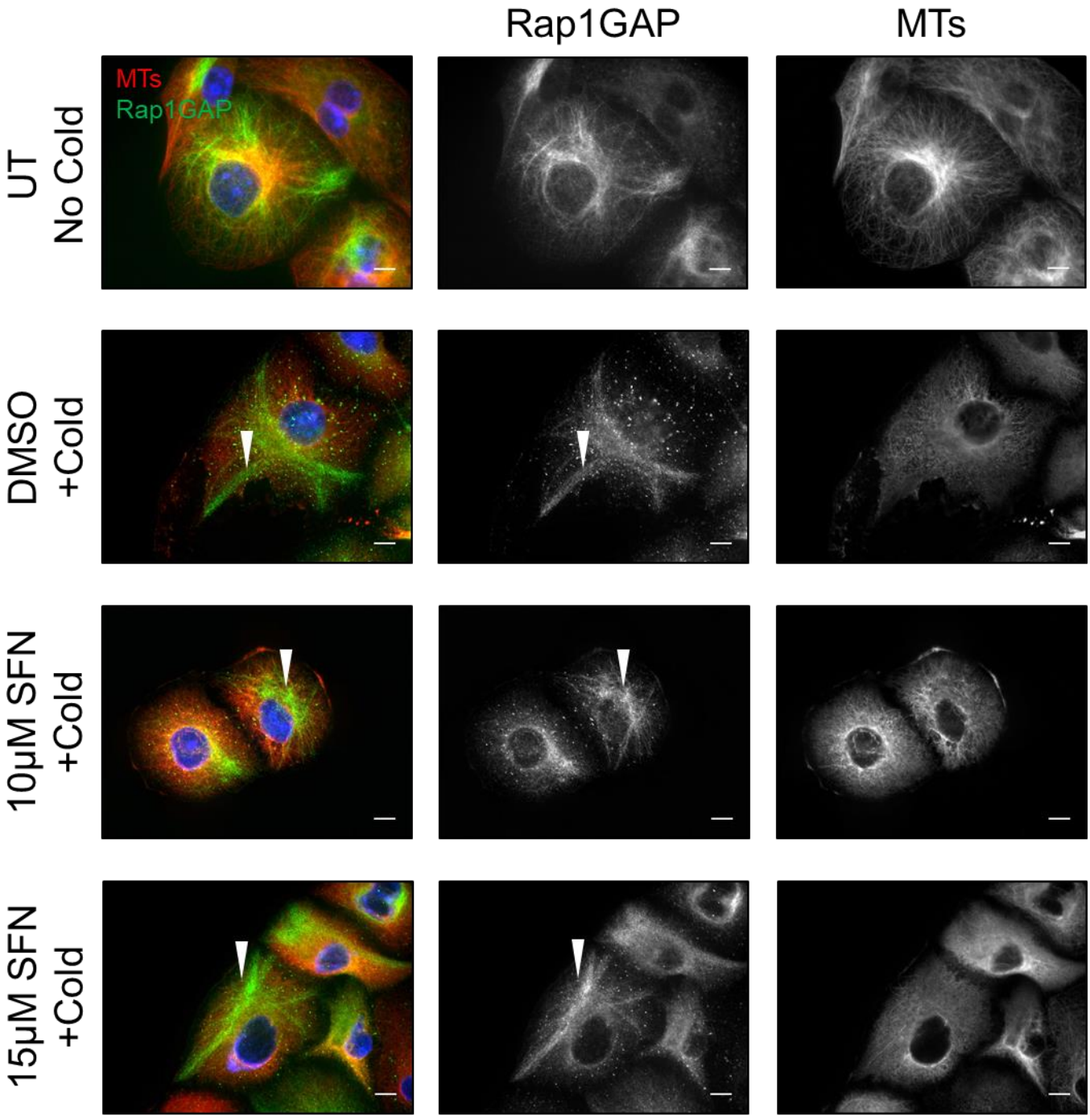

Figure 37 – Network-like localisation indicated in Panc-1 cells by Abcam Rap1GAP antibodies are resistant to cold treatment. The filament-like arrangements of Rap1GAP detected by the Abcam antibody are likely not due to Rap1GAP, or erroneous antibody, association with MTs as they are resistant to cold treatment, which leads to depolymerisation of the majority of the radial MT network in cells. Scale bars = 10μm images representative of 15 cells per condition.

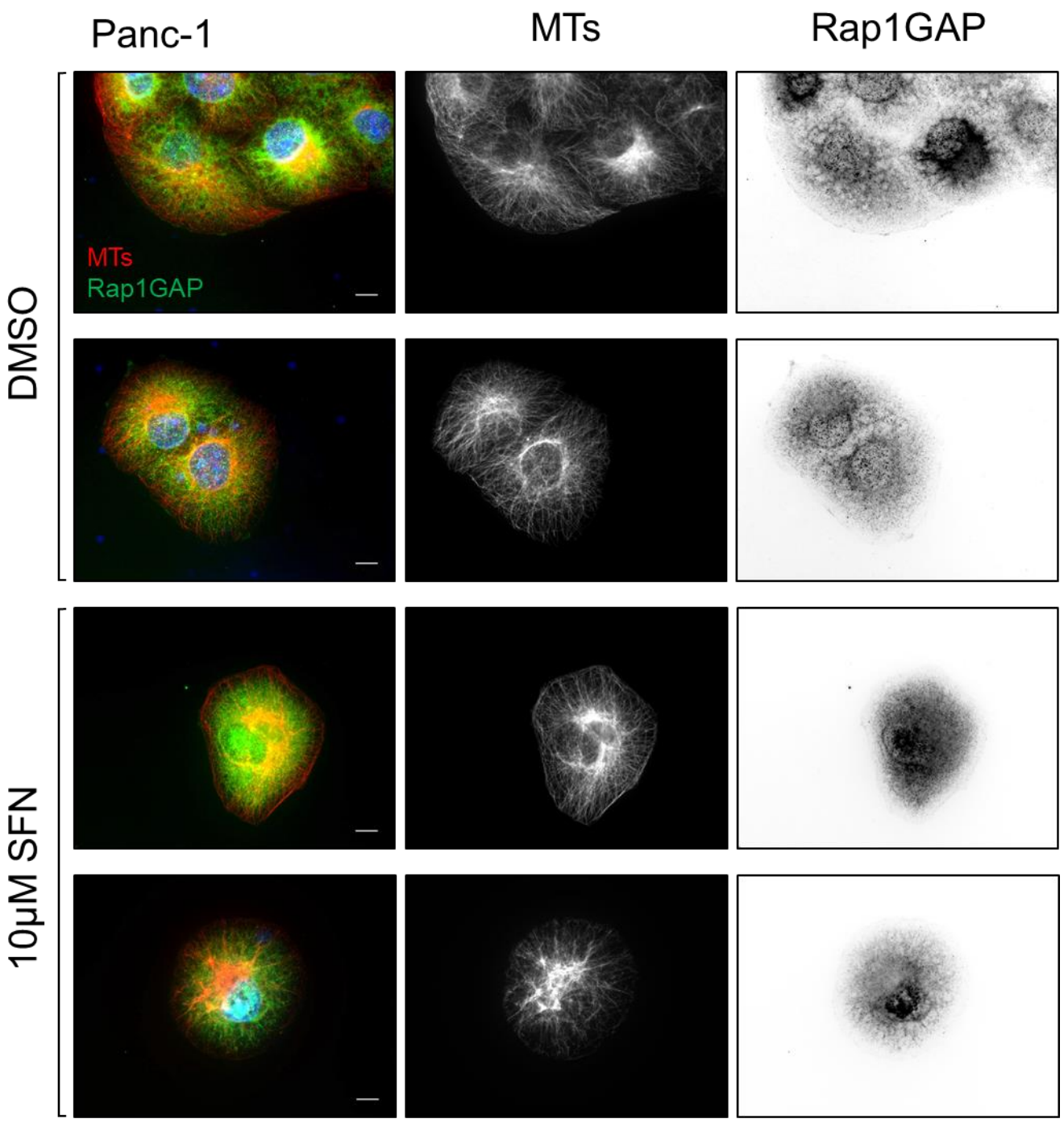

Figure 38 – Labelling of Panc-1 cells with anti-Rap1GAP antibody from santa cruz indicates global, punctate distribution of Rap1GAP, with no filamentous localisation. Filament-like localisation, as seen with the Abcam antibody, is not indicated by a different antibody from Sant Cruz biosciences, indicating that there may be potential off-target binding of the Abcam antibody. Scale bars = 10μm, images representative of 15 cells per condition.

like localisation patterns indicated by the abcam anti-Rap1GAP antibody were resistant to cold treatment, and persisted in cells after 15min on ice, despite the loss of radial microtubule networks (Fig. 37). However, when Panc-1 cells were labelled using a different anti-Rap1GAP antibody obtained from Santa Cruz Biotechnology these networks were not detected (Fig. 38), and instead Rap1GAP appeared to localise in a diffuse manner throughout the cells. The diffuse staining throughout Panc-1 cells detected using the Santa Cruz antibody was not dissimilar to the localisation patterns present in another epithelial cell line, ARPE-19, when labelled with the Abcam antibody, a cell line in which no filamentous distribution of Rap1GAP was apparent (data not shown).

To determine if the filamentous pattern was co-localising with actin filaments, Panc-1 cells were labelled for Rap1GAP and actin, using phalloidin in PHEMO fixed cells (Fig. 39A-F), and there appears to be co-localised clusters of Rap1GAP and actin near the cell periphery in protrusions resembling lamellipodia in both control cells and those treated with 10μM SFN (Fig. 39G-H). These points could potentially be focal adhesions. However, these regions are not observed when actin is labelled with antibody in MeOH fixed Panc-1 cells (Fig. 40A-F). Some co-localisation between Rap1GAP and actin can be detected at the cell cortex (Fig. 40G-J) To try and determine if Rap1GAP is present at FAs, Panc-1 cells were labelled for both Rap1GAP and FA component, paxillin, however, no apparent co-localisation between the two proteins was observed, even following incubation with 10 and 15μM SFN for 24hr (Fig. 41), at odds with the earlier indication of localisation with actin at adhesion points (Fig. 40).

Due to Rap1GAP being a putative TSG, and suggestions that EB2 may be a factor in cancer progression, localisation of both these proteins was assessed by immunofluorescence to determine if cells expressing high levels of EB2 had supressed Rap1GAP, facilitating a more aggressive and invasive phenotype. In some cells with relatively high EB2 levels there does appear to be lower levels of Rap1GAP, while those with high Rap1GAP have lower EB2 levels. However, some cells appear to have intermediary levels of each protein (Fig. 42).

Immunofluorescence techniques were also used to investigate the localisation of the Rap1GAP target, Rap1A, in epithelial cell lines. In untreated ARPE-19, MDA-MB-231 and Panc-1 cells Rap1A appears to localise in puncta throughout the cell (Fig. 43A-I), with some evidence of co-localisation with MTs, which may be protein contained in vesicles being transported along filaments (Fig. 43J-L). In MDA

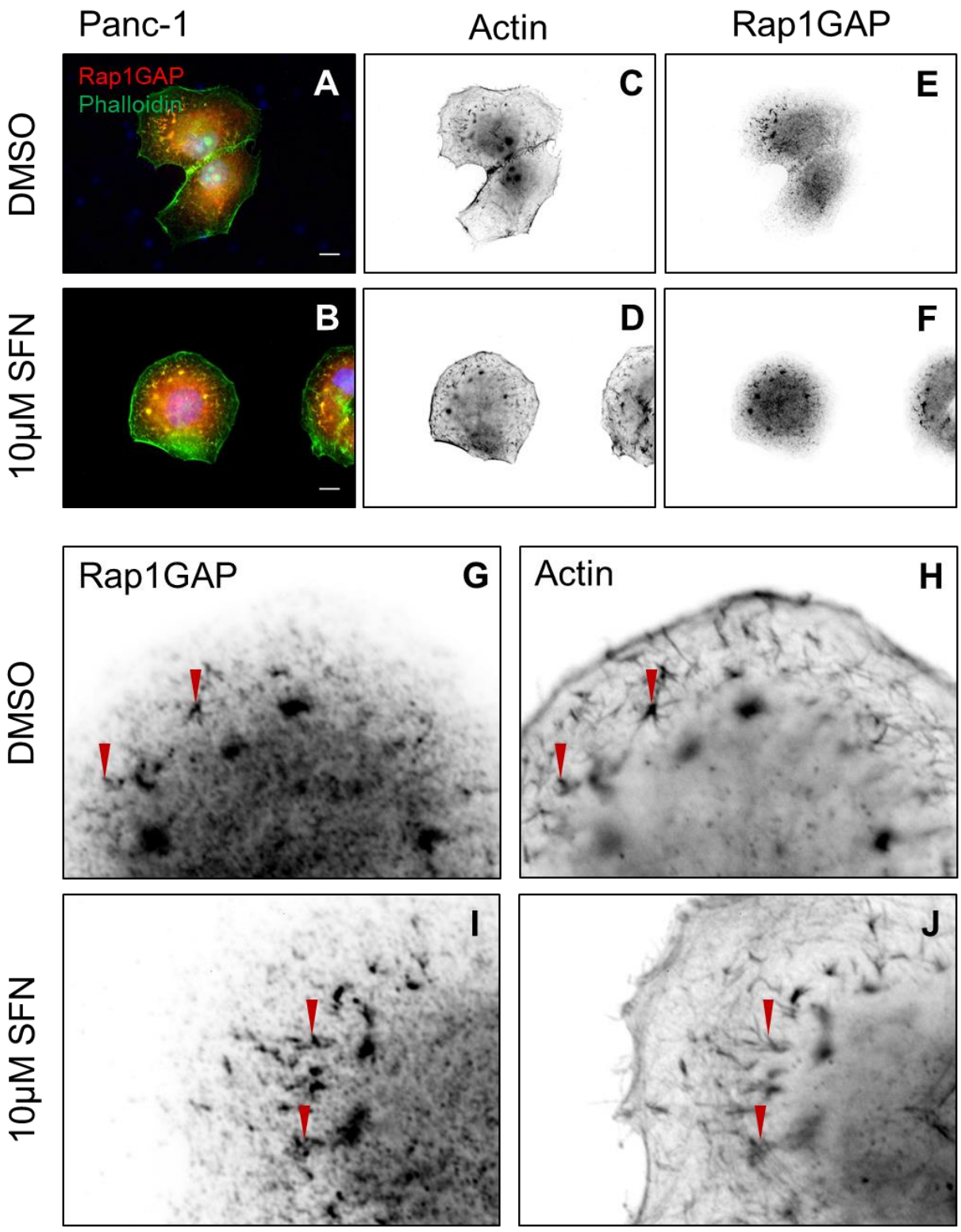

Figure 39 – Rap1GAP and actin, as detected by phalloidin, in Panc-1 cells indicates some co-localisation at adhesion sites. PHEMO-fixed Panc-1 cells labelled for actin and Rap1GAP appear to indicate some co-localisation at points near the cell periphery, potentially focal adhesions (A,B). Actin in Panc-1 cells appears disorganised, and is principally present at the cell cortex with very little evidence of bundled stress fibres in both control and treated cells (C,D). Rap1GAP appears as large and small puncta throughout the cells (E,F), with collections of the protein co-localising with collections of short actin fibres which appear to congregate on one point, potentially focal adhesions (G-J; red arrows), even in the presence of 10μM SFN. Scale bars = 10μm, images representative of 15 cells per condition.

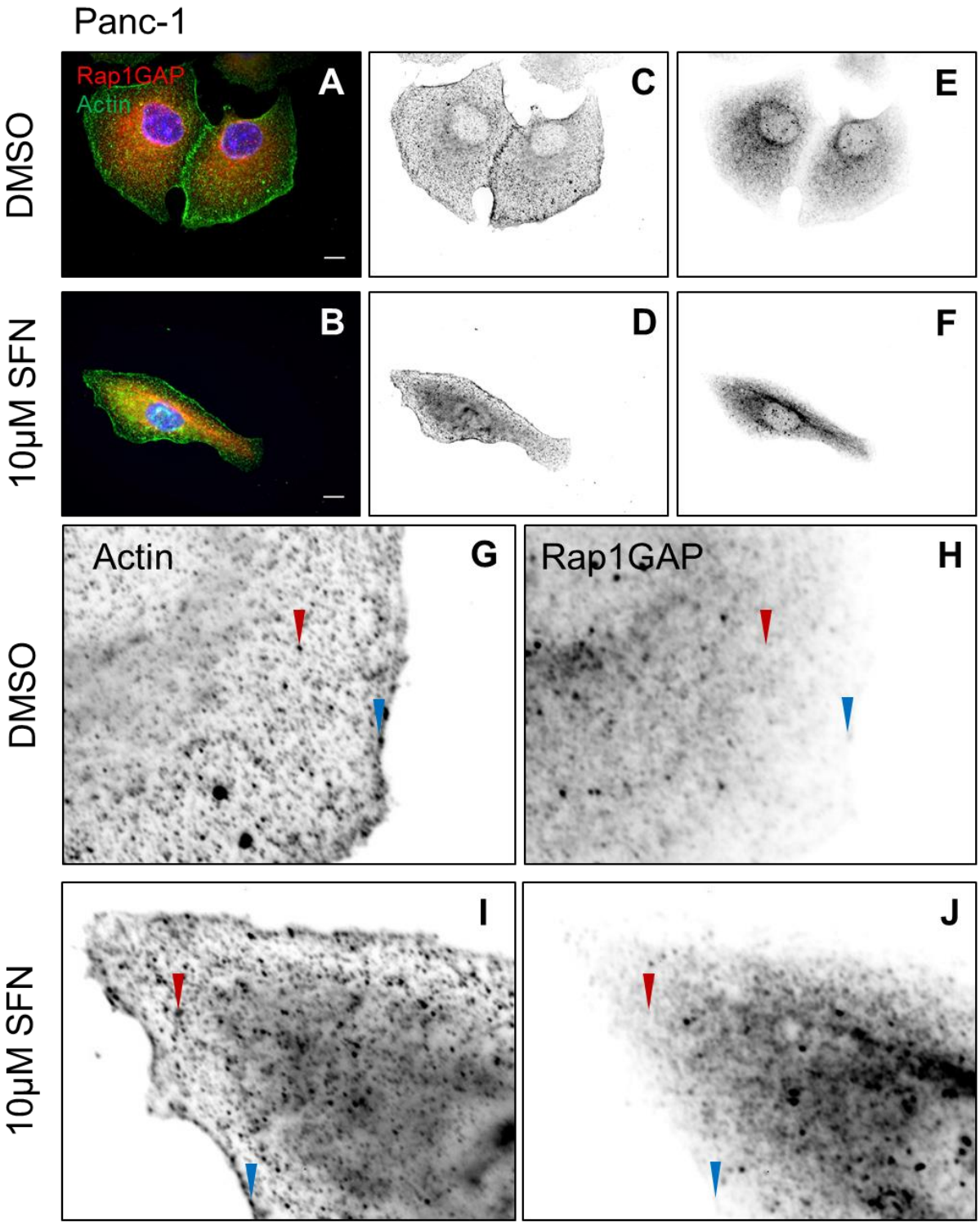

Figure 40 – Actin, as detected with an antibody, doesn't appear to show co-localisation with Rap1GAP following treatment with 10μM SFN. No extensive co-localisation between Rap1GAP and actin was seen when actin was labelled with an antibody instead of phalloidin as in Fig. 34 (A,B). Actin was still seen mostly at the cell periphery, with little evidence of stress fibres or the potential focal adhesion regions seen in phalloidin labelled cells (C,D). Rap1GAP can be seen in a diffuse pattern within the cell, without the large collections of proteins in regions near the cell periphery (E,F). In close up views of both actin and Rap1GAP labelling large amounts of co-localisation are not readily identifiable at potential focal adhesion sites (G-J; red arrows), however, there does appear to be some co-localisation of Rap1GAP with actin at the cell cortex (blue arrows). Scale bars = 10μm, images representative of 15 cells per condition.

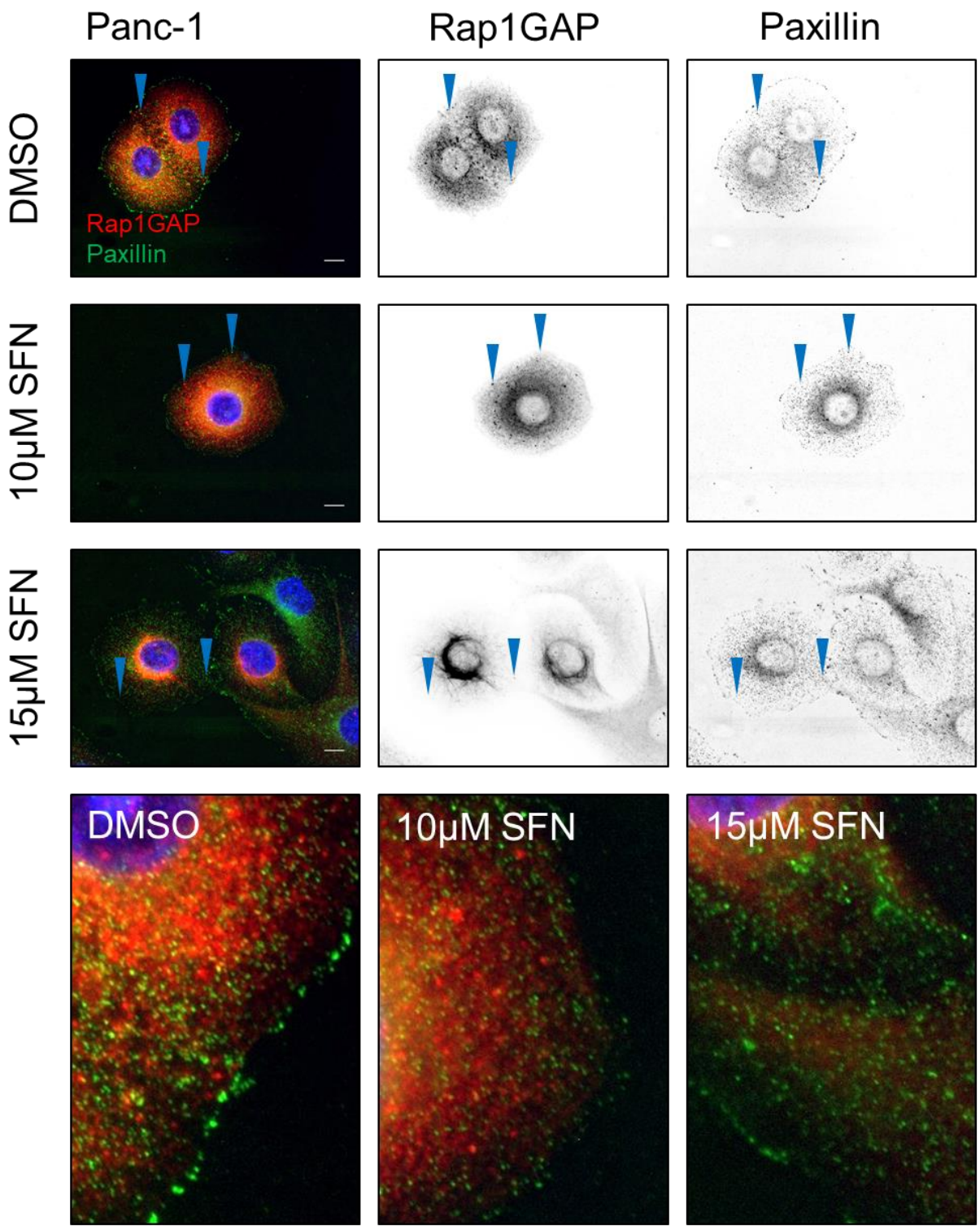

Figure 41 – Immunofluorescence labelling of FA protein paxillin didn't indicate colocalisation with Rap1GAP, even in the presence of 10 and 15μM SFN. Panc-1 cells treated with DMSO and 10 or 15μM SFN for 24hr and labelled for Paxillin and Rap1GAP did not show colocalisation between the two proteins (blue arrows). Scale bars = 10μm, images representative of 15 cells per condition.

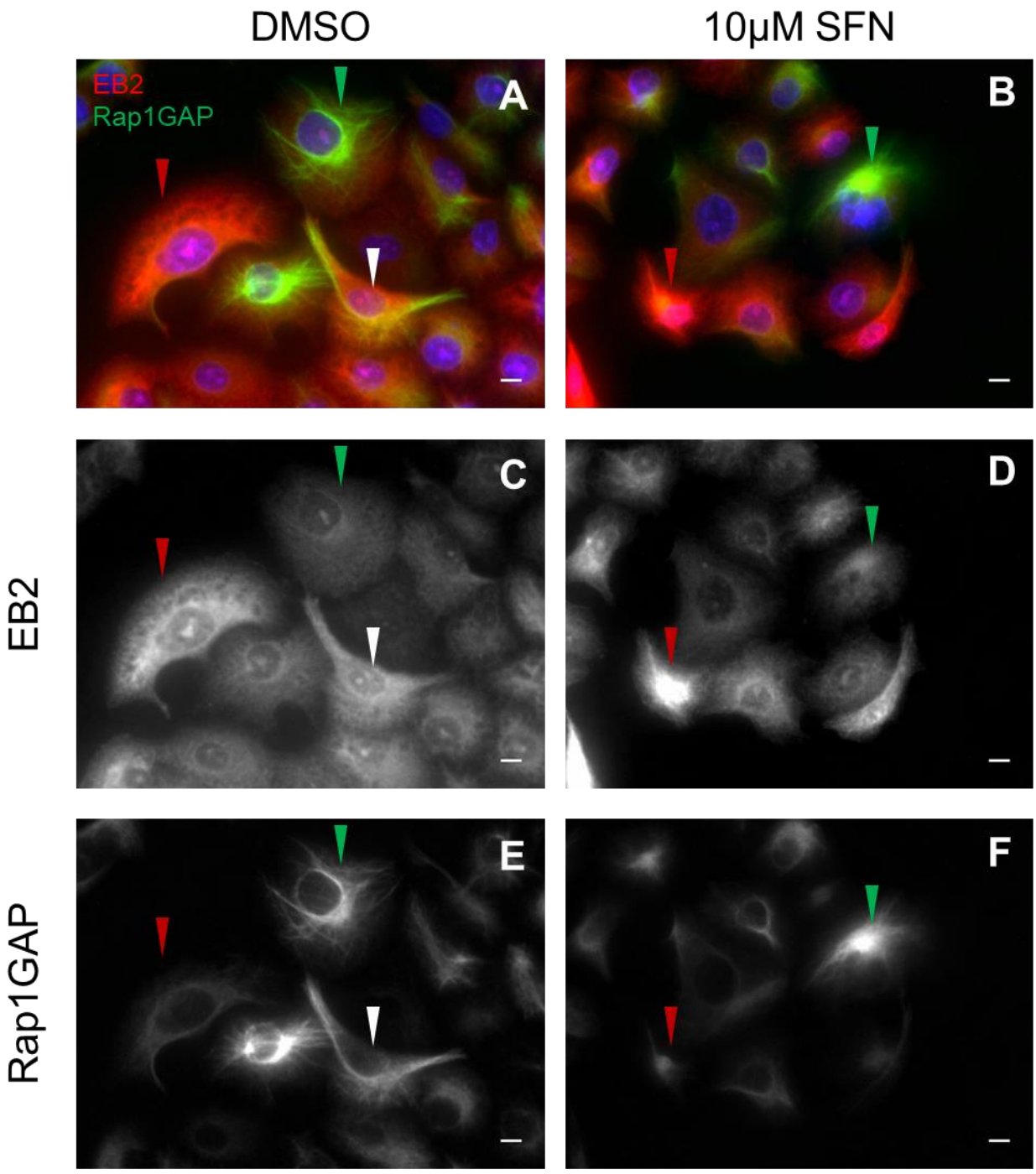

Figure 42 – Low Rap1GAP levels seem to coincide with higher levels of EB2 in Panc-1 cells, even following treatment with 10μM SFN. Panc-1 cells treated with 10μM SFN for 24hr were labelled for EB2 and Rap1GAP. Control and treated cells containing comparatively high levels of EB2 do not contain high levels of Rap1GAP (red arrows), while cells containing lower levels of EB2 have higher levels of Rap1GAP (green arrows). Certain cells contain intermediate levels of both proteins (white arrows). Scale bars = 10μm, images representative of 15 images per condition.

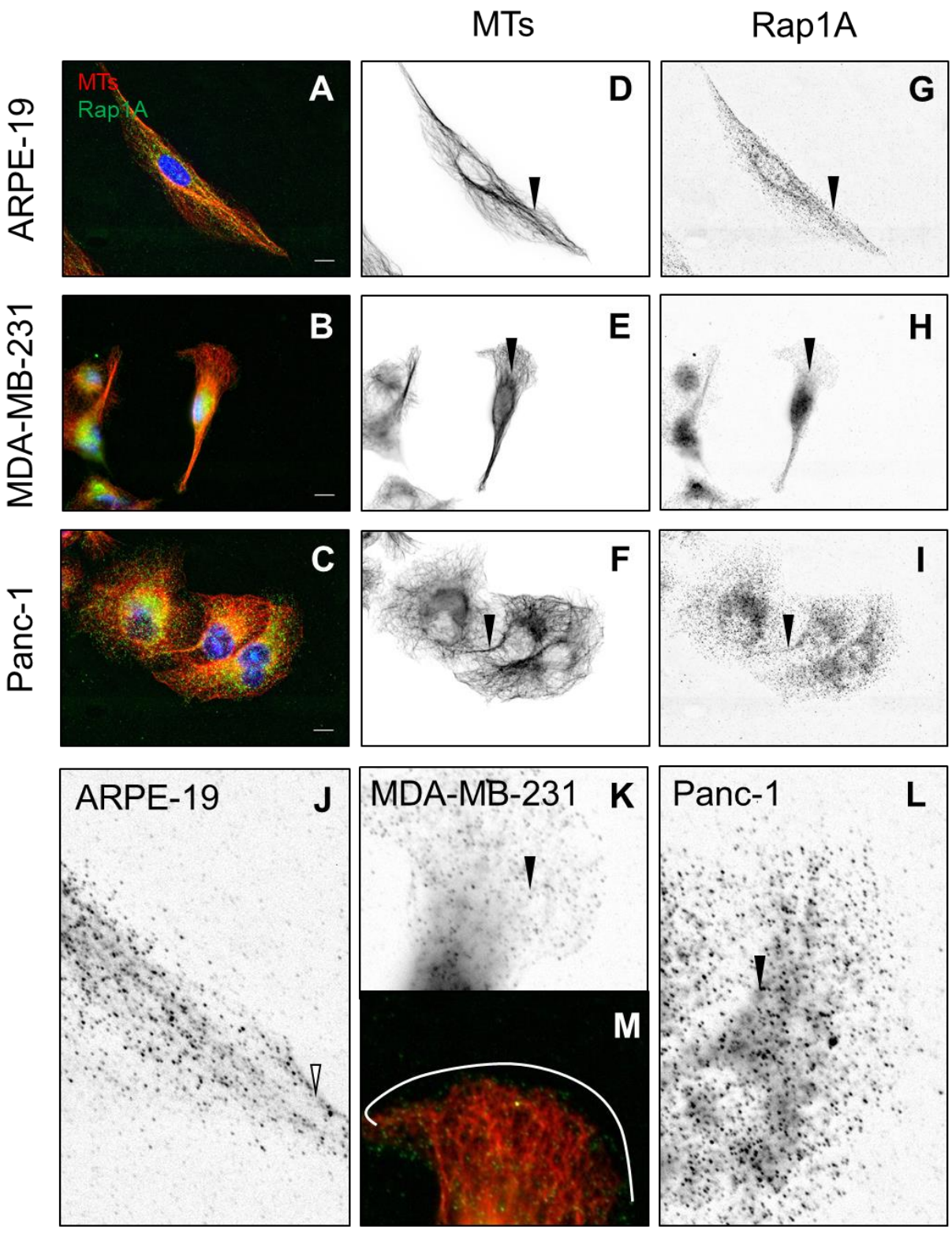

Figure 43– Localisation of Rap1A in relation to MTs in untreated ARPE, MDA-MB-231 and Panc-1 cells. Untreated ARPE-19, MDA-MB-231 and Panc-1 cells were labelled for MTs and Rap1 to assess the localisation of Rap1 in each cell line (A-C). All three cell lines possess radial MT arrays (D-F) and Rap1 localises as diffuse punctae throughout the cell with some evidence of co-localisation with MTs (white arrow indicating fibre-like distribution). This can be seen in close up sections from the images (J-L). In MDA-MB-231 cells, which tend to exhibit lamellipodia-like protrusions when grown on 2D surfaces, Rap1 can be seen at the leading edge of these structures ahead of the ends of MTs, with the edge of the cell indicated by the white line (M). Scale bars = 10μm, images representative of 15 cells per condition.

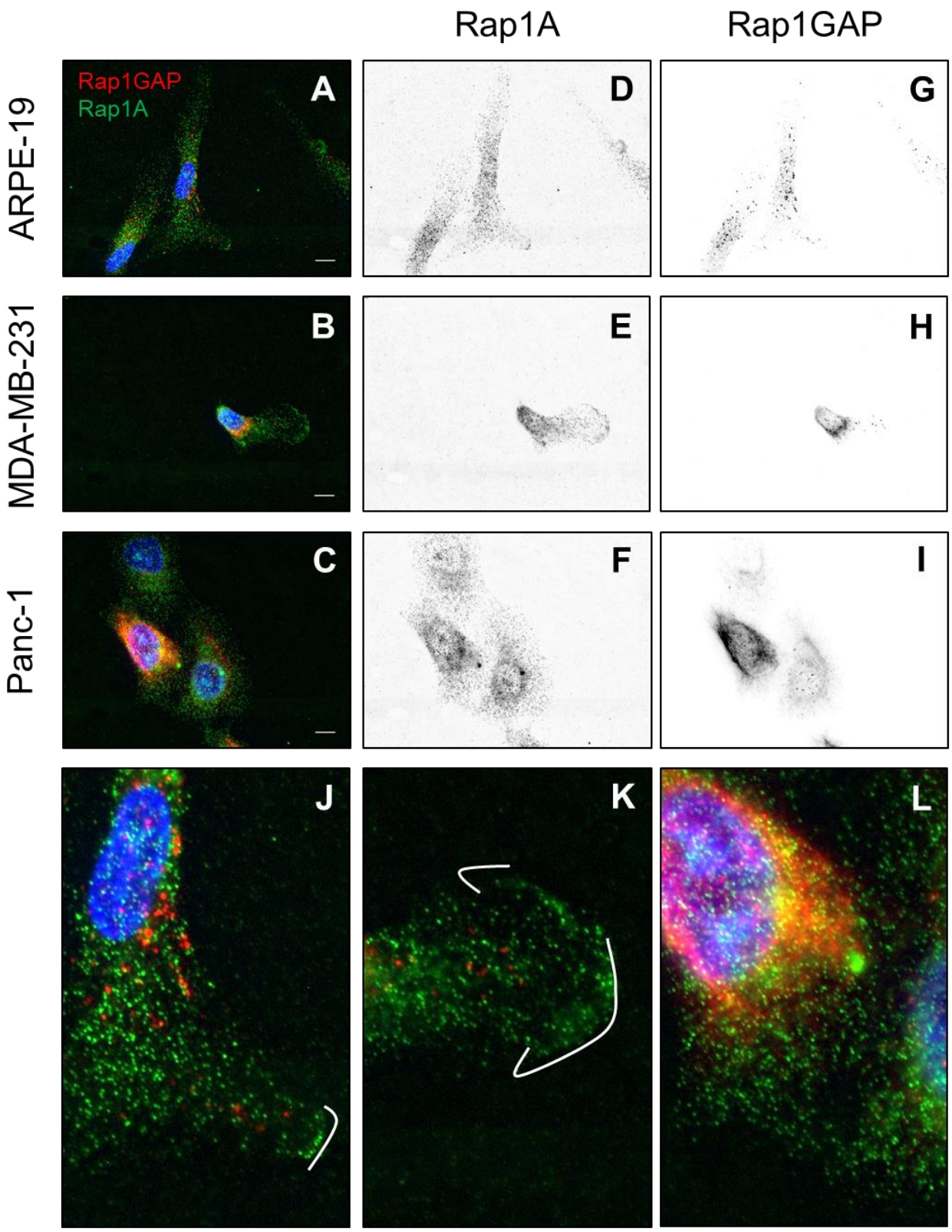

Figure 44 – There is no apparent co-localisation of Rap1A and Rap1GAP in untreated ARPE, MDA-MB-231 and Panc-1 cells. Rap1 appears to be present through a larger area of the cell than Rap1GAP, with Rap1GAP occupying the space closer to the cell nucleus while Rap1 is found out to the cell periphery (A-I), and at the edge of lamellipodia-like protrusions in cells (J,K). Punctae of Rap1 and Rap1GAP appear to rarely co-localise in cells as shown by close up merged images (J-L), with white lines indicating the edge of cell protrusions. Scale bars = 10μm, images representative of 10 cells per condition..

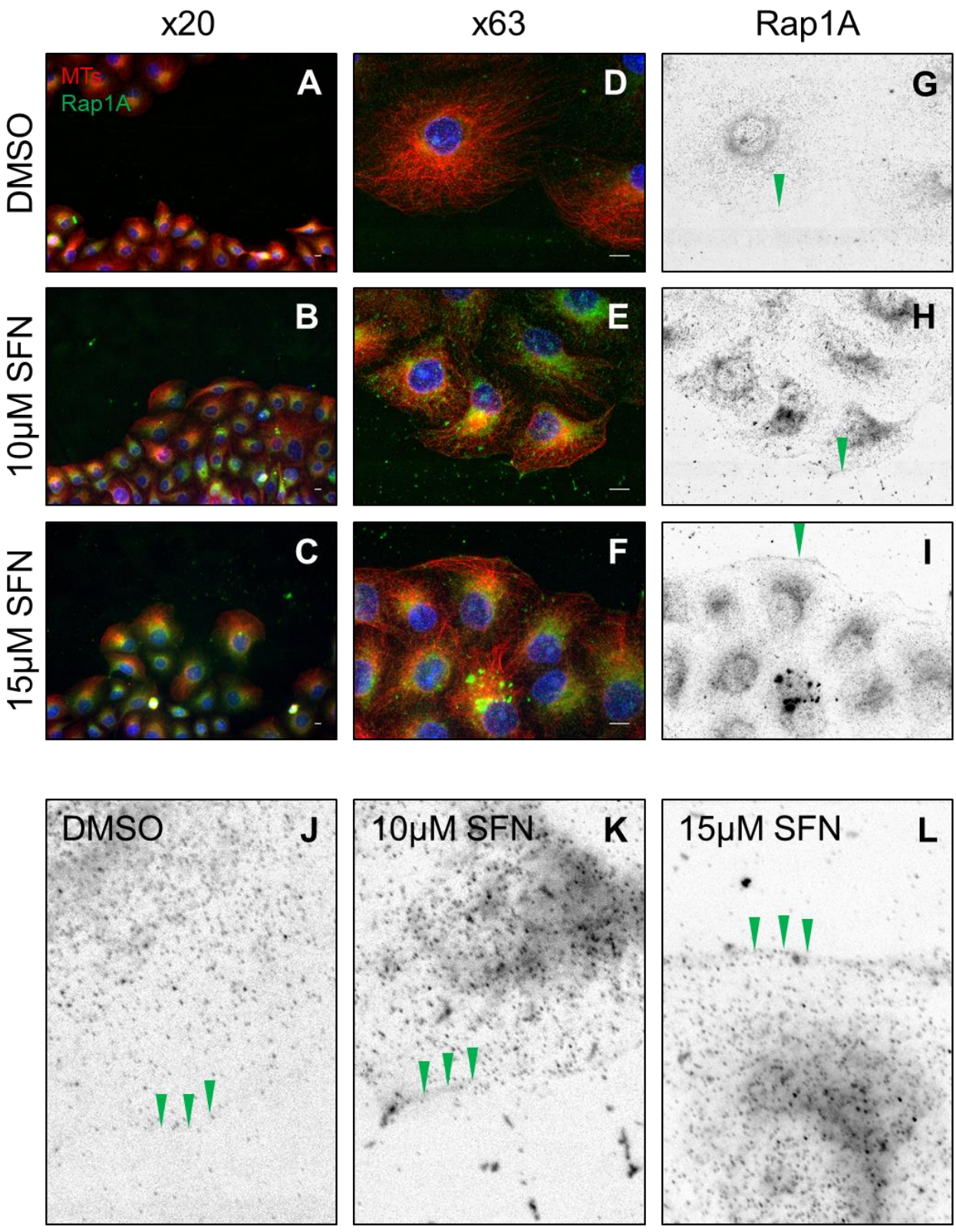

Figure 45 – Rap1 can be observed at the leading edge of Panc-1 cells in the closing scratch wound even after treatment with 10 and 15μM SFN. Wounds treated with SFN for 17hr were labelled for MTs and Rap1A and images using x20 (A-C) and x63 objectives (D-F). At x63 Rap1A can be identified at the leading edges of cells at the wound front in control cells and those treated with 10 or 15μM SFN (green arrows). This can be seen more closely in enlarged sections of the images (J-L, green arrows). Scale bars = 10μm, images representative of 20 leading edge images per condition.

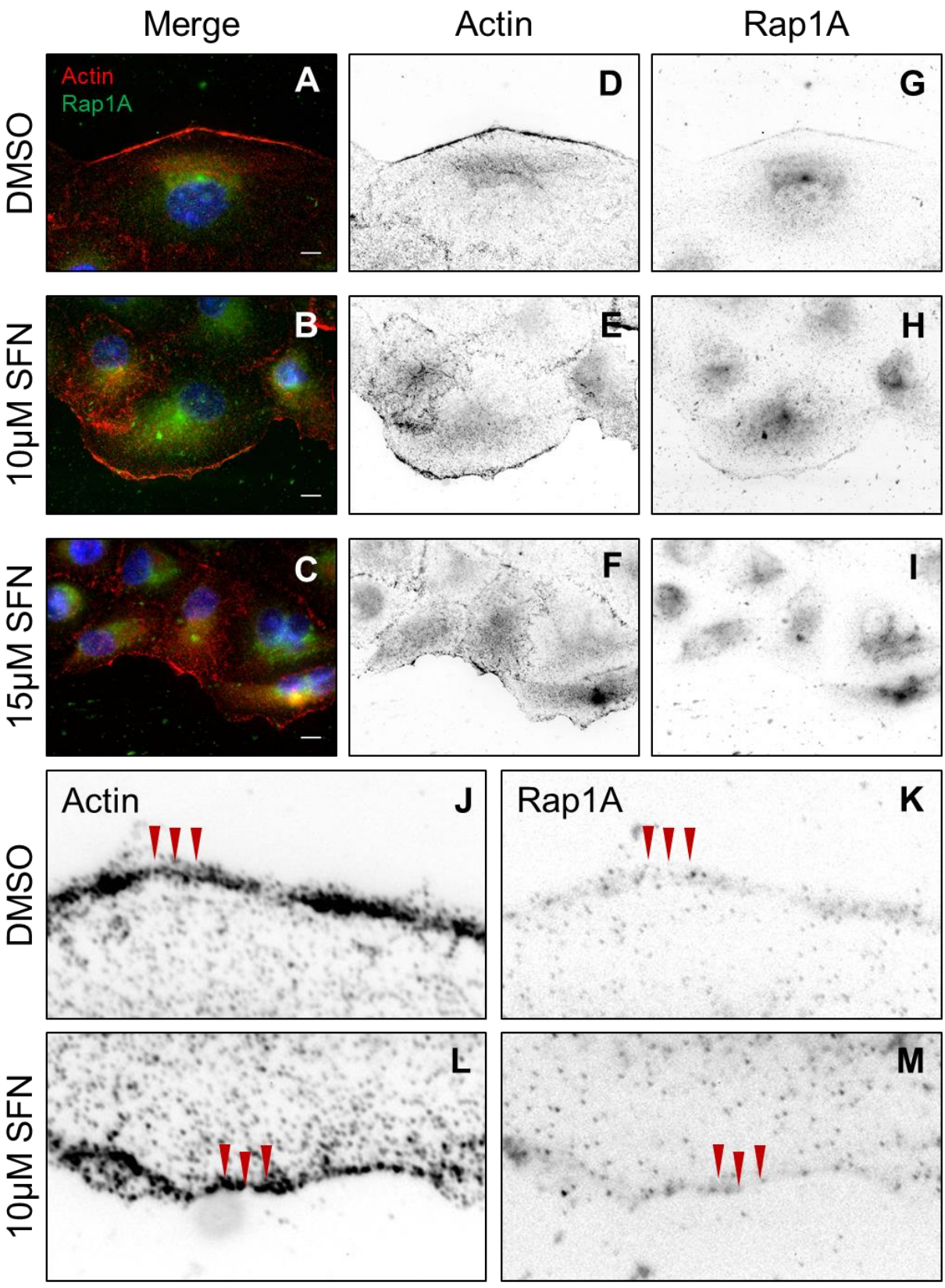

Figure 46 – Rap1A co-localises with Actin at the leading edge of Panc-1 cells at the wound front, even following treatment with 10 and 15μM SFN. Wounds treated fro 17hr with 10 and 15μM SFN were labelled for actin and Rap1A (A-C), with actin (D-F) and Rap1A G-I) being present at the leading edges of cells at the wound front, where they colocalise as seen in the enlarged images (J-M; red arrows). Scale bars = 10μm, images representative of 20 leading edge images per condition.

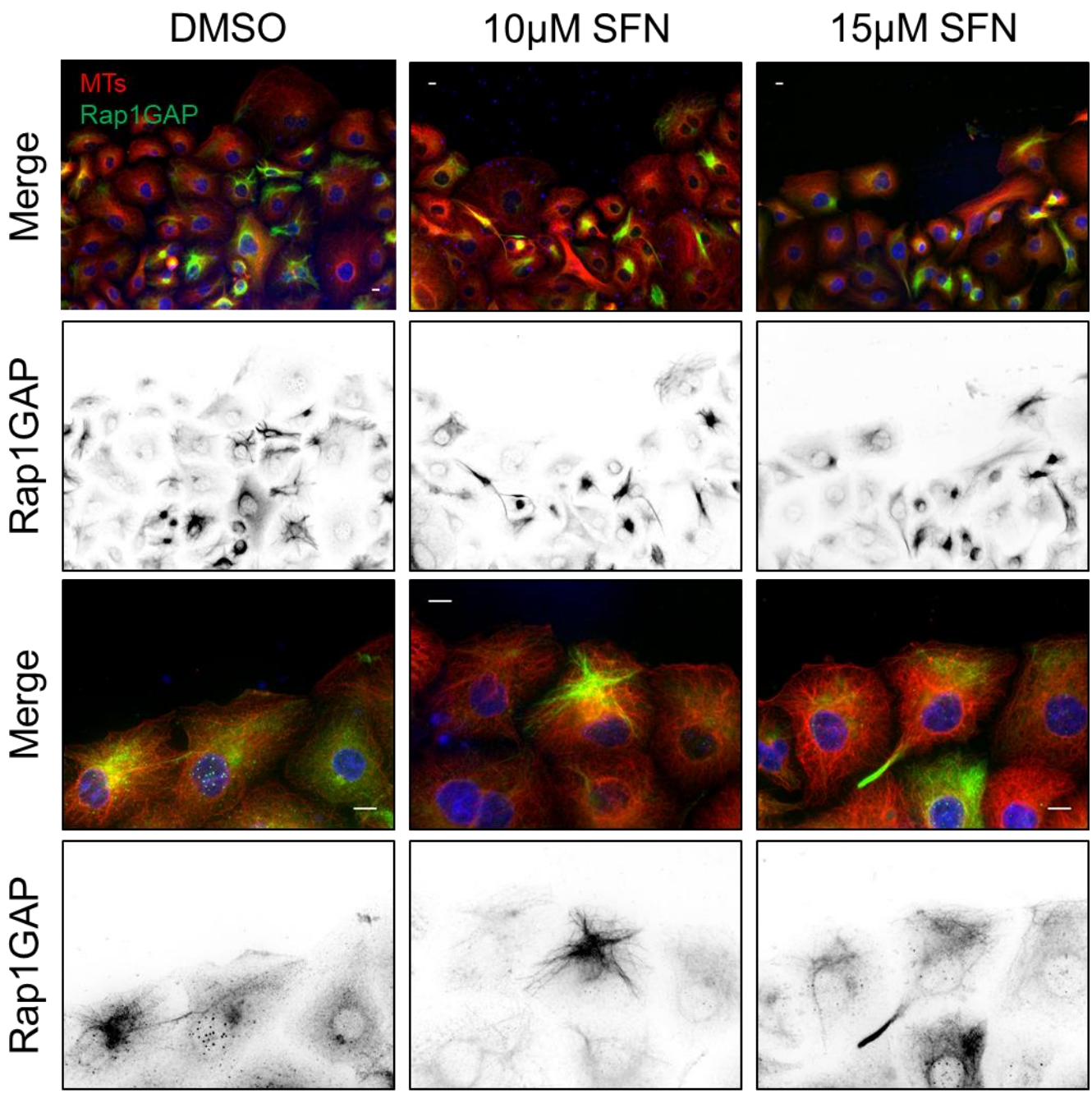

Figure 47 – Rap1GAP is still widely expressed in cells at the wound frontier in Panc-1 cells following treatment with 10 and 15μM SFN. There does not appear to be a global suppression of Rap1GAP in the leading cells at the edge of scratch wounds, with some cells still exhibiting higher levels of Rap1GAP at the wound edge. Scale bars = 10μm, images representative of 20 leading edge images per condition.

cells a region of Rap1A in front of the plus ends of MTs in lamellipodia-like protrusions can be observed (Fig. 43M). Labelling of both Rap1A and Rap1GAP in these three epithelial cell lines did not indicate any visible co-localisation between the two punctate proteins (Fig. 44A-I), however, fronts of Rap1A at potential migratory protrusions were seen again in MDA cells (Fig. 44K).

4.2.3. Rap1A and Rap1GAP in the closing scratch wound

Results presented in the previous chapter indicated that SFN significantly reduces the percentage wound closure in Panc-1 cell monolayers, and that this is likely to still be the case even when SFN inhibition of cell division is taken out of the equation. In order to learn more about this effect, the localisation of proteins in migrating cells during scratch wound closure in the presence of SFN was assessed via immunoflourescence labelling of scratch wounds on coverslips. When closing wounds were labelled for Rap1A, this protein could be seen at the leading edges of cells at the migrating front, even after treatment with 10 and 15μM SFN (Fig. 45), and this region appears to co-localise with regions of actin at the leading edge as detected by anti-actin antibodies (Fig. 46). Labelling of Rap1GAP in the closing wounds does not indicate particular patterns of Rap1GAP in cells at the leading edge of the wound, with some cells showing high levels of Rap1GAP and others at the wound front showing very low levels (Fig. 47).

4.3. Discussion

Rap1GAP was found to be upregulated in Panc-1 cells at both the level of RNA, via microarray analysis following 48hr treatment with 10μM SFN, and protein, via western blotting, following 24hr treatment with 10 and 15μM SFN. If the indication of LogFC is taken from the microarray then there could be an almost 4-fold upregulation of Rap1GAP in cells treated with SFN. When Rap1GAP protein levels

were investigated via western blotting in MDA-MB-231 cells an upregulation was not seen, however, this experiment did indicate that MDA-MB-231 cells appear to express higher levels of Rap1GAP than Panc-1 cells in all treatment conditions. This is not an expected result, as MDA-MB-231 cells originate from highly aggressive triple negative breast cancer, so their high expression of a putative TSG is unusual, and further investigation into this could be performed.

A number of immunofluorescence experiments were completed to examine the localisation of Rap1GAP and its target GTPase Rap1 in certain epithelial cell lines, particularly Panc-1 cells. These indicated that both of these proteins are diffusely expressed in cells, aside from the filamentous localisation seen in Panc-1 cells when using the Abcam antibody, which may be due to an off-target effect in this particular cell line, as these patterns are not detected using a different antibody made by Santa Cruz. However, further investigation would be needed to determine which antibody, if any, is giving an accurate depiction of Rap1GAP localisation. These antibodies do bind to different regions of the protein, with the Abcam antibody binding tyrosine 134 and the Santa Cruz antibody binding an epitope between amino acids 23 and 40 of the Rap1GAP protein, therefore any off-target binding sites recognised by the Abcam antibody would not necessarily be bound by the Santa Cruz antibody and vice versa. Regarding the relationship between high EB2 expression in the Panc-1 cell line used in these experiments and Rap1GAP expression, it appeared that low levels of Rap1GAP appear to be found in cells with higher expression of EB2, potentially contributing to a more invasive phenotype, where Rap1A activity is more persistent.

Rap1A, the target of RAP1GAP, was found to be present at the leading edge of lamellipodia-like projections in cells, particularly those at the frontier of closing scratch wounds, and this was not noticeably perturbed by treatment with SFN. This is likely to be where Rap1A is acting in the process of inside-out activation of integrins at the leading edge to form adhesions during migration. Although addition of SFN

does not seem to disturb this localisation, the antibody used does not distinguish between active and inactive forms of Rap1A, so it may still be present at the leading edge but could possibly be inactivated by SFN, explaining the slowing of wound closure in the presence of SFN. In the future, an antibody which specifically recognises active Rap1 could be used to determine if levels of activation at the leading edge are altered by SFN treatment at 10 or 15μM.

Western blotting and many of the immunofluorescence experiments were carried out prior to the indication that the initial antibody, purchased from Abcam, may not be exclusively binding Rap1GAP. Therefore, much of the data presented here may not be reliable, however, western blotting could be repeated using the Santa Cruz antibody as part of the further validation required before determining if the Abcam antibody is unreliable.

Further from these investigations, once experiments had been repeated with the replacement antibody, the upregulation of Rap1GAP RNA should be verified by TaqMan RT-PCR to ensure the protein increase is due to mRNA upregulation and to confirm the results seen in the microarray. Elucidation of the full mechanism behind Rap1GAP upregulation by SFN in Panc-1 cells would be the next logical avenue to follow. Based on available published evidence and further results in the microarray data there are two possible hypotheses which could be pursued using various molecular techniques (Fig. 48). The first potential mechanism, and most in agreement with data found by our microarray, involves inhibitor of differentiation (Id) proteins which associate with basic helix-loop-helix (bHLH) transcription factors to inhibit their DNA binding capacity. Generally, these proteins act to inhibit differentiation and promote proliferation, and they are involved in genetic regulation of progenitor expansion and cell fate decisions in cells (Sikder et al., 2003), including the pancreatic epithelium (Hua et al., 2006), however, these proteins have been shown to be upregulated in tumours, including in pancreatic cancer (Maruyama et al., 1999), and linked to tumour aggressiveness and coordination of stem cell-like

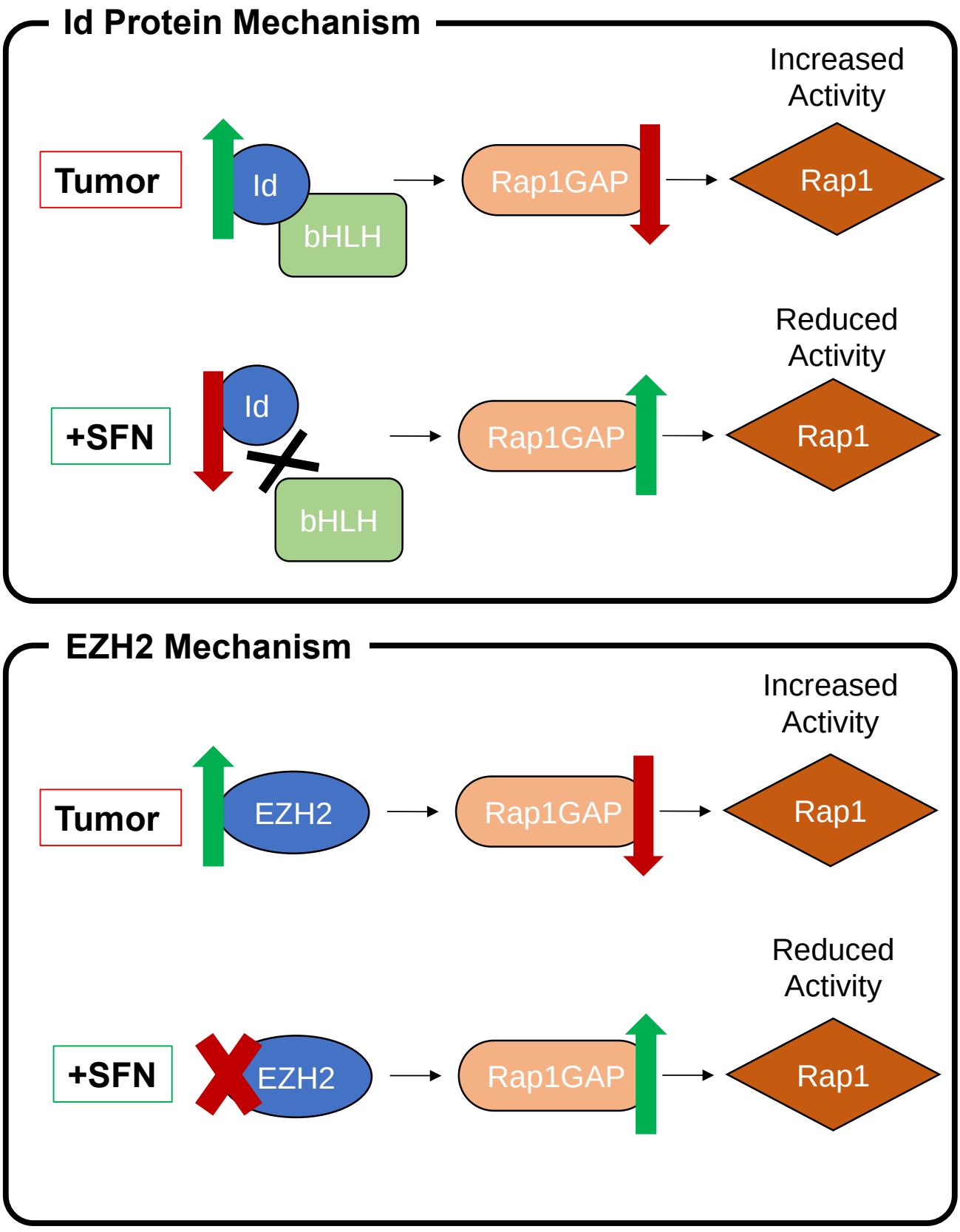

Figure 48 – Schematic representation of the two potential mechanisms of Rap1GAP expression increase by SFN. In tumours, Id proteins become upregulated, leading to increased inhibition of bHLH transcription factors and reduced expression of, among other genes, Rap1GAP. This facilitates increased activity of Rap1. SFN may downregulate Id proteins, reducing bHLH inhibition and facilitating Rap1GAP expression and Rap1 deactivation. Alternatively, the methyltransferase EZH2, normally upregulated in cancer leading to Rap1GAP promoter hypermethylation, could be downregulated or marked for degradation by SFN. This reduces Rap1GAP promoter methylation and allows Rap1 inhibition.

phenotypes by cancer cells (Lasorella et al., 2014). This upregulation of Id proteins has been shown to lead to decreased Rap1GAP expression and therefore prolonged Rap1 activity which mediates cell adhesion and is associated with more aggressive tumours, such as high-grade gliomas which are often incurable (Niola et al., 2013). This axis, involving Id-1, has also been shown to play a role in the normal differentiation of neuronal stem cells, where downregulation of Id-1 has been shown to increase levels of Rap1GAP and reduce active Rap1 in murine neuronal stem cells (Tan et al., 2012). Both Id-2 and Id-3 were shown to be downregulated after 48hr SFN treatment in Panc-1 cells via microarray, suggesting the possibility that bHLH transcription factors would then be permitted to bind the Rap1GAP promoter and elicit expression of this gene, thereby reducing Rap1 activity and restoring tumour suppressive activity of Rap1GAP.

The other possibility is a mechanism by which SFN could reduce the hypermethylation of the Rap1GAP promoter by targeting the histone methyltransferase Enhancer of Zeste Homolog 2 (EZH2), which constitutes the catalytic component of the polycomb repressive complex 2 (PRC2; Banerjee et al., 2011). It has been shown that overexpression of EZH2, observed in a number of cancers including squamous cell carcinoma, leads to Rap1GAP silencing via increased methylation of the gene promoter at Lysine 23 of histone 3 ($H3K23^{Me}$; Banerjee et al., 2011). EZH2 has been shown to be a target of SFN (Fisher et al., 2015), and treatment of cells with SFN has been shown to lead to reduced expression of EZH2, however, this gene was not a significant hit on our microarray data. Despite this, work in skin cancer cell lines has suggested that reduction in EZH2 protein levels may occur via proteasome-dependent mechanisms (Balasubramanian et al., 2011), which would not be detected by RNA analysis methods such as microarrays. As such, future work to investigate these potential mechanisms would need to incorporate analysis of both RNA and protein levels in cells following SFN treatment.

The microarray data shown in this chapter was obtained from cells following 48hr of treatment, therefore, due to the rapid metabolism of SFN by cells, there may be other genetic changes which have occurred within this timeframe and been missed. Therefore, further microarray analysis at shorter time-points, such as 6, 12 and 24hr, may show other gene expression changes and shed light on the chronology of these changes and their potential functional implications. RNA from these different time-points could also be used for qRT-PCR to determine when the upregulation of Rap1GAP begins, and to verify any other lead genes which come out of these microarrays, such as CD24 which could also represent an anticancer mechanism of SFN in Panc-1 cells. Previous research has linked doses of SFN as low as 5μM to an inhibition of growth and reduction of self-renewal in pancreatic CSCs (Srivastava et al., 2011). However, no link was made in this study to the reduction of CD24 in cells, therefore, further investigation of this as a potential mechanism of CSC targeting by SFN is needed.

Chapter Five

Conclusions

Current cancer treatments, although often affording patients extended survival, if not full remission, from the disease, are often limited in terms of dosage by their toxicity and accompanied by a range of side effects. Therefore, a large amount of research effort is being put into further understanding how cancer develops and progresses, and how potential new therapeutics interfere with these processes, in order to find new treatments which can better distinguish between healthy and cancerous cells to reduce unwanted side effects. Plant secondary metabolites, particularly the ITC SFN derived from glucoraphanin, have attracted attention in recent years as potential future anticancer compounds. Previous investigations of SFN have shown that this compound has a large number of effects when it is taken up into cells, including inhibition of cell cycle progression, protection from oxidative stress and modulation of phase 1 and 2 enzymes. Only a very small proportion of this literature was focused on the effects of SFN on cell migration and the cellular cytoskeleton, particularly microtubules. The project described in the previous chapters set out to further investigate the effect of SFN on the microtubule cytoskeleton and cell migration, particularly in epithelial cells, which are thought to be the cell of origin for around 90% of cancers. These effects were investigated through indirect immunofluorescence, scratch wound assays and western blotting experiments performed using a range of epithelial cell lines.

The results from scratch wound experiments suggest that SFN does reduce the ability of cells to migrate, as percentage closure of these wounds is reduced at doses of 10-15μM. There is little in the literature in terms of comprehensive investigation involving tumour cells treated with SFN, however, 3D modified Boyden chamber assays using B16F-10 melanoma cells indicated a significant reduction in invasion through type I collagen following 10hr in the presence of 5μM SFN. Further *in vivo* investigation of lung metastasis induced by B16F-10 cells in mice, indicated that administration of 500μg/kg SFN over 10 consecutive days (giving a daily dose

of approximately 10μg per mouse based on average weight of 20g) either prior to, consecutive with or following tail vein injection of B16F-10 cells reduces tumour nodules in the lungs at 21 days post tumour cell injection (Thejass and Kuttan, 2006). Reduction of migration in scratch wound assays has been reported in non-cancerous smooth muscle cells, where it was linked to reduction in MMP-9 activity (Hung et al., 2013). Therefore, the data reported here, in which SFN significantly reduced the percentage wound closure in Panc-1 and MDCKII cells, most likely represents a novel finding in relation to pancreatic cancer cell lines. In this instance, the authors did not include any analysis of the effect of SFN on the velocity of B16F-10 cells exposed to SFN, whereas in the present investigation velocity, and average total distance, was analysed in both Panc-1 and MDCKII cells, where SFN was shown to reduce both of these parameters at 10 and 15μM doses. These results make sense in the context of reduced wound closure, especially when the persistence of the effect on wound closure despite a thymidine mitotic block is considered, it is highly likely that SFN is reducing cell migration in these cell lines from doses of 10μM. Further investigation to characterise this effect on cells could include monitoring random cell migration on slides or chemotaxis assays, in which cells are monitored as they migrate towards a chemoattractant, using this more data on single cell migration could be gathered. In the future, it would be relevant to investigate this effect in more cancer cell lines through scratch assays and determine if this effect is still observed in 3D contexts using assays such as Boyden Chambers with ECM coatings, as used by Thejass and Kuttan (2006).

Apparent shortening of EB1 comets in breast cancer cell lines following SFN treatment in the same dose range would appear to suggest that this reduction in migration is linked in some way to reduction of MT dynamics and growth, as slower growing MTs would have smaller comets of EB1 at their plus ends due to a smaller GTP cap. Due to the lack of fixed exposure images of these experiments, the

shortening of EB1 comets could not be quantified at this time. Reduction of MT dynamics has been previously reported by (Azarenko et al., 2008), however, further exploration of the mechanism behind these effects is needed, as it could be potentially linked in to the covalent modification of cysteines in tubulin which has been previously reported to alter tertiary structure of the protein (Mi et al., 2008), which could affect its polymerisation and interaction with other proteins. Repeats of the experiments presented here, with fixed exposure images for analysis, plus further live imaging of MTs and EB1 at the leading edge of cells during migration in 2D and 3D environments would provide more information on these effects.

It appears that SFN may not only have direct effects on the cytoskeleton but may also affect GTPases and their regulators involved in cell adhesion and guidance of migration. Rap1GAP, the inactivating regulatory protein of the small Rap1 GTPases, which are linked to cell adhesion regulation and migration, was reported by microarray analysis conducted prior to this project to be upregulated approximately 4-fold following 48hr treatment with 10μM SFN. Rap1GAP is a putative tumour suppressor gene, with its downregulation linked to increased invasiveness of tumour cells (Tsygankova et al., 2013). Because of this, further investigation into the upregulation and localisation of Rap1GAP, and Rap1, in epithelial cells treated with SFN was performed. Upregulation of Rap1GAP at the protein level was confirmed via western blotting, however, the Abcam antibody used in these experiments did not show the same localisation as another anti-Rap1GAP antibody purchased from Santa Cruz, indicating filamentous patterns of localisation that was not shown by the Santa Cruz antibody in Panc-1 cells, from which lysates were collected for western blot analysis. Therefore, the blotting experiments presented in Chapter Four would need to be repeated using the Santa Cruz antibody to assess if this antibody indicates the same upregulation, however, it is possible that the Abcam antibody is more effective when used in western blotting than in immunofluorescence experiments. Further confirmation of Rap1GAP mRNA upregulation via RT-PCR would validate

the microarray analysis and allow investigation of more timepoints, such as 12 and 24hr, to determine the timescale and magnitude of Rap1Gap upregulation.

If Rap1GAP is being upregulated by SFN, then the mechanism behind this should be considered. Two such hypothesised mechanisms, based on published data and previous microarray data, were presented in Chapter Four. Briefly, such upregulation may either be mediated by downregulation of Id proteins, and subsequent release of bHLH transcription factors to increase Rap1GAP transcription or inhibition/degradation of EZH2, the catalytic component of the methylating Polycomb Repressive Complex 2, reducing the methylation of the Rap1GAP promoter. In Panc-1 cells the former mechanism seems more probable, as Id-2 and Id-3 were flagged as being significantly downregulated on the microarray (with a LogFC of 0.53 and 0.62 respectively), whereas changes in EZH2 were not significant. However, it is possible that while EZH2 mRNA is being produced, it may be being targeted for degradation by SFN, as shown in previous work (Fisher et al., 2015), an effect that would be seen via western blotting. These mechanisms are purely speculative, and further investigations via immunolabelling, western blotting and functional studies would be required to resolve these questions in the future.

Interestingly, SFN treatment also appears to significantly downregulate CD24 mRNA. A small, cell surface protein, CD24 functions in cell-cell and cell-matrix interactions in cells, and its expression has been linked to cancer progression and metastasis, leading to a great deal of interest in CD24 as a CSC marker (Jaggupilli and Elkord, 2012). Overexpression of CD24 has been linked to poor prognoses in breast cancer, with increased lymph node metastasis and significantly shorter survival in patients with tumours expressing high levels of CD24. Upregulation of CD24 has also been documented in pancreatic ductal adenocarcinoma (Durko et al., 2017), and expression of CD24 often correlates with advanced stages of disease. Cells expressing CD24 and CD44 have been identified as cancer stem cells, which are thought to be instrumental in disease relapse following treatment as they can

repopulate tumours via increased replicative potential (Li et al., 2007). Previous reports have linked SFN to inhibition of CSCs in the breast (Li et al., 2010) and pancreas (Rausch et al., 2010; Li et al., 2013), potentially through its action on NF-κB (Rausch et al., 2010). The value of these markers in identification of CSCs is still under debate, and further investigation would be required to determine if modulation of CD24 expression in Panc-1 cells was related to a reduction in stem cell-like behaviour of cells.

It has been indicated in small human trials in 8 patients that blood plasma SFN concentrations of around 100μM can be achieved through oral dosing of broccoli sprouts containing approximately 200μM SFN, however, tissue concentrations only appear to reach picomolar/mg of tissue levels at this dose (Cornblatt et al., 2007). As yet, no evidence of toxicity towards animals or humans ingesting SFN has been shown, so a much larger dose is likely to be well tolerated by the body, allowing achievement of higher, micromolar, tissue concentrations approaching those used in these investigations. Therefore, the anti-migratory effect observed in this investigation could potentially be achieved in the body to exert an anti-metastatic effect on tumours. One major block in the movement of SFN from promising *in vitro* studies into the clinic is the inherent instability of SFN, as the compound is sensitive to temperature, pH and oxygen (Wu et al., 2014). In 2010 Evgen Pharma acquired the rights to a synthetic form of SFN stabilised in a sugar lattice, known as Sulforadex®, and has subsequently been optimising this compound for pharmaceutical use, with Phase II clinical trials in the treatment of breast cancer and inflammation following subarachnoid haemorrhages currently underway.

There appears to be a future for SFN, and indeed other ITCs, in cancer prevention and treatment. In some respects, its reported ability, at low dietary doses, to prevent carcinogen activation and aid in carcinogen exclusion from cells is arguably more tantalising than the effects on established cancer cells. In the case of

cancer, which possesses a complicated and, in some respects, relatively mysterious, aetiology, and is often able to adapt and overcome any blocks placed by therapeutic intervention, it may be that finding an easily implementable method to prevent the development of the disease may be a more fruitful endeavour than the discovery and production of a highly effective cure. If SFN, or indeed a combination of bioactive plant secondary metabolites, could be administered as a daily supplement, much like vitamin tablets or aspirin, and exert the same preventative effect as when consumed as part of the diet, a large number of cancer cases could potentially be prevented. This would not only circumvent a large amount of suffering for patients, but also be highly cost effective, avoiding the long process of diagnosis, treatment and follow-up care associated with cancers. Indeed, SFN tablets and broccoli extracts can already be purchased, however a large scale long-term study of the efficacy of these supplements has not been conducted. The use of SFN in the clinic may extend beyond cancer, as SFN has shown efficacy in reducing tissue damage following subarachnoid haemorrhage via effects on the Nrf2 pathway, protecting cells from oxidative stress (Zhao et al., 2016). A potential to slow the progression of neurodegenerative conditions such as Alzheimer's, which as the population ages is becoming an ever-growing issue, has also been seen with SFN treatment. It has been demonstrated that SFN can inhibit the generation of amyloid plaques, which are thought to build up to toxic levels in neurons during the disease, leading to improvements in memory in mouse models of Alzheimer's (Hou et al., 2018). Therefore, SFN appears to be a compound with a huge potential for future therapeutic use, however, these uses may only be fully exploited following full understanding and characterisation of its effects in cells.

Bibliography

Ahmadian, M.R., Stege, P., Scheffzek, K., Wittinghofer, A. (1997) Confirmation of the arginine-finger hypothesis for the GAP-stimulated GTP-hydrolysis reaction of Ras. Nature Structural Biology. 4; 686-689.

Alison, M.R., Lin, W.R., Lim, S.M.L., Nicholson, L.J. (2012) Cancer stem cells: In the line of fire. Cancer Treatment Reviews. 38; 589-598.

Aldana-Masangkay, G.I., Sakamoto, K.M. (2011) The role of HDAC6 in cancer. Journal of Medicine and Biotechnology. 2011; article ID 875824.

Aman, A., Piotrowski, T. (2010) Cell migration during morphogenesis. Developmental Biology. 341; 20-33.

Ambrosone, C.B., McCann, S.E., Freudenheim, J.L., Marshall, J.R., Zhang, Y., Sheilds, P.G. (2004) Breast cancer risk in premenopausal women is inversely associated with consumption of broccoli, a source of isothiocyanates, but is not modified by GST genotype. Journal of Nutrition. 134; 1134-1138.

Andréasson, E., Jørgensen, L.B., Höglund, A.-S., Rask, L., Meijer, J. (2001) Different myrosinase and idioblast distribution in Arabidopsis and *Brassica napus*. Plant Physiology. 127(4); 1750-1763.

Azarenko, O., Okouneva, T., Singletary, K.W., Jordan, M.A., Wilson, L. (2008) Suppression of microtubule dynamic instability and turnover in MCF7 breast cancer cells by sulforaphane. Carcinogenesis. 29(12); 2360-2368.

Badin-Larcon, A.C., Boscheron, C., Soleilhac, J.M., Piel, M., Mann, C., Denarier, E., Fourest-Lieuvin, A., Lafanechere, L., Bornens, M., Job, D. (2004) Suppression of nuclear oscillations in saccharomyces cerevisiae expressing Glu tubulin. Proceedings of the National Academy of Sciences of the United States of America. 101; 5577-5582.

Balasubramanian, S., Chew, Y.C., Eckert, R.L. (2011) Sulforaphane suppresses polycomb group protein level via a proteasome-dependent mechanism in skin cancer cells. Molecular Pharmacology. 80(5); 870-878.

Banerjee, R., Mani, R.S., Russo, N., Scanlon, C.S., Tsodikov, A., Jing, X., Cao, Q., Palanisamy, N., Metwally, T., Inglehart, R.C., Tomlins, S., Bradford, C., Carey, T., Wolf, G., Kalyana-Sundaram, S., Chinnaiyan, A.M., Varambally, S., D'Silva, N.J. (2011) The tumour suppressor gene Rap1GAP is silenced by mir-101-mediated EZH2 overexpression in invasive squamous cell carcinoma. Oncogene. 30(42); 4339-4349.

Barker, N., Ridgway, R.A., van Es, J.H., van de Wetering, M., Begthel, H., van den Born, M., Danenberg, E., Clarke, A.R., Sansom, O.J., Clevers, H. (2009) Crypt stem cells as the cells-of-origin of intestinal cancer. Nature. 457; 608-611.

Basten, G.P., Bao, Y., Williamson, G. (2002) Sulforaphane and its glutathione conjugate but not sulforaphane nitrile induce UDP-glucuronosyl transferase (UGT1A1) and glutathione transferase (GSTA1) in cultured cells. Carcinogenesis. 23(8); 1399-1404.

Bellett, G., Carter, J.M., Keynton, J., Goldspink, D., James, C., Moss, D.K., Mogensen, M.M. (2009) Microtubule plus-end and minus-end capture at adherens junctions is involved in the assembly of apico-basal arrays in polarised epithelial cells. Cell Motility and the Cytoskeleton. 66(10); 893-908.

Bieling, P., Kandels-Lewis, S., Telley, I.A., van Dijk, J., Janke, C., Surrey, T. (2008) CLIP-170 tracks growing microtubule ends by dynamically recognising composite EB1/tubulin binding sites. Journal of Cell Biology. 183; 1223-1233.

Bieling, P., Laan, L., Schek, H., Munteanu, E.L., Sandblad, L., Dogterom, M., Brunner, D., Surrey, T. (2007) Reconstitution of a microtubule plus end tracking system in vitro. Nature. 450; 1100-1105.

Boettner, B., Van Aelst, L. (2009) Control of cell adhesion dynamics by Rap1 signalling. Current Opinion in Cell Biology. 21; 684-693.

Boggs, A.E., Vitolo, M.I., Whipple, R.A., Charpentier, M.S., Goloubeva, O.G., Ioffe, O.B., Tuttle, K.C., Slovic, J., Lu, Y., Mills, G.B., Martin, S.S. (2014) α-Tubulin acetylation elevated in metastatic and basal-like breast cancer cells promotes microtentacle formation, adhesion and invasive migration. Cancer research. 75(1); 203-215.

Bos, J.L. (1998) All in the family? New insights and questions regarding interconnectivity of Ras, Rap1 and Ral. The EMBO Journal. 17; 6776-6782.

Bos, J.L. (2005) Linking Rap to cell adhesion. Current Opinion in Cell Biology. 17; 123-128.

Bos, J.L., de Rooij, J., Reedquist, K.A. (2001) Rap1 signalling: Adhering to new models. Nature Reviews Molecular Cell Biology. 2; 369-377.

Bourne, H.R., Sanders, D.A., McCormick, F. (1991) The GTPase superfamily: conserved structure and molecular mechanism. Nature. 349; 117-127.

Bowne-Anderson, H., Hibbel, A., Howard, J. (2015) Regulation of microtubule growth and catastrophe: Unifying theory and experiment. Trends in Cell Biology. 25 (12); 769-779.

Bravo-Cordero, J.J., Hodgson, L., Condeelis, J. (2012) Directed cell invasion and migration during metastasis. Current Opinion in Cell Biology. 24; 277-283.

Brokowska, J., Hać, A., Węgrzyn, G., Herman-Antosiewicz, A. (2016) Sulforaphane reduces the level of exogenous mutated huntingtin protein in normal human fibroblasts. Journal of Neurology, Neurosurgery and Psychiatry. 87(Suppl.1); A94.

Brown, A.F., Yousef, G.G., Jeffery, E.H., Klein, B.P., Wallig, M.A., Kushad, M.M., Juvik, J.A. (2002) Glucosinolate profiles in broccoli: variation in levels and implications in breeding for cancer chemoprotection. Journal of the American Society for Horticultural Science. 127; 807-813.

Buday, L., Downward, J. (2008) Many faces of Ras activation. Biochimica et Biophysica Acta. 1786; 178-187.

Burbank, K.S., Mitchison, T.J. (2006) Microtubule dynamic instability. Current Biology. 16(14); R516-R517.

Bush, K.E., Brunner, D. (2004) The microtubule plus end tracking proteins mal3p and tip1p cooperate for cell-end targeting of interphase microtubules. Current Biology. 14; 548-559.

Busiek, K.K., Margolin, W. (2011) Split decision: a thaumarchaeon encoding both FtsZ and Cdv cell division proteins chooses Cdv for cytokinesis. Molecular Microbiology. 82(3); 535-538.

Calderwood, D.A. (2015) The Rap1-RIAM pathway prefers β2 integrins. Blood. 126; 2658-2659.

Carey, S.P., Martin, K.E., Reinhart-King, C.A. (2017) Three-dimensional collagen matrix induces a mechanosensitive invasive epithelial phenotype. Scientific Reports. 7; 42088.

Caron, E. (2003) Cellular functions of the Rap1GTP-binding protein: a pattern emerges. Journal of Cell Science. 116; 435-440.

Chaffer, C.L., Weinberg, R.A. (2011) A perspective on cancer metastasis. Science. 331(6024); 1559-1564.

Chambers, A.F., Groom, A.C., MacDonald, I.C. (2002) Disemmination and growth of cancer cells in metastatic sites. Nature Reviews Cancer. 2; 563-572.

Chang, C., Werb, Z. (2001) The many faces of metalloproteases: Cell growth, invasion, angiogenesis and metastasis. Trends in Cell Biology. 11(S1); S37-S43.

Chen, J., Zhang, M. (2013) The Par3/Par6/aPKC complex and epithelial cell polarity. Experimental Cell Research. 319(10); 1357-1364.

Chiao, J.W., Chung, F.L., Kancherla, R., Ahmed, T., Mittelman, A., Conaway, C.C. (2002) Sulforaphane and its metabolite mediate growth arrest and apoptosis in human prostate cancer cells. International Journal of Oncology. 20; 631-636.

Clark, A.G., Vignjevic, D.M. (2015) Modes of cancer cell invasion and the role of the microenvironment. Current Opinion in Cell Biology. 36; 13-22.

Clark, E.A., Golub, T.R., Lander, E.S., Hynes, R.O. (2000) Genomic analysis of metastasis reveals an essential role for RhoC. Nature. 406(6795); 532-535.

Clarke, J.D., Dashwood, R.H., Ho, E. (2008) Multi-targeted prevention of cancer by sulforaphane. Cancer Letters. 269; 291-304.

Conde, C., Cáceres, A. (2009) Microtubule assembly, organisation and dynamics in axons and dendrites. Nature Reviews Neuroscience. 10; 319-332.

Cook, S.J., Rubinfield, B., Albert, I., McCormick, F. (1993) RapV12 antagonizes Ras-dependent activation of ERK1 and ERK2 by LPA and EGF in Rat-1 fibroblasts. The EMBO Journal. 12; 3475-3485.

Cornblatt, B.S., Ye, L., Dinkova-Kostova, A.T., Erb, M., Fahey, J.W., Singh, N.K., Chen, M.S.A., Stierer, T., Garrett-Mayer, E., Argani, P., Davidson, N.E., Talalay, P., Kensler, T.W., Visvanathan, K. (2007) Preclinical and clinical evaluation of sulforaphane for chemoprevention in the breast. Carcinogenesis. 28(7); 1485-1490.

Daumke, O., Weyand, M., Chakrabarti, P.P., Vetter, I.R., Wittinghofer, A. (2004) The GTPase-activating protein Rap1GAP uses a catalytic asparagine. Nature. 429; 197-201.

de Forges, H., Bouissou, A., Perez, F. (2012) Interplay between microtubule dynamics and intracellular organization. The International Journal of Biochemistry & Cell Biology. 44; 266-274.

DeVita, V.T.Jr, Chu, E. (2008) A history of cancer chemotherapy. Cancer Research. 68(21); 8643-8653.

Dey, P., Togra, J., Mitra, S. (2014) Intermediate filament: Structure, function and applications in cytology. Diagnostic Cytopathology. 42(7); 628-635.

Dinicola, S., Fabrizi, G., Masiello, M.G., Proietti, S., Palombo, A., Minini, M., Harrath, A.H., Alwasel, S.H., Ricci, G., Catizone, A., Cucina, A., Bizzarri, M. (2016) Inositol induces mesenchymal-epithelial reversion in breast cancer cells through cytoskeleton rearrangement. Experimental Cell Research. 345(1); 37-50.

Dinkova-Kostova, A.T., Fahey, J.W., Kostov, R.V., Kensler, T.W. (2017) KEAP1 and done? Targeting the NRF2 pathway with sulforaphane. Trends in Food Science & Technology. In Press.

Dixit, R., Barnett, B., Lazarus, J.E., Tokito, M., Goldman, Y.E., Holzbaur, E.L. (2009) Microtubule plus-end tracking by CLIP-170 requires EB1. Proceedings of the National Academy of Sciences of the United States of America. 106; 492-497.

Dong, X., Liu, F., Sun, L., liu, M., Li, D., Su, D., Zhu, Z., Dong, J.T., Fu, L., Zhou, J. (2010) Oncogenic function of microtubule end-binding protein 1 in breast cancer. The Journal of Pathology. 220(3); 361-369.

Downing, K.H., Nogales, E. (1998) Tubulin and microtubule structure. Current Opinion in Cell Biology. 10; 16-22.

Doxsey, S. (1998) The centrosome – a tiny organelle with big potential. Nature Genetics. 20; 104-106.

Druker, B.J., Guilhot, F., O'Brien, S.G., Gathmann, I., Kantarjian, H., Gattermann, N., Deininger, M.W.N., Silver, R.T., Goldman, J.M., Stone, R.M., Cervantes, F., Hochhaus, A., Powell, B.L., Gabrilove, J.L., Rousselot, P., Reiffers, J., Cornelissen, J.J., Hughes, T., Agis, H., Fischer, T., Verhoef, G., Shepherd, J., Saglio, G., Gratwohl, A., Nielsen, J.L., Radich, J.P., Simonsson, B., Taylor, K., Baccarani, M., So, C., Letvak, L., Larson, R.A. (2006) Five-year follow-up of patients receiving imatinib for chronic myeloid leukemia. The New England Journal of Medicine. 355; 2408-2417.

Dumontet, C., Jordan, M.A. (2010) Microtubule-binding agents: a dynamic field of cancer therapeutics. Nature Reviews Drug Discovery. 9; 790-803.

Durko, L., Wlordarski, W., Stasikowska-Kanicka, O., Wagrowska-Danilewicz, M., Danilewicz, M., Hogendorf, P., Strzelczyk, J., Malecka-Panas, E. (2017) Expression and clinical significance of cancer stem cell markers CD24, CD44 and CD133 in pancreatic ductal adenocarcinoma and chronic pancreatitis. Disease Markers. 2017; 3276806.

Eira, J., Silva, C.S., Sousa, M.M., Liz, M.A. (2016) The cytoskeleton as a novel therapeutic target for old neurodegenerative disorders. Progress in Neurobiology. 141; 61-82.

Ezratty, E.J., Bertaux, C., Marcantonio, E.E., Gundersen, G.G. (2009) Clathrin mediates integrin endocytosis for focal adhesion disassembly in migrating cells. Journal of Cell Biology. 187(5); 733-747.

Ezratty, E.J., Partridge, M.A., Gundersen, G.G. (2005) Microtubule-induced focal adhesion disassembly is mediated by dynamin and focal adhesion kinase. Nature Cell Biology. 156(2); 349-359.

Fahey, J.W., Haristoy, X., Dolan, P.M., Kensler, T.W., Scholtus, I., Stephenson, K.K., Talalay, P., Lozniewski, A. (2002) Sulforaphane inhibits extracellular, intracellular and antibiotic-resistant strains of *Helicobacter pylori* and prevents benzo[a]pyrene-induced stomach tumours. Proceedings of the National Academy of Sciences of the United States of America. 99; 7610-7615.

Fahey, J.W., Zalcmann, A.T., Talalay, P. (2001) The chemical diversity and distribution of glucosinolates and isothiocyanates among plants. Phytochemistry. 56; 5-51.

Fellous, A., Francon, J., Lennon, A.M., Nunez, J. (1977) Microtubule assembly *in vitro*. European Journal of Biochemistry. 78; 167-174.

Fimognari, C., Hrelia, P. (2007) Sulforaphane as a promising molecule for fighting cancer. Mutation Research. 635(2-3); 90-104.

Fisher, M.L., Adhikary, G., Grun, D., Kaetzel, D.M., Eckert, R.L. (2015) The ezh2 polycomb group protein drives an aggressive phenotype in melanoma cancer stem cells and is a target of diet derived sulforaphane. Molecular Carcinogenesis. 55(12); 2024-2036.

Fletcher, D.A., Mullins, R.D. (2010) Cell mechanics and the cytoskeleton. Nature. 463; 485-492.

Friedl, P., Locker, J., Sahai, E., Segall, J.E. (2012) Classifying collective cancer cell invasion. Nature Cell Biology. 14; 777-783.

Frixione, E. (2000) Recurring views on the structure and function of the cytoskeleton: A 300-year epic. Cell Motility and the Cytoskeleton. 46; 73-94.

Fujii, T., Iwane, A.H., Yanagida, T., Namba, K. (2010) Direct visualisation of secondary structures of F-actin by electron cryomicroscopy. Nature. 467; 724-728.

Gandalovičova, A., Rosel, D., Fernandes, M., Veselỳ, P., Heneberg, P., Čermák, V., Petruželka, L., Kumar, S., Sanz-Moreno, V., Brábek, J. (2017) Migrastatics – anti-metastatic and anti-invasion drugs: Promises and challenges. Trends in Cancer. 3(6); 391-406.

Gamet-Payrastre, L., Li, P., Lumeau, S., Cassar, G., Dupont, M.A., Chevolleau, S., Gase, N., Tulliez, J., Tercé, F. (2000) Suforaphane, a naturally occurring isothiocyanate, induces cell cycle arrest and apoptosis in HT29 human colon cancer cells. Cancer Research. 60; 1426-1433.

Gamet-Payrastre, L., lumeau, S., Gasc, N., Cassar, G., Rollin, P., Tulliez, J. (1998) Selective cytostatic and cytotoxic effects of glucosinolates hydrolysis products on human colon cancer cells in vitro. Anticancer Drugs. 9; 141-148.

Gant Luxton, G.W., Gundersen, G.G (2011) Orientation and function of the nuclear-centrosomal axis during cell migration. Current Opinion in Cell Biology. 23(5); 579-588.

Garnham, C.P., Roll-Mecak, A. (2012) The chemical complexity of cellular microtubules: tubulin post-translational modification enzymes and their roles in tuning microtubule functions. Cytoskeleton. 69 (7); 442-463.

Gatenby, R.A., Gillies, R.J., Brown, J.S. (2010) The evolutionary dynamics of cancer prevention. Nature Reviews Cancer. 10; 526-527.

Gerdes, M.J., Yuspa, S.H. (2005) The contribution of epidermal stem cells to skin cancer. Stem Cell Reviews. 1; 225-231.

Getahun, S.M., Chung, F.L. (1999) Conversion of glucosinolates to isothiocyanates in humans after ingestion of cooked watercress. Cancer Epidemiology, Biomarkers & Prevention. 8; 447-451.

Gibbs, A., Schwartzman, J., Deng, V., Alumkal, J. (2009) Sulforaphane destabilises the androgen receptor in prostate cancer cells by inactivating histone deacetylase 6. Proceedings of the National Academy of Sciences of the United States of America. 106(9); 16663-16668.

Goldspink, D. A., Rookyard, C., Tyrrell, B.J., Gadsby, J., Perkins, J., Lund, E.K., Galjart, N., Thomas, P., Wileman, T., Mogensen, M.M. (2017) Ninein is essential for apico-basal microtubule formation and CLIP-170 facilitates its redeployment to non-centrosomal microtubule organising centres. Open Biology. 7(2); 160274.

Guo, L., Yang, R., Wang, Z., Guo, Q., Gu, Z. (2014) Glucoraphanin, sulforaphane and myrosinase activity in germinating broccoli sprouts as affected by growth temperature and plant organs. Journal of Functional Foods. 9; 70-77.

Gyan, E., Frew, M., Bowen, D., Beldjord, C., Preudhomme, C., Lacombe, C., Mayeux, P., Dreyfus, F., Porteu, F., Fontenay, M. (2005) Mutation in RAP1 is a rare event in myelo-dysplastic syndromes. Leukemia. 19; 1678-1680.

Hahn, W.C., Weinberg, R.A. (2002) Modelling the molecular circuitry of cancer. Nature Reviews Cancer. 2(5); 331-341.

Hall, A. (2009) The cytoskeleton and cancer. Cancer and Metastasis Reviews. 28; 5-14.

Hammond, J.W., Cai, D., Verhey, K.J. (2008) Tubulin modifications and their cellular functions. Current Opinion in Cell Biology. 20; 71-76.

Hanahan, D., Weinberg, R.A. (2000) The hallmarks of cancer. Cell. 100(1); 57-70.

Hanahan, D., Weinberg, R.A. (2011) Hallmarks of cancer: The next generation. Cell. 144(5); 646-674.

Hancock, J.F. (2003) Ras proteins: different signals from different locations. Nature Reviews Molecular Cell Biology. 4; 373-384.

Hansson, L.E., Nyren, O., Bergström, R., Wolk, A., Lindgren, A., Baron, J., Adami, H.O. (1993) Diet and risk of gastric cancer. A population-based case-control study in Sweden. International Journal of Cancer. 55; 181-189.

Haren, L., Remy, M.H., Bazin, I., Callebaut, I., Wright, M., Merdes, A. (2008) NEDD-1-dependent recruitment of the γ-tubulin ring complex to the centrosome is necessary for centriole duplication and spindle assembly. Journal of Cell Biology. 172(4); 505-515.

Harless, W., Qui, Y. (2006) Cancer: A medical emergency. Medical Hypotheses. 67(5); 1054-1059.

Helfand, B.T., Chang, L., Goldman, R.D. (2004) Intermediate filaments are dynamic and motile elements of cellular architecture. Journal of Cell Science. 117; 133-141.

Herzog, W., Weber, K. (1977) In vitro assembly of pure tubulin into microtubules in the absence of microtubule-associated proteins and glycerol. Proceedings of the National Academy of the Sciences of the United States of America. 74(5); 1860-1864.

Honnappa, S., Gouveia, S.M., Weisbrich, A., Damberger, F.F., Bhavesh, N.S., Jawhari, H., Grigoriev, I., van Rijssel, F.J.A., Buey, R.M. (2009) An EB1-binding motif acts as a microtubule tip localisation signal. Cell. 138(2); 366-376.

Hou, T.T., Yang, H.Y., Wu, Q.Q., Tian, Y.R., Jia, J.P. (2018) Sulforaphane inhibits the generation of Amyloid-β oligomer and promotes spatial learning and memory in Alzheimer's disease (PS1V97L) transgenic mice. Journal of Alzheimer's Disease. 62(4); 1803-1813.

Hu, C.D., Kariya, K., Kotani, G., Shirouzu, M., Yokoyama, S., Kataoka, T. (1997) Coassociation of Rap1A and Ha-Ras with Raf-1 terminal region interferes with ras-dependent activation of Raf-1. Journal of Biological Chemistry. 272; 11702-11705.

Hu, R., Khor, T.O., Shen, G., Jeong, W.S., Hebbar, V., Chen, C., Xu, C., Reddy, B., Chada, K., Kong, A.N.T. (2006) Cancer chemoprevention of intestinal polyposis in ApcMin/+ mice by sulforaphane, a natural product derived from cruciferous vegetable. Carcinogenesis. 27(10); 2038-2046.

Hua, H., Zhang, Y.Q., Dabernat, S., Kritzik, M., Dietz, D., Sterling, L., Sarvetnick, N. (2006) BMP4 regulates pancreatic progenitor cell expansion through Id2. Journal of Biological Chemistry. 281(19); 13574-13580.

Hubbert, C., Guardiola, A., Shao, R., Kawaguchi, Y., Ito, A., Nixon, A., Yoshida, M., Wang, X.F., Yao, T.P. (2002) HDAC6 is a microtubule associated deacetylase. Nature. 417; 455-458.

Huber, F., Boire, A., López, M.P., Koenderink, G.H. (2014) Cytoskeletal crosstalk: when three different personalities team up. Current Opinion in Cell Biology. 32; 39-47.

Hung, C.N., Huang, H.P., Lii, C.K., Liu, K.L., Wang, C.J. (2013) Sulforaphane inhibits smooth muscle cell proliferation and migration by reducing MMP-9 activity via the Ras and RhoA/ROCK pathways. Journal of Functional Foods. 5(3); 1097-1107.

Insall, R.H., Machesky, L.M. (2009) Actin dynamics at the leading edge: from simple machinery to complex networks. Developmental Cell. 17; 310-322.

Itoh, M., Nelson, C.M., Myers, C.A., Bissell, M.J. (2007) Rap1 integrates tissue polarity, lumen formation and tumorigenic potential in human breast epithelial cells. Cancer Research. 67; 4759-4766.

Jacquemet, G., Hamidi, H., Ivaska, J. (2015) Filopodia in cell adhesion, 3D migration and cancer cell invasion. Current Opinion in Cell Biology. 36; 23-31.

Jackson, S.J.T., Singletary, K.W. (2004) Sulforaphane: a naturally occurring mammary carcinoma mitotic inhibitor which disrupts tubulin polymerization. Carcinogenesis. 25(2); 219-227.

Jackson, S.J.T., Singletary, K.W., Venema, R.C. (2007) Sulforaphane supresses angiogenesis and disrupts endothelial mitotic progression and microtubule polymerization. Vascular Pharmacology. 46; 77-84.

Jaggupilli, A., Elkord, E. (2012) Significance of CD44 and CD24 as cancer stem cell markers: an enduring ambiguity. Clinical and Developmental Immunology. 2012; 708036.

Juge, N., Mithen, R.F., Traka, M. (2007) Molecular basis for chemoprevention by sulforaphane: a comprehensive review. Cellular and Molecular Life Sciences. 64; 1105-1127.

Kabsch, W., Mannherz, H.G., Suck, D., Pai, E.F., Holmes, K.C. (1990) Atomic structure of the actin:DNase I complex. Nature. 347; 37-44.

Kakiuchi, M., Nishizawa, T., Ueda, H., Gotoh, K., Tanaka, A., Hayashi, A., Yamamoto, S., Tatsuno, K., Katoh, H., Watanabe, Y., Ichimura, T., Ushiku, T., Funahashi, S., Tateishi, K., Wada, I., Shimizu, N., Nomura, S., Koike, K., Seto, Y., Fukayama, M., Aburatani, H., Ishikawa, S. (2014) Recurrent gain-or-function mutations of RHOA in diffuse-type gastric carcinoma. Nature Genetics. 46(6); 583-587.

Kanematsu, S., Yoshizawa, K., Uehara, N., Miki, H., Sasaki, T., Kuro, M., Lai, Y.C., Kimura, A., Yuri, T., Tsubara, A. (2011) Sulforaphane inhibits the growth of KPL-1 human breast cancer cells *in vitro* and supresses the growth and metastasis of orthotopically transplanted KPL-1 cells in female anthymic mice. Oncology Reports. 26; 603-608.

Katagiri, K., Maeda, A., Shimonaka, M., Kinashi, T. (2003) RAPL, a Rap1 binding molecule that mediates Rap1 induced adhesion through spatial regulation of LFA-1. Nature Immunology. 4; 741-748.

Kato, C., Miyazaki, K., Nakagawa, A., Ohira, M., Nakamura, Y., Ozaki, T., Imai, T., Nakagawara, A. (2004) Low expression of human tubulin tyrosine ligase and supressed tubulin tyrosination/detyrosination cycle are associated with impaired neuronal differentiation in neuroblastomas with poor prognosis. International Journal of Cancer. 112; 365-375.

Kavallaris, M. (2010) Microtubules and resistance to tubulin-binding agents. Nature Reviews Cancer. 10; 194-204.

Kaverina, I., Krylyshkina, O., Small, J.V. (1999) Microtubule targeting of substrate contacts promotes their relaxation and dissociation. Journal of Cell Biology. 146; 1033-1044.

Kim, W.J., Gersey, Z., Daaka, Y. (2012) Rap1GAP regulates renal cell carcinoma invasion. Cancer Letters. 320(1); 65-71.

Kitayama, H., Sugimoto, Y., Matsuzaki, T., Ikawa, Y., Noda, M. (1989) A ras-related gene with transformation suppressor activity. Cell. 56; 77-84.

Knox, A.L., Brown, N.H. (2002) Adherens junction positioning and cell adhesion. Science. 295; 1285-1288.

Kollman, J.M., Zelter, A., Muller, E.G.D., Fox, B., Rice, L.M., Davis, T.N., Agard, D.A. (2008) The structure of the γ-tubulin small complex: implications of its architecture and flexibility for microtubule nucleation. Molecular Biology of the Cell. 19; 207-215.

Komarova, Y.A., Akhmanova, A.S., Kojima, S., Galjart, N., Borisy, G.G. (2002) Cytoplasmic linker proteins promote microtubule rescue in vivo. Journal of Cell Biology. 159; 589-599.

Komarova, Y.A., De Groot, C.O., Grigoriev, I., Gouveia, S.M., Munteanu, E.L., Schober, J.M., Honnappa, S., Buey, R.M., Hoogenraad, C.C., Dogterom, M., Borisy, G.G., Steinmetz, M.O., Akhmanova, A. (2009) Mammalian end binding proteins control perisistent microtubule growth. Journal of Cell Biology. 184; 691-706.

Koroleva, O.A., Gibson, T.M., Cramer, R., Stain, C. (2010) Glucosinolate-accumulating S-cells in Arabidopsis leaves and flower stalks undergo programmed cell death at early stages of differentiation. The Plant Journal. 64; 456-469.

Lafanechere, L., Courtay-Cahen, C., Kawakami, T., Jacrot, M., Rudiger, M., Wehland, J., Job, D., Margolis, R.L. (1998) Suppression of tubulin tyrosine ligase during tumour growth. Journal of Cell Science. 111; 171-181.

Lagarrigue, F., Anekal, P.V., Lee, H.S., Bachir, A.I., Ablack, J.N., Horwitz, A.F., Ginsberg, M.H. (2015) A RIAM/lamellipodin-talin-integrin complex forms the tip of sticky fingers that guide cell migration. Nature Communications. 6; article number 8492.

Lamouille, S., Xu, J., Derynck, R. (2014) Molecular mechanisms of epithelial-mesenchymal transition. Nature Reviews Molecular Cell Biology. 15(3); 178-196.

Lasorella, A., Benezra, R., Iavarone, A. (2014) The ID proteins: Master regulators of cancer stem cells and tumour aggressiveness. Nature Reviews Cancer. 14; 77-91.

Lauffenburger, D.A., Horwitz, A.F. (1996) Cell migration: A physically integrated molecular process. Cell. 84; 359-369.

Lazebnik, Y. (2010) What are the hallmarks of cancer? Nature Reviews Cancer. 10; 232-233.

Lee, E.Y.H.P., Muller, W.J. (2010) Oncogenes and tumour suppressor genes. Cold Spring Harbour Perspectives in Biology. 2; a003236.

Lee, J.H., Jeong, J.K., Park, S.Y. (2014) Sulforaphane induced autophagy flux prevents prion protein-mediated neurotoxicity through AMPK pathway. Neuroscience. 278; 31-39.

Lee, J.M., Dedhar, S., Kalluri, R., Thompson, E.W. (2006) The epithelial-mesenchymal transition: new insights in signalling, development, and disease. Journal of Cell Biology. 172(7); 973-981.

Li, C., Heidt, D.G., Dalerba, P., Burant, C.F., Zhang, L., Adsay, V., Wicha, M., Clarke, M.F., Simeone, D.M. (2007) Identification of pancreatic cancer stem cells. Cancer Research. 67(3); 1030-1037.

Li, L., Yang, X.J. (2015) Tubulin acetylation: responsible enzymes, biological functions and human diseases. Cellular and Molecular Life Sciences. 72(22); 4237-4255.

Li, S.H., Fu, J., Watkins, D.N., Srivastava, R.K., Shankar, S. (2013) Sulforaphane regulates self-renewal of pancreatic cancer stem cells through the modulation of sonic hedgehog-GLI pathway. Molecular and Cellular Biochemistry. 1(2); 217-227.

Li, Y., Zhang, T., Korkaya, H., Liu, S., Lee, H.F., Newman, B., Yu, Y., Clouthier, S.G., Schwartz, S.J., Wicha, M.S., Sun, D. (2010) Sulforaphane, a dietary component of broccoli.broccoli sprouts, inhibits breast cancer stem cells. Clinical Cancer Research. 16(9); 2580-2590.

Liao, G., Gundersen, G.G. (1998) Kinesin is a candidate for cross-bridging microtubules and intermediate filaments. Selective binding of kinesin to detyrosinated tubulin and vimentin. Journal of Biological Chemistry. 273; 9797-9803.

Lim, E., Vaillant, F., Wu, D., Forrest, N.C., Pal, B., Hart, A.H., Asselin-Labat, M.L., Gyorki, D.E., Ward, T., Partanen, A., Feleppa, F., Huschtscha, L.I., Thorne, H.J., kConFab, Fox, S.B., Yan, M., French, J.D., Brown, M.A., Smyth, G.K., Visvader, J.E., Lindeman, G.J. (2009) Aberrant luminal progenitors as the candidate target population for basal tumour development in BRCA1 mutation carriers. Nature Medicine. 15; 907-913.

Lim, J., Thiery, J.P. (2012) Epithelial-mesenchymal transitions: Insights from development. Development. 139; 3471-3486.

Lin, H.J., Probst-Hensch, N.M., Louie, A.D., Kau, I.H., Witte, J.S., Ingles, S.A., Frankl, H.D., Lee, E.R., Haile, R.W. (1998) Glutathione transferase null genotype, broccoli, and lower prevalence of colorectal adenomas. Cancer Epidemiology, Biomarkers & Prevention. 7; 647-652.

Liu, C.Y., lin, H.H., Tang, M.J., Wang, Y.K. (2015) Vimentin contributes to epithelial-mesenchymal transition cancer cell mechanics by mediating cytoskeletal organisation and focal adhesion maturation. Oncotarget. 6(18); 15966-15983.

Liu, H., Smith, A.J.O., Lott, M.C., Bao, Y., Bowater, R.P., Reddan, J.R., Wormstone, I.M. (2013) Sulforaphane can protect lens cells against oxidative stress: Implications for cataract protection. Investigative Opthalmology & Visual Science. 54(8); 5236-5248.

Loehrer, P.J., Einhorn, L.H., Elson, P.J., Crawford, E.D., Keubler, P., Tannock, I., Raghavan, D., Stuart-Harris, R., Sarosdy, M.F., Lowe, B.A., Blumenstein, B., Trump, D. (1992) A randomized comparison of cisplatin alone or in combination with methotrexate, vinblastine, and doxorubicin in patients with metastatic urothelial carcinoma: A cooperative group study. Journal of Clinical Oncology. 10; 1066-1073.

López-Lázaro, M. (2018) The stem cell division theory of cancer. Critical Reviews in Oncology/Hematology. 123; 95-113.

Löwe, J., Amos, L.A. (2009) Evolution of cytomotive filaments: The cytoskeleton from prokaryotes to eukaryotes. The International Journal of Biochemistry & Cell Biology. 41; 323-329.

Luzzi, K.J., MacDonald, I.C., Schmidt, E.E., Kerklivet, N., Morris, V.L., Chambers, A.F., Groom, A.C. (1998) Multistep nature of metastatic inefficiency: Dormancy of solitary cells after successful extravasation and limited survival of early micro-metastases. The American Journal of Pathology. 153; 865-873.

Macara, I.G., Guyer, R., Richardson, G., Huo, Y., Ahmed, S.M. (2014) Epithelial homeostasis. Current Biology. 24; R815-R825.

Machesky, L.M., Gould, K.L. (1999) The Arp2/3 complex: a multifunctional actin organizer. Current Opinion in Cell Biology. 11(1); 117-121.

Magge, R. S., DeAngelis, L.M. (2015) The double-edged sword: Neurotoxicity and chemotherapy. Blood Reviews. 29(2); 93-100.

Martinez-Villaluenga, C., Peñas, E., Ciska, E., Piskula, M.K., Kozlowska, H., Vidal-Valverde, C., Frias, J. (2010) Time dependence of bioactive compounds and antioxidant capacity during germination of different cultivars of broccoli and radish seeds. Food Chemistry. 120; 710-716.

Maruyama, H., Kleef, J., Wildi, S., Friess, H., Büchler, M.W., Israel, M.A., Korc, M. (1999) Id-1 and Id-2 are overexpressed in pancreatic cancer and dysplastic lesions in chronic pancreatitis. The American Journal of Pathology. 155(3); 815-822.

Maurer, S.P., Fourniol, F.J., Bohner, G., Moores, C.A., Surrey, T. (2012) EBs recognize a nucleotide-dependent structural cap at growing microtubule ends. Cell. 149; 371-382.

McCaffrey, L.M., Macara, I.G. (2011) Epithelial organisation, cell polarity and tumorigenesis. Trends in Cell Biology. 21(12); 727-735.

McDonald, P.C., Fielding, A.B., Dedhar, S. (2008) Integrin-linked kinase – essential roles in physiology and cancer biology. Journal of Cell Science. 121(19); 3121-3132.

Mi, L., Xiao, Z., Hood, B.L., Dakshanamurthy, S., Wang, X., Govind, S., Conrads, T.P., Veenstra, T.D., Chung, V.L. (2008) Covalent binding to tubulin by isothiocyanates. The Journal of Biological Chemistry. 283(32); 22136-22146.

Mialhe, A., Lefanechere, L., Treilleux, I., Peloux, N., Dumontet, C., Bremond, A., Panh, M.H., Payan, R., Wehland, J., Margolis, R.L., Job, D. (2001) Tubulin detyrosination is a frequent occurrence in breast cancers of poor prognosis. Cancer Research. 61(13); 5024-5027.

Mishra, A.K., Lambright, D.G. (2016) Small GTPases and their GAPs. Biopolymers. 105(8); 431-448.

Mitra, S.K., Hanson, D.A., Schlaepfer, D.D. (2005) Focal adhesion kinase: In command and control of cell motility. Nature reviews Molecular Cell Biology. 6(1); 56-58.

Mogensen, M.M. (1999) Microtubule release and capture in epithelial cells. Biology of the Cell. 91(4-5); 331-341.

Mogensen, M.M. (2004) Microtubule organising centres in polarised epithelial cells. In Centrosomes in Development and Disease (Ed Nigg, E.A.). Weinheim: Wiley-VCH; 299-319.

Mogensen, M.M., Mackie, J.B., Doxsey, S.J., Stearns, T., Tucker, J.B. (1997) Centrosomal deployment of gamma-tubulin and pericentrin: evidence for a microtubule-nucleating domain and a minus-end docking domain in certain mouse epithelial cells. Cell Motility and the Cytoskeleton. 36(3); 276-290.

Mogensen, M.M., Malik, A., Piel, M., Bouckson-Castaing, V., Bornens, M. (2000) Microtubule minus-end anchorage at centrosomal and non-centrosomal sites: the role of ninein. Journal of Cell Science. 113(Pt 17); 3013-3023.

Mogensen, M.M., Tucker, J.B., Mackie, J.B., Prescott, A.R., Nathke, I.S. (2002) The adenomatous polyposis coli protein unambiguously localises to microtubule plus ends and is involved in establishing parallel arrays of microtubule bundles in highly polarised epithelial cells. Journal of Cell Biology. 157(6); 1041-1048.

Molyneux, G., Geyer, F.C., Magnay, F.A., McCarthy, A., Kendrick, H., Natrajan, R., MacKay, A., Grigoriadis, A., Tutt, A., Ashworth, A., Reis-Filho, J.S., Smalley, M.J. (2010) BRCA1 basal-like breast cancers originate from luminal epithelial progenitors and not from basal stem cells. Cell Stem Cell. 7; 403-417.

Moon, D.O., Kim, M.O., Kang, S.H., Choi, Y.H., Kim, G.Y. (2009) Sulforaphane suppresses TNF-α-mediated activation of NF-κB and induces apoptosis through activation of reactive oxygen species-dependent caspase-3. Cancer Letters. 274; 132-142.

Moss, D.K., Bellett, G., Carter, J.M., Liovic, M., Keynton, J., Prescott, A.R., Lane, B., Mogensen, M.M. (2007) Ninein is released from the centrosome and moves bi-directionally along microtubules. Journal of Cell Science. 120; 3064-3074.

Myzak, M.C., Dashwood, W.M., Orner, G.A., Ho, E., Dashwood, R.H. (2006) Sulforaphane inhibits histone deacetylase in vivo and supresses tumorigenesis in *Apc*^{min} mice. The FASEB Journal. 20(3); 506-508.

Nagano, M., Hoshino, D., Koshikawa, N., Akizawa, T., Seiki, M. (2012) Turnover of focal adhesions and cancer cell migration. International Journal of Cell Biology. 2012; Article ID 310616.

Nakaya, Y., Sheng, G. (2008) Epithelial to mesenchymal transition during gastrulation: An embryological view. Development, Growth and Differentiation. 50; 755-766.

Naumov, G.N., MacDonald, I.C., Weinmeister, P.M., Kerkvliet, N., Nadkarni, K.V., Wilson, S.M., Morris, V.L., Groom, A.C., Chambers, A.F. (2002) Persistence of solitary mammary carcinoma cells in a secondary site: a possible contributor to dormancy. Cancer Research. 62(7); 2162-2168.

Nellore, A., Paziana, K., Ma, C., Tsygankova, O.M., Wang, Y., Puttaswamy, K., Iqbal, A.U., Franks, S.R., Lv, Y., Troxel, A.B., Feldman, M.D., Meinkoth, J.L., Brose, M.S. (2009) Loss of Rap1GAP in papillary thyroid cancer. The Journal of Clinical Endocrinology & Metabolism. 94(3); 1026-1032.

Niola, F., Zhao, X., Singh, D., Sullivan, R., Castano, A., Verrico, A., Zoppoli, P., Friedmann-Morvinski, D., Sulman, E., Barrett, L., Zhuang, Y., Verma, I., Benezra, R., Aldape, K., Iavarone, A., Lasorella, A. (2013) Mesenchymal high-grade glioma is maintained by the ID-RAP1 axis. The Journal of Clinical Investigation. 123(1); 405-417.

Ocana, O.H., Corcoles, R., Fabra, A., Moreno-Bueno, G., Acloque, H., Vega, S., Barrallo-Gimeno, A., Cano, A., Nieto, M.A. (2012) Metastatic colonization requires the repression of the epithelial-mesenchymal transition inducer Prrx1. Cancer Cell. 22; 709-724.

Oda, T., Iwasa, M., Aihara, T., Maeda, Y., Narita, A. (2009) The nature of the globular- to fibrous- actin transition. Nature. 457; 441-445.

Panková, K., Rösel, D., Novotn□, M., Brábek, J. (2010) The molecular mechanisms of transition between mesenchymal and amoeboid invasiveness in tumor cells. Cellular and Molecular Life Sciences. 67; 63-71.

Pappa, G., Bartsch, H., Gerhäuser, C. (2007) Biphasic modulation of cell proliferation by sulforaphane at physiologically relevant exposure times in a human colon cancer cell line. Molecular Nutrition & Food Research. 51; 977-984.

Perdiz, D., Mackeh, R., Poüs, C., Baillet, A. (2011) The ins and outs of tubulin acetylation: more than just a post-translational modification? Cellular Signalling. 23(5); 763-771.

Peris, L., Thery, M., Fauré, J., Saoudi, Y., Lafanechère, L., Chilton, J.K., Gordon-Weeks, P., Galjart, N., Bornens, M., Wordeman, L., Wehland, J., Andrieux, A., Job, D. (2006) Tubulin tyrosination is a major factor affecting the recruitment of CAP-Gly proteins at microtubule plus ends. Journal of Cell Biology. 174(6); 839-849.

Pierson, G.B., Burton, P.R., Himes, R.H. (1978) Alterations in number of protofilaments in microtubules assembled in vitro. The Journal of Cell Biology. 76; 223-228.

Piperno, G., Fuller, M.T. (1985) Monoclonal antibodies specific for an acetylated form of alpha-tubulin recognize the antigen in cilia and flagella from a variety of organisms. Journal of Cell Biology. 101(6); 2085-2094.

Pledgie-Tracy, A., Sobolewski, M.D., Davidson, N.E. (2007) Sulforaphane induces cell type-specific apoptosis in human breast cancer cell lines. Molecular Cancer Therapeutics. 6(3); 1013-1021.

Pocasap, P., Weerapreeyakul, N., Thumanu, K. (2018) Structures of isothiocyanates attributed to reactive oxygen species generation and microtubule depolymerisation in HepG2 cells. Biomedicine and Pharmacotherapy. 101; 698-709.

Pollard, T.D., Borisy, G.G. (2003) Cellular motility driven by assembly and disassembly of actin filaments. Cell. 112; 453-465.

Prior, I.A., Muncke, C., Parton, R.G., Hancock, J.F. (2003) Direct visualisation of Ras proteins in spatially distinct cell surface microdomains, Journal of Cell Biology. 160; 165-170.

Prochaska, H.J., Santamaria, A.B. (1988) Direct measurement of NAD(P)H:quinone reductase from cells cultured in microtiter wells: a screening assay for anticarcinogenic enzyme inducers. Analytical Biochemistry. 169; 328-336.

Raaijmakers, J.H., Bos, J.L. (2009) Specificity in Ras and Rap signalling. Journal of Biological Chemistry. 284; 10995-10999.

Raftopoulou, M., Hall, A. (2004) Cell migration: Rho GTPases lead the way. Developmental Biology. 265; 23-32.

Raman, R., Savio, C., Sonawane, M. (2018) Polarised organisation of the cytoskeleton: Regulation by cell polarity proteins.Journal of Molecular Biology. In Press.

Rangkadilok, N., Tomkins, B., Nicolas, M.E., Premier, R.R., Bennett, R.N., Eagling, D.R., Taylor, P.W.J. (2002) The effect of post-harvest and packaging treatments on glucoraphanin concentration in broccoli (*Brassica oleracia* var. *italica*). Journal of Agriculture and Food Chemistry. 50; 7386-7391.

Rask, L., Andréasson, E., Ekbom, B., Eriksson, S., Pontoppidan, B., Meijer, J. (2000) Myrosinase: gene family evolution and herbivore defence in Brassicaceae. Plant Molecular Biology. 42; 93-113.

Rausch, V., Liu, L., Kallifatidis, G., Baumann, B., Mattern, J., Gladkich, J., Wirth, T., Schemmer, P., Büchler, M.W., Zöller, M., Salnikov, A.V., Herr, I. (2010) Synergistic activity of sorafenib and sulforaphane abolishes pancreatic cancer stem cell characteristics. Cancer Research. 70(12); 5004-5013.

Reed, N.A., Cai, D., Blasius, T.L., Jih, G.T., Meyhofer, E., Gaertig, J., Verhey, K.J. (2006) Microtubule acetylation promotes kinesin-1 binding and transport. Current Biology. 16; 2166-2172.

Richman, E.L., Carroll, P.R., Chan, J.M. (2012) Vegetable and fruit intake after diagnosis and risk of prostate cancer progression. International Journal of Cancer. 131(1); 201-210.

Rid, R., Schiefermeier, N., Grigoriev, I., Small, J.V., Kaverina, I. (2005) The last but not the least: the origin and significance of trailing adhesions in fibroblastic cells. Cell Motility and the Cytoskeleton. 61; 161-171.

Ridley, A.J., Schwartz, M.A., Burridge, K., Firtel, R.A., Ginsberg, M.H., Borisy, G., Parsons, J.T., Horwitz, A.R. (2003) Cell migration: integrating signals from front to back. Science. 302(5651); 1704-1709.

Roll-Mecak, A. (2015) Intrinsically disordered tubulin tails: complex tuners of microtubule functions? Seminars in Cell and Developmental Biology. 37; 11-19.

Roy, M., Sarkar, R., Mukherjee, S., Mukherjee, A., Biswas, J. (2015) Sulforaphane inhibits metastatic events in breast cancer cells through genetic and epigenetic regulation. Journal of Carcinogenesis & Mutagenesis. 6(4); doi: 10.4172/2157-2518.1000231.

Rudolf, E., Andelová, H., Červinka, M. (2009) Activation of several concurrent proapoptotic pathways by sulforaphane in human colon cancer cells SW620. Food and Chemical Toxicology. 47(9); 2366-2373.

Rudolf, E., Červinka, M. (2011) Sulforaphane induces cytotoxicity and lysosome- and mitochondria-dependent cell death in colon cancer cells with deleted p53. Toxicology in Vitro. 25(7); 1302-1309.

Sak, K. (2012) Chemotherapy and dietary phytochemical agents. Chemotherapy Research and Practice. 2012; 282570.

Sasse, R., Gull, K. (1988) Tubulin post-translational modifications and the construction of microtubular organelles in Trypanosoma brucei. Journal of Cell Science. 90(Pt4); 577-589.

Schmidt, B., Ribnicky, D.M., Poulev, A., Logendra, S., Cefalu, W.T., Raskin, I. (2008) A natural history of botanical therapeutics. Metabolism Clinical and Experimental. 57(Suppl 1); S3-S9.

Schulze, E., Asai, D.J., Bulinski, J.C., Kirschner, M. (1987) Posttranslational modification and microtubule stability. Journal of Cell Biology. 105(5); 2167-2177.

Schuyler, S.C., Pellman, D. (2001) Microtubule “plus-end-tracking proteins”: the end is just the beginning. Cell. 105; 421-424.

Seow, A., Yuan, J.M., Sun, C.L., van den Berg, D., Lee, H.P., Yu, M.C. (2002) Dietary isothiocyanates, glutathione S-transferase polymorphisms and colorectal cancer risk in the Singapore Chinese Health Study. Carcinogenesis. 23; 2055-2061.

Shah, S., Brock, E.J., Ji, K., Mattingly, R.R. (2018) Ras and Rap1: A tale of two GTPases. Seminars in Cancer Biology. In Press.

Shah, S.P., Roth, A., Goya, R., Oloumi, A., Ha, G., Zhao, Y., Turashvili, G., Ding, J., Tse, K., Haffari, G., Bashashati, A., Prentice, L.M., Khattra, J., Burleigh, A., Yap, D., Bernard, V., McPherson, A., Shumansky, K., Crisan, A., Giuliany, R., Heravi-Moussavi, A., Rosner, J., Lai, D., Birol, I., Varhol, R., Tam, A., Dhalla, N., Zeng, T., Ma, K., Chan, S.K., Griffith, M., Moradian, A., Cheng, S.W.G., Morin, G.B., Watson, P., Gelmon, K., Chia, S., Chin, S.F., Curtis, C., Rueda, O.M., Pharoah, P.D., Damaraju, S., Mackey, J., Hoon, K., Harkins, T., Tadigotla, V., Sigaroudinia, M., Gascard, P., Tlsty, T., Costello, J.F., Meyer, I.M., Eaves, C.J., Wasserman, W.W., Jones, S., Huntsman, D., Hirst, M., Caldas, C., Marra, M.A., Aparicio, S. (2012) The clonal and mutational evolution spectrum of primary triple-negative breast cancers. Nature. 486; 395-399.

Shan, Y., Zhang, L., Bao, Y., Li, B., He., C., Gao, M., Feng, X., Xu, W., Zhang, X., Wang, S. (2013) Epithelial-mesenchymal transition, a novel target of sulforaphane via COX-2/MMP2, 9/Snail, ZEB1 and miR-200c/ZEB1 pathways in human bladder cancer cells. Journal of Nutritional Biochemistry. 24(6); 1062-1069.

Shankar, S., Ganapathy, S., Srivastava, R.K. (2008) Sulforaphane enhances the therapeutic potential of TRAIL in prostate cancer orthotopic model through regulation of apoptosis, metastasis and angiogenesis. Clinical Cancer Research. 14(21); 6855-6866.

Shi, L., Xiao, R., Wang, M., Zhang, M., Weng, N., Zhao, X., Zheng, X.F.S., Wang, H., Mai, S. (2018) MicroRNA-342-3p supresses proliferation and invasion of nasopharyngeal carcinoma cells by directly targeting Cdc42. Oncology Reports. doi: 10.3892/or.2018.6642.

Shin, K., Straight, S., Margolis, B. (2005) PATJ regulates tight junction formation and polarity in mammalian epithelial cells. Journal of Cell Biology. 168(5); 705-711.

Sikder, H.A., Devlin, M.K., Dunlap, S., Ryu, B., Alani, R.M. (2003) Id proteins in cell growth and tumourigenesis. Cancer Cell. 3(6); 525-530.

Singh, M., Yelle, N., Venugopal, C., Singh, S.K. (2018) EMT: Mechanisms and therapeutic implications. Pharmacology and Therapeutics. 182; 80-94.

Singh, S.V., Herman-Antosiewicz, A., Sing, A.V., Lew, K.L., Srivastava, S.K., Kamath, R., Brown, K.D., Zhang, L., Baskaran, R. (2004) Sulforaphane-induced G_2/M phase cell cycle arrest involves checkpoint kinase 2-mediated phosphorylation of cell division cycle 25C. The Journal of Biological Chemistry. 279(24); 25813-25822.

Singh, S.V., Warin, R., Xiao, D., Powolny, A.A., Stan, S.D., Arlotti, J.A., Zeng, Y., Hahm, E.R., Marynowski, S.W., Bommareddy, A., Desai, D., Amin, S., Parise, R.A., Beumer, J.H., Chambers, W.H. (2009) Sulforaphane inhibits prostate carcinogenesis and pulmonary metastasis in TRAMP mice in association with increased cytotoxicity of natural killer cells. Cancer Research. 69(5); 2117-2125.

Smith, K.J., Levy, D.B., Maupin, P., Pollard, T.D., Vogelstein, B., Kinzler, K.W. (1994) Wild-type but not mutant APC associates with the microtubule cytoskeleton. Cancer Research. 54; 3672-3675.

Snider, N.T., Omary, M.B. (2014) Post-translational modifications of intermediate filament proteins: mechanisms and functions. Nature Reviews Molecular and Cell Biology. 15(3); 163-177.

Soucek, K., Kamid, A., Phung, A.D., Kubala, L., Bulinski, J.C., Harper, R.W., Eiserich, J.P. (2006) Normal and prostate cancer cells display distinct molecular profiles of alpha tubulin posttranslational modifications. Prostate. 66; 954-965.

Spano, D., Heck, C., De Antonellis, P., Christofori, G., Zollo, M. (2012) Molecular networks that regulate cancer metastasis. Seminars in Cancer Biology. 22(3); 234-249.

Spitz, M.R., Duphorne, C.M., Detry, M.A., Pillow, P.C., Amos, C.I., Lei, L., de Andrade, M., Gu, X., Hong, W.K., Wu, X. (2000) Dietary intake of isothiocyanates: evidence of a joint effect with glutathione S-transferase polymorphisms in lung cancer risk. Cancer Epidemiology, Biomarkers & Prevention. 9; 1017-1020.

St Johnston, D., Sanson, B. (2011) Epithelial polarity and morphogenesis. Current Opinion in Cell Biology. 23; 540-546.

Steinart, P.M. (1993) Structure, function and dynamics of keratin intermediate filaments. The Journal of Investigative Dermatology. 100(6); 729-734.

Stephen, A.G., Esposito, D., Bagni, R.K., McCormick, F. (2014) Dragging Ras back in the ring. Cancer Cell. 25; 272-281.

Steward, O., Goldschmidt, R.B., Sutula, T. (1984) IV. Neurotoxicity of colchicine and other tubulin-binding agents: A selective vulnerability of certain neurons to the disruption of microtubules. Life Sciences. 35(1); 43-51.

Stoker, A.W. (2005) Protein tyrosine phosphatases and signalling. Journal of Endocrinology. 185(1); 19-33.

Stypula-Cyrus, Y., mutyal, N.H., Cruz, M.D., Kunte, D.P., Radosevich, A.J., Wali, R., Roy, H.K., Backman, V. (2014) End-binding protein 1 (EB1) up-regulation is an early event in colorectal carcinogenesis. FEBS Letters. 588(5); 829-835.

Su, L.K., Qi, Y. (2001) Characterisation of human *MAPRE* genes and their proteins. Genomics. 71; 142-149.

Svitkina, T.M. (2018) Ultrastructure of the actin cytoskeleton. Current Opinion in Cell Biology. 54: 1-8.

Takai, Y. Sasaki, T., Matozaki, T. (2001) Small GTP-binding proteins. Physiological Reviews. 81; 153-208.

Tamate, M., Tanaka, R., Osogami, H., Matsuura, M., Satohisa, S., Iwasaki, M., Saito, T. (2017) Rap1GAP inhibits tumour progression in endometrial cancer. Biochemical and Biophysical Research Communications. 485(2); 476-483.

Tan, R., Lee, Y.J., Chen, X. (2012) Id-1 plays a key role in cell adhesion in neural stem cells through the preservation of Rap1 signalling. Cell Adhesion & Migration. 6(1); 1-3.

ten Klooster, J.P., Hordijk, P.L. (2007) Targeting and localised signalling by small GTPases. Biology of the Cell. 99; 1-12.

Tepass, U. (2012) The apical polarity protein network in Drosophila epithelial cells: regulation of polarity, junctions, morphogenesis, cell growth and survival. Annual Review of Cell and Developmental Biology. 28; 655-685.

Thejass, P., Kuttan, G. (2006) Antimetastatic activity of sulforaphane. Life Sciences. 78(26); 3043-3050.

Tsai, J.H., Donaher, J.L., Murphy, D.A., Chau, S., Yang, J. (2012) Spatiotemporal regulation of epithelial-mesenchymal transition is essential for squamous cell carcinoma metastasis. Cancer Cell. 22; 725-736.

Tsygankova, O.M., Wang, H., Meinkoth, J.L. (2013) Tumor cell migration and invasion are enhanced by depletion of Rap1 GTPase activating protein (Rap1GAP). Journal of Biological Chemistry. 288; 24636-24646.

Tucker, J.B., Paton, C.C., Richardson, G.P., Mogensen, M.M., Russell, I.J. (1992) A cell surface-associated centrosomal layer of microtubule-organising material in the inner pillar cell of the mouse cochlea. Journal of Cell Science. 102; 215-226.

Ueda, K., Cardarelli, C., Gottesman, M.M., Pastan, I. (1987) Expression of a full-length cDNA for the human “MDR1” gene confers resistance to colchicine, doxorubicin and vinblastine. Proceedings of the National Academy of Sciences of the United States of America. 84(9); 3004-3008.

Ueda, M., Gräf, R., MacWilliams, H.K., Schliwa, M., Euteneuer, U. (1997) Centrosome positioning and directionality of cell movements. Proceedings of the National Academy of Sciences of the United States of America. 94(18); 9674-9678.

Vaughn, S.F., Berhow, M.A. (2005) Glucosinolate hydrolysis products from various plant sources: pH effects, isolation and purification. Industrial Crops and Products. 21; 193-202.

Verhey, K.J., Gaertig, J. (2007) The tubulin code. Cell Cycle. 6; 2152-2160.

Verhovsky, A.B., Svitkina, T.M., Borisy, G.G. (1999) Self-polarisation and directional motility of cytoplasm. Current Biology. 9(1); 11-20.

Vetter, I.R., Wittinghofer, A. (2001) The guanine nucleotide binding switch in three dimensions. Science. 294; 1299-1304.

Vigil, D., Cherfils, J., Rossman, K.L., Der, C.J. (2010) Ras superfamily GEFs and GAPs: Validated and tractable targets for cancer therapy? Nature Reviews Cancer. 10; 842-857.

Wade, R.H., Chrétien, D., Job, D. (1990) Characterisation of microtubule protofilament numbers. How does that surface lattice accommodate? Journal of Molecular Biology. 212(4); 775-786.

Wade, R.H., Hyman, A.A. (1997) Microtubule structure and dynamics. Current Opinion in Cell Biology. 9; 12-17.

Wang, L.I., Giovannucci, E.L., Hunter, D., Neuberg, D., Su, L., Christiani, D.C. (2004a) Dietary intake of cruciferous vegetables, glutathione S-transferase (GST) polymorphisms and lung cancer risk in a Caucasian population. Cancer Causes & Control. 15; 977-985.

Wang, L., Liu, D., Ahmed, T., Chung, F.L., Conaway, C., Chiao, J.W. (2004b) Targeting cell cycle machinery as a molecular mechanism of sulforaphane in prostate cancer prevention. International Journal of Oncology. 24; 187-192.

Wang, X., Kruithof-de Julio, M., Economides, K.D., Walker, D., Yu, H., Halili, M.V., Hu, Y.P., Price, S.M., Abate-Shen, C., Shen, M.M. (2009) A luminal epithelial stem cell is a cell of origin for prostate cancer. Nature. 461; 495-500.

Wegner, A., Isenberg, G. (1983) 12-fold difference between the critical monomer concentrations of the two ends of actin filaments in physiological salt conditions. Proceedings of the National Academy of Sciences of the United States of America. 80; 4922-4925.

Wu, Y., Mao, J., You, Y., Liu, S. (2014) Study on degradation kinetics of sulforaphane in broccoli extract. Food Chemistry. 155; 235-239.

Wynne, J.P., Wu, J., Su, W., Mor, A., Patsoukis, N., Boussiotis, V.A., Hubbard, S.R., Philips, M.R. (2012) Rap1-interacting adapter molecule (RIAM) associates with the plasma membrane via a proximity detector. Journal of Cell Biology. 199(2); 317-330

Xing, F., Sharma, S., Liu, Y., Mo, Y.Y., Wu, K., Zhang, Y.Y., Pochampally, R., Martinez, L.A., lo, H.W., Watabe, K. (2015) miR-509 suppresses brain metastasis of breast cancer cells by modulating RhoC and TNF-α. Oncogene. 34(37); 4890-4900.

Yancik, R. (2005) Population aging and cancer: A cross-national concern. The Cancer Journal. 11; 437-441.

Yang, Z. (2002) Small GTPases. Plant Cell. 14(Suppl); s375-s388.

Yilmaz, M., Christofori, G. (2009) EMT, the cytoskeleton, and cancer cell invasion. Cancer and Metastasis Reviews. 28; 15-33.

Yoshida, J., Horiuchi, A., Kikuchi, N., Hayashi, A., Osada, R. Ohira, S., Shiozawa, T., Konishi, I. (2009) Changes in the expression of E-cadherin repressors, Snail, Slug, SIP1 and Twist, in the development and progression of ovarian carcinoma: the important role of Snail in ovarian tumorigenesis. Medical Molecular Morphology. 42(2); 82-91.

Yu, C., He, Q., Zheng, J., Li, L.Y., Hou, Y.H., Song, F.Z. (2017) Sulforaphane improves outcomes and slows cerebral ischemic/reperfusion injury via inhibition of NLRP3 inflammasome activation in rats. International Immunopharmacology. 45; 74-78.

Yunpeng, L., Wang, S., Tang, L., Wang, X., Chen, L., Song, X., Wang, L., Chen, A. (2016) Sulforaphane alleviates myocardial ischemia/reperfusion injury by up-regulation of autophagy via AMPK/mTOR pathway. Journal of the American College of Cardiology. 68(16) Suppl S; C27.

Zhang, H., Chang, Y.C., Brennan, M.L., Wu, J. (2014) The structure of Rap1 in complex with RIAM reveals specificity determinants and recruitment mechanism. Journal of Molecular Cell Biology. 6(2); 128-139.

Zhang, L., Chenwei, L., Mahmood, R., van Golen, K., Greenson, J., Li, G., D'Silva, N.J., Li, X., Burant, C.F., Logsdon, C.D., Simeone, D.M. (2006) Identification of a putative tumor suppressor gene Rap1GAP in pancreatic cancer. Cancer Research. 66(2); 898-906.

Zhang, R., Alushin, G.M., Brown, A., Nogales, E. (2015) Mechanistic origin of microtubule dynamic instability and its modulation by EB proteins. Cell. 162; 849-859.

Zhang, Y. (2004) Cancer-preventive isothiocyanates: measurement of human exposure and mechanism of action. Mutation Research. 555; 173-190.

Zhang, Y., Kensler, T.W., Cho, C.G., Posner, G.H., Talalay, P. (1994) Anticarcinogenic activities of sulforaphane and structurally related synthetic norbornyl isothiocyanates. Proceedings of the National Academy of Sciences of the United States of America. 91; 3147-3150.

Zhang, Y., Tang, L. (2007) Discovery and development of sulforaphane as a cancer chemopreventive phytochemical. Acta Pharmalogica Sinica. 28(9); 1343-1354.

Zhang, Y.L., Wang, R.C., Cheng, K., Ring, B.Z., Su, L. (2017) Roles of Rap1 signaling in tumor cell migration and invasion. Cancer Biology & Medicine. 14(1); 90-99.

Zhang, Z., Mitra, R.S., Henson, B.S., Datta, N.S., McCauley, L.K., Kumar, P., Lee, J.S.J., Carey, T.E., D'Silva, N.J. (2006) Rap1GAP inhibits tumour growth in oropharyngeal squamous cell carcinoma. The American Journal of Pathology. 168(2); 585-596.

Zhang, Z., Yamashita, H., Toyama, T., Sugiura, H., Omoto, Y., Ando, Y., Mita, K., Hamaguchi, M., Hayashi, S.-I., Iwase, H. (2004) HDAC6 expression is correlated with better survival in breast cancer. Clinical Cancer Research. 10(20); 6962-6968.

Zhao, X., Wen, L., Dong, M., Lu, X. (2016) Sulforaphane activates the cerebral vascular Nrf2-ARE pathway and supresses inflammation to attenuate cerebral vasospasm in rat with subarachnoid hemorrhage. Brain Research. 1653; 1-7.

Zuo, H., Gandhi, M., Edreira, M.M., Hochbaum, D., Nimgaonkar, V.L., Zhang, P., DiPaola, J., Evdokimova, V., Altschuler, D.L., Nikiforov, Y.E. (2010) Downregulation of Rap1Gap through epigenetic silencing and loss of heterozygosity promotes invasion and progression of thyroid tumours. Cancer Research. 70(4); 1389.